# The PHILOSOPHICAL MAGAZINE

FIRST PUBLISHED IN 1798

. 41 SEVENTH SERIES No. 320 September, 1950

## *A Journal of Theoretical Experimental and Applied Physics*



PRICE 10s.
Annual Subscription £5 2s. 6d. payable in advance.

D AND PUBLISHED BY TAYLOR & FRANCIS LTD., RED LION COURT, FLEET ST., LONDON, E.C.4

# CONTENTS OF No. 320.




**All communications for the Philosophical Magazine should be addressed, post-paid, to the Editors, c/o Messrs. Taylor and Francis, Ltd., Red Lion Court, Fleet Street, London, England.

# LXXVIII. *Calibration of Proportional Counters by the Excitation of Flourescence Radiation with Radioactive Sources.*

By G. M. Insch,
Department of Natural Philosophy, Glasgow University*.

[Received July 3, 1950].

Summary.

The calibration of proportional counters by means of a very few suitably chosen radioactive sources which are used to excite the fluorescence radiation of various elements is described. The efficiency of excitation is high and the method is of wide application. The accurate identification of isomeric transitions using proportional tubes is demonstrated.

## Introduction.

The Investigations carried out in this laboratory using proportional counters (*Phil. Mag.* 1949) have necessitated detailed examination of various calibration techniques. Information on this subject has already been

Fig. 1.

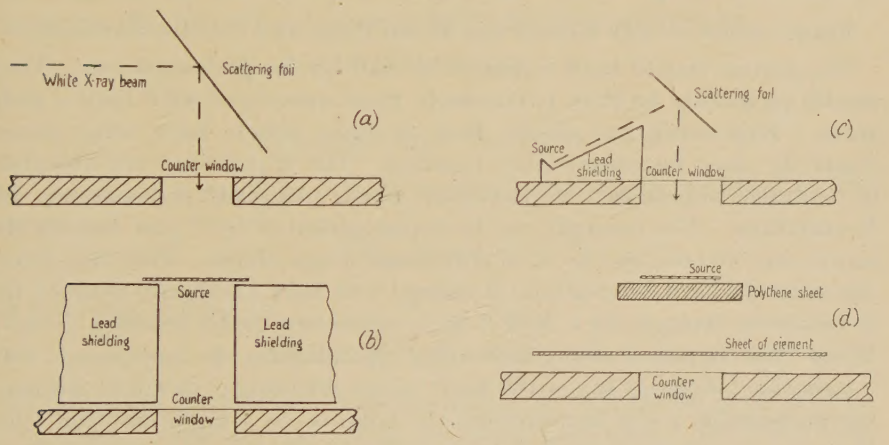


published by Rothwell and West (1950). However, during the course of our work considerable progress has been made in overcoming the various problems involved, and it is the aim of this paper to correlate some of the results obtained. The chief method described here is original and it is described in reasonable detail since it is of wide application.

In the early investigations the beam from an ordinary A.C.-operated X-ray machine, adjusted to operate at a small output intensity and which emitted white radiation was allowed to fall on a thin foil and the scattered radiation was detected in the counter at an angle to the beam direction (fig. 1(*a*)), (Curran, Angus and Cockroft 1949). This radiation entering the

* Communicated by the Author.

tube consisted mainly of the fluorescence X-rays of the scattering element. However, this method is not ideal. The X-ray machine is cumbersome, may give rise to spurious pulses (due to electrical interference), and calibration is accompanied by an increase in the " background " of the counter due to the detection of the white radiation. In addition the tube in ageing fails to self-rectify adequately and hence the pulses appear grouped on part of alternate half-cycles of the mains supply. For these reasons, new calibration techniques were explored and normally preferred. Pile-activated sources, which decayed by K-capture, or which showed nuclear isomersion or strong internal conversion of their $\gamma$-radiation, were found suitable as agents for the production of beams of homogeneous X-radiation or electrons. Sometimes the sources were used directly, but two methods of greatly entending their usefulness were established. The sources which have been most commonly applied in the course of several studies are shown in Table I.

TABLE I.

| Isotope | Half life | Transition | Approx. energy of X-ray | Associated radiation |
|---|---|---|---|---|
| $In^{114}$ | 50 days | isomeric | 24·1 KeV. | 1·98 MeV. $\beta+\gamma$'s |
| $Sn^{113}$ | 105 days | K-capture | 24·1 KeV. | $\gamma$'s and $e^-$ |
| $Ge^{71}$ | 11 days | K-capture | 9·2 KeV. | negligible |
| $Fe^{55}$ | 4 years | K-capture | 5·9 KeV. | none if pure. |

ELIMINATION OF THE EFFECTS OF HARD BETA AND GAMMA RADIATION.

The sources should have a reasonable half life for prolonged use. They should preferably be thin, particularly when associated with hard $\gamma$-radiation. Experience has shown that isotopes which have long period $\beta$-activity may be comfortably handled. The $\beta$-particles are absorbed by suitable thicknesses of polythene which has good transparency for X-radiation. For example, in the investigation of $In^{114}$ (see below) the source was covered by a layer of polythene, 6 mm. thick. This completely absorbed the hard $\beta$-radiation (of energy 1·98 MeV.) and only reduced the X-radiation (energy 24·1 KeV.) by a relatively small fraction ($\sim$1/4). When the required soft calibrating X-radiation is associated with $\gamma$-radiation (of energy say $\sim$100 KeV.) some shielding is useful in reducing the undesirable $\gamma$-ray flux through the counter to a miniumm (fig. 1(*b*)). However, this method can only be applied with advantage to relatively soft $\gamma$-rays. In the case of still harder $\gamma$-radiation ($\sim$·25 MeV. upwards) the source is most conveniently examined when placed really close to the counter window. This simple geometry results in the best solid angle for soft radiation passing into the counter and makes use of the higher efficiency of the counter for such radiation. Usually it is possible to secure a ratio of at least 10 : 1 in efficiency of detection in favour of the soft X-radiation. To obtain optimum results when examining the source in this way, care must be taken to eliminate the " end-effect " of the tube, since a small fraction of the radiation detected penetrates to the region of variable gas gain.

### Production of Modified Radiation.

Calibrating agents which gave homogeneous X-radiation covering the whole range from say 3 KeV. to 50 KeV. in small energy increments were found extremely useful. Since this coverage cannot be accomplished readily by use of radioactive sources alone new methods were devised. These involved the excitation of the desired radiation by homogeneous X-rays of higher energy originating from a radioactive source. This process is one of high efficiency and it was achieved in practice either by allowing the initial radiation to fall on a thin sheet of the appropriate element and detecting the excited radiation emitted from the front face (reflection (fig. 1(*c*)), or by placing a suitable thickness of the element between the source and the window (transmission). In the former case, the fluorescence radiation greatly predominates in intensity within the counter and its homogeneity is nearly independent of the thickness of the reflecting sheet. In the second case (transmission) a suitable thickness of the sheet can readily be calculated. For example, consider a source emitting homogeneous X-rays of wavelength $\lambda_1$ exciting a radiation of wavelength $\lambda_2$ in a sheet of the chosen element placed between the source and the counter window. Let this sheet have mass absorption coefficients $\mu_1$ and $\mu_2$ corresponding to $\lambda_1$ and $\lambda_2$. Let it be of thickness $l$ and density $p$.

It can be shown that the number of fluorescence X-ray quanta entering the counter (fig. 1(*d*)) when $I_0$ quanta fall on the sheet is given by

$$N=K_1I_0[e^{-K_2}-e^{-K_1}]/(K_1-K_2),$$

where

$$K_1=\mu_1 pl \quad \text{and} \quad K_2=\mu_2 pl.$$

The number of unmodified X-rays transmitted through the sheet to the counter is

$$T=I_0e^{-K_1}$$

and the ratio of these is

$$R=N/T=K_1[e^{K_1-K_2}-1]/(K_1-K_2). \quad . \quad . \quad . \quad . \quad . \quad (1)$$

Examination of equation (1) shows that the ratio R can be made as large as required ($>100$ say) by using sufficient thickness $l$, provided that $\mu_2<\mu_1$, a condition which is always satisfied in the usual experimental arrangements. (Furthermore this argument is strengthened by the fact that the modified radiation is usually the more efficiently detected). However, in practice large $l$ values may necessitate strong sources and in some cases it may be difficult to secure adequate intensity. On the other hand, if $R\sim1$ is regarded as suitable (peaks due to modified and unmodified radiations of equal intensity) the method can be used with very weak sources. (see fig. 2).

Regarding the reflection method (fig. 1(*c*)) it is sufficient to note that it can be readily applied in almost every case, but it may be inferior to the transmission method when very weak sources are employed.

These methods were applied to excite the fluorescence radiations of a number of elements (see Table II.). In this Table $E_0$ is the approximate energy of the initial X-radiation falling on the element and $E_m$ is the approximate energy of the modified radiation.

With the simple geometry demonstrated in fig. 1(*c*) it was possible to detect a) modified radiation ~5 per cent of the total radiation emanating

Fig. 2.

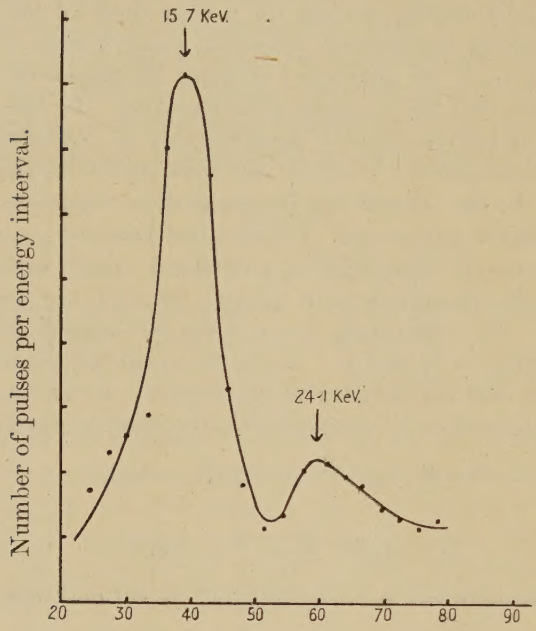


from the source. Hence a source strength of $<1\mu$ curie total activity proved sufficient. Indium and Geranium sources were found adequate for excitation of the flourescence radiations from less than 5 KeV. upwards, which considerably increased the number of homogeneous X-ray calibrating agents available within this energy range.

Table II.

| Source | Excited element | $E_0$ in KeV. | $E_m$ | Type of geometry | Histogram |
|---|---|---|---|---|---|
| $In^{114}$ | Zr | 24·1 | 15·7 | Tramsnission | fig. 2 |
| $In^{114}$ | Cu | 24·1 | 8·05 | Reflection | fig. 3(*a*) |
| $Ge^{71}$ | Ni | 9·2 | 7·5 | Reflection | fig. 3(*b*) |
| $Ge^{71}$ | Fe | 9·2 | 6·4 | Reflection | fig. 3(*c*) |

New calibrating agents are at present being examined for use with proportional counters in magnetic fields. Curran, Cockroft and Insch (1950) have recently used proportional tubes to measure particle energies >1 MeV. These examinations demand calibration radiations of several

hundred KeV. energy. Sources which decay by $\gamma$-ray transitions (not associated with $\beta$-activity) and which show strong internal conversion, are being studied (*e. g.* $Sn^{113}$; $\gamma$-ray energy 392 KeV. and ~70 per cent internal conversion) Such sources are introduced into the counter.

### Identification of Isomeric Transitions.

The primary phenomena externally observable in an isomeric transition are the emission of $\gamma$-radiation and usually conversion electrons. Accompanying the latter is a K X-radiation which is detected with high efficiency and accuracy by a proportional counter. Since this X-radiation is

Fig. 3.

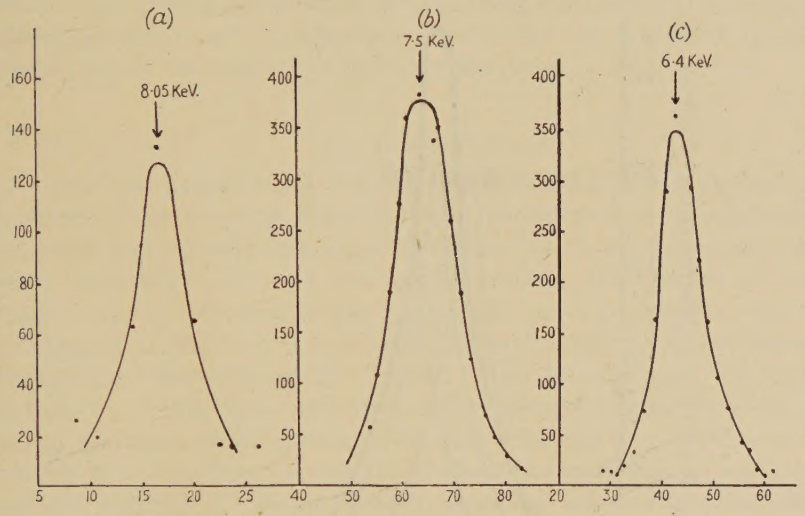


frequently difficult to identify with certainty, the method described here is an important aid. The isomeric transition in $In^{114}$ was studied and the K$\alpha$ fluorescence X-ray histogram is shown in fig. 4, curve A. At the same time, the K$\alpha$ fluorescence radiations of cadmium (energy 23·1 KeV.) Indium (24·1 KeV.) and tin (25·2 KeV.) were excited and compared with the radiation arising in the nuclear process. The three histograms are shown in fig. 4, curves B, C and D. This demonstrates at once that the known $\gamma$-ray energy 192 KeV., which is strongly converted, is emitted prior to any transition in which Z changes. The importance of this method for the accurate identification of isomeric processes is obvious.

In the course of this work argon was used as the absorbing gas. For the energies investigated it is superior to the gases of greater atomic number, such as Xenon and Krypton, which have a relatively small Auger effect, causing homogeneous X-radiation to yield two peaks of comparable intensity, which can lead to uncertainties. One peak corresponds to the case when the argon X-ray escapes from its own atom and is not detected. The Auger effect in argon is high and an independent value for this effect

was obtained during the work described above. This was accomplished by studying an X-ray histogram obtained when the fluorescence K X-rays of iron were excited by a germanium source. Two peaks were evident, one due to the fluorescence Kα X-radiation of iron of energy 6·4 KeV., and one to the photoelectrons (energy 3·4 KeV.) from the K level of argon when the X-ray escaped and did not form an Auger electron.

Fig. 4.

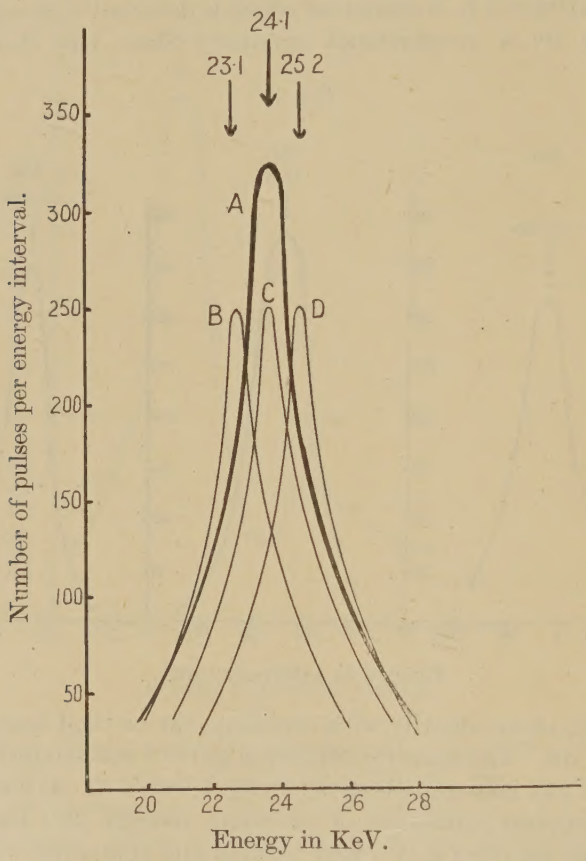


The effect on the smaller energy peak, due to 3 KeV. X-radiation caught in the gas was calculated and the " background " spectrum of the counter was subtracted from the histogram. Using this the Auger effect in argon was found to be 94 per cent in reasonable agreement with previous work (Compton and Allison 1936).

Throughout this work a counter $5\frac{1}{2}''$ internal diameter was used with a filling of 60 cm. Hg. of argon and 15 cm. Hg. of methane.

## References.

Rothwell, P., and West, D., 1950, *Proc. Phys. Soc.*, **63**, 541.
Curran, S. C., Angus, J., and Cockroft, A. L., 1949, *Phil. Mag.*, **40**, 36.
Curran, S. C., Cockroft, A. L., and Insch, G. M., in the press.
Compton, A. H., and Allison, S. K., 1936, *X-rays* (Macmillan).

# LXXIX. *Transit-time Phenomena in Electron Streams.*—II.

By D. K. C. MacDonald,
Clarendon Laboratory, Parks Road, Oxford *.

[Received July 13, 1950.]

Abstract.

A density modulated electron stream will suffer amplitude reduction and phase variation with transit time due to the statistical velocity distribution of the electrons. The problem is considered in relation to that of noise generation in a beam due to velocity fluctuation; the analysis developed is then used in examining the variation of space-charge reduction factor ($\Gamma^2$) under particular laws of potential distribution which present themselves in physical problems.

## § 1. Introduction.

In a previous paper in this Journal † (MacDonald 1949 a) we analysed the problem of an electron beam initially accelerated to a relatively high potential and initially ordered in density ($\Gamma^2=0$), which becomes progressively disordered ($\Gamma^2 \to 1$) due to the random distribution of velocities present in the electron beam. We wish now to consider the related problem of an electron stream with thermal velocities which has a given density-modulated sinusoidal "signal" initially imposed; the amplitude and phase of this signal will then suffer alteration with transit-time due to the thermal energy spread. We shall examine the significance of this relationship and then proceed to analyse the variation of such a signal and the related $\Gamma^2$ under certain potential laws of physical interest. The theoretical predictions will be compared with such experimental evidence as is available and the significance of the results discussed.

## § 2. Reduction of Signal Amplitude.

Since (I) was published, both van der Ziel (1949) and MacDonald (1949 b) have independently considered the variation during drift time $\tau$ of a sinusoidal density-variation in an electron stream of thermal energy distribution

$$\left.\begin{aligned} p(\mathrm{E})d\mathrm{E} &= 1/k\theta \,.\, \exp(-\mathrm{E}/k\theta)d\mathrm{E}, \quad (\mathrm{E}>0) \\ &= 0 \qquad\qquad\qquad\quad , \quad (\mathrm{E}<0) \end{aligned}\right\} \tag{1}$$

($k$ : Boltzmann's constant. $\theta$ : Absolute temperature)

which has been initially accelerated very rapidly to energy $\Phi$.

If the beam-density before "drifting" ($\tau=0$) is given by

$$n_{(0)}=\mathrm{N}_0+\mathrm{A}_0 \sin \omega t,$$

* Communicated by the Author.

† Referred to as (I) here.

then one shows readily by considering the loss and gain of electrons in a short interval of time that

$$n_{(\tau)}=\frac{2\Phi}{k\theta\tau}\int_0^\infty \exp\left(-\frac{2\Phi x}{k\theta\tau}\right).(N_0+A_0\sin\omega t\cos\omega x+A_0\sin\omega x\cos\omega t)dx$$

$$=N_0+A_0\sin\omega t\left\{\frac{1}{1+a^2}\right\}+A_0\cos\omega t\left\{\frac{a}{1+a^2}\right\}, \quad . . . . . (2)$$

where $$a=\omega t\left(\frac{k\theta}{2\Phi}\right).$$

The unvarying (" d.c. ") component, $N_0$, remains unchanged, as we should expect, but the oscillatory (" a.c. ") component suffers reduction in magnitude and a change in phase. It is perhaps interesting to observe that for the large values of $\tau$ the phase-shift approaches $\pi/2$ asymptotically.

## § 3. Relationship with Noise-Reduction Factor, $\Gamma^2$.

Equation (2) is in itself of interest ; by comparison with (I), however, where we found $\Gamma^2=\frac{a^2}{1+a^2}$, we may show immediately

$$A_\tau=A_0\sqrt{(1-\Gamma^2)}\sin(\omega t+\alpha), \quad . . . . . (3)$$

$$\left[\alpha=\tan^{-1}\sqrt{\left(\frac{\Gamma^2}{1-\Gamma^2}\right)}\right],$$

where $A_\tau$ is the signal after drift time, $\tau$. The variation of the signal components and of $\Gamma^2$ are plotted in fig. 1, particularly for comparison with the later work.

Equation (3) may be interpreted as follows. Consider a wholly disordered stream (full " shot effect ", $\Gamma^2=1$); then the noise current $\overline{\delta I^2}$ may be considered as distributed in a frequency spectrum according to the well-known expression

$$\overline{\delta I_f^2}=2eI\,df. \quad . . . . . (3)$$

After drifting for a time $\tau$, according to (3), the magnitude will have diminished to

$$\overline{\delta I_{f,\tau}^2}=2eI(1-\Gamma^2)\,df. \quad . . . . . (4a)$$

On the other hand, the d.c. component, I, which we have effectively considered as " smooth " by distributing the fluctuation throughout the frequency spectrum in (4), will, by (I), have become partially disordered according to the law

$$\overline{\delta I^2}=2eI\Gamma^2\,df. \quad . . . . . (4b)$$

The net sum of (4*a*) and (4*b*) is thus simply $2eIdf$. The irreversible maintenance of full shot effect (equation (4)) in the beam may thus be regarded as the " detailed balancing " of these two mechanisms always proceeding at the same rate at any instant. When we consider the

problem, as in (I), of the beam with zero shot effect, then only one process can occur and we thus witness the so-called irreversible approach towards full shot effect *. We remark also that the *signal-noise (power) ratio* will evidently deteriorate following a law $\sim \frac{1-\Gamma^2}{\Gamma^2}$.

With the equivalence demonstrated above the calculation of $\Gamma^2$ in certain problems is simplified.

## § 4. Lemma—Case of Initial $\Gamma^2 \neq 0$.

Before continuing to a detailed analysis of the problems in view we state a simple lemma. Thus far we have assumed that $\Gamma^2 = 0$ initially; we ask now how the noise will grow if initially

$$\overline{\delta I_f^2} = 2e\mathrm{I}\Gamma_0^2\, df \qquad (0 < \Gamma_0^2 \leqslant 1).$$

Fig. 1.

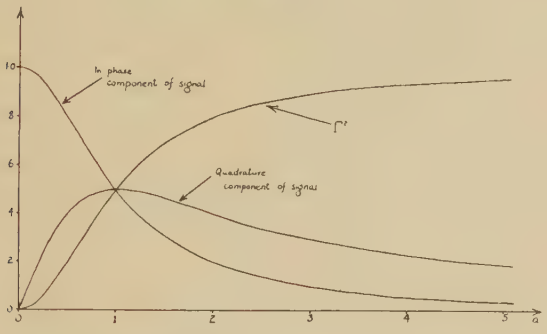


Variation of signal components and $\Gamma^2$ for accelerated electron-stream.

If $\Gamma_{\tau,0}^2$ be the noise factor due to transit calculated for an initially smooth beam ($\Gamma_0^2 = 0$), then the overall factor (say $\Gamma_\tau^2$) is given by

$$\Gamma_\tau^2 = \Gamma_0^2 + (1-\Gamma_0^2)\Gamma_{\tau,0}^2. \quad . \quad . \quad . \quad . \quad . \quad . \quad . \quad . \quad (5)$$

A simple demonstration may be given by splitting the current, I say, into an initially "noisy" component of magnitude $\mathrm{I}\Gamma_0^2$ and an initially "smooth" one of magnitude $\mathrm{I}(1-\Gamma_0^2)$ (*cf.* (I), p. 565).

## § 5. $\Gamma^2$ in Various Potential Distributions †.

In (I) we assumed that the electron beam was injected into the drift region at relatively high energy, $\Phi$, with $\Gamma^2 = 0$. In practice the electron stream is derived from a structure ("electron gun") similar in principle

* v. d. Ziel's communication (*loc. cit.*) is on somewhat similar lines to the foregoing. He suggests, however, that $\Gamma^2$ is derivable *à priori* from an equation equivalent to (2) of this paper. We have reason to prefer to regard the two analyses as of *individual* significance, demonstrating also, however, *under these assumptions* (*e. g.* no space-charge interaction) the equivalence shown above.

† It should perhaps be remarked that we are here throughout interested in the dynamics of an electron stream—that is, in the convective part of the current. The experimental data used below for comparison refer indeed to such currents.

to a simple thermionic diode, of anode voltage $\Phi/e$ (measured from the potential minimum, strictly speaking), having a hole in the anode for projection of the electron beam. The smoothing in density of the emitted current fluctuations occurs through the medium of the variable potential minimum which is present between cathode and anode when the current is limited by space-charge. At medium frequencies the overall transit time in the electron gun is so short that a quasi-steady state may be assumed in the "classical" analysis (*cf.* North (1940), Schottky and Spenke (1937)); consequently one need not consider what region of the "valve" is dynamically responsible for the smoothing process. At very high frequencies, however, the very existence of a high degree of smoothing in diodes and long beams (Kompfner *et al.* 1946; Kompfner 1947) suggests that the action must occur effectively within a very small fraction of the total diode transit time. Further, the general assumption that the "compensating" stream of electrons released is of almost zero energy (relative to the space-charge minimum) suggests that essentially only a small region about the potential minimum is significant for the initial smoothing.

As a first analytical model, then, on the basis of these considerations, we shall assume that the space-charge smoothing is effectively complete immediately beyond the potential minimum. We would emphasize that no theory as yet exists for the detailed space-charge interaction of electrons in a valve at very high frequencies; we hope in the future to be able to make some progress in this direction. If a satisfactory detailed theory is forthcoming we should then be able to specify with greater certainty the "initial conditions" of our present problem.

We turn thus to consider the current fluctuations in the electron gun itself. We measure potential, $V$, transit time, $\tau$, and distance, $x$, from the potential minimum. In line with the foregoing discussion, we assume first a smooth current "injected" at $x=0$; this corresponds to the assumption that the smoothing mechanism can be idealized, in the first place, to occur at $x=0$.

(*a*): *Linear potential variation* *.

Let $V=Cx$; we first require the law of transit-time, $\tau_E$, from $V=0$ at $x=0$ to potential $V_0$ at $x=x_0$, say, with variation of initial (thermal) energy, E.

Thus
$$\tau_E=\sqrt{\left(\frac{m}{2e}\right)}\int_0^{x_0}\frac{dx}{\sqrt{(V+E/e)}} \quad . \quad . \quad . \quad . \quad . \quad . \quad (6)$$

$$=\tau_0(1-(E/eV_0)^{1/2}), \quad . \quad . \quad . \quad . \quad . \quad . \quad . \quad . \quad (7)$$

where $\tau_0$ is transit time for $E=0$. Equation (6) then replaces the equation for $\tau$ appropriate in (I) and in § 2 of this paper, namely

$$\tau_E=\tau_0(1-E/2\Phi).$$

* It is of course understood that a linear law could not exist fundamentally in the immediate neighbourhood of the minimum; it is chosen simply as an obvious overall first approximation.

To calculate $\Gamma^2$ we rely on the equivalence demonstrated in §3 above. We find in this case that $S_\tau \equiv A_\tau/A_0$ is given by

$$S_\tau = \sin \omega t \int_0^\infty \epsilon^{-x^2} \cos\left(\frac{\omega x}{\beta}\right) 2x\,dx + \cos \omega t \int_0^\infty \epsilon^{-x^2} \sin\left(\frac{\omega x}{\beta}\right) 2x\,dx, \quad . \quad (8)$$

where $$\beta = \frac{1}{\tau}(eV_0/k\theta)^{1/2},$$

assuming that the electrons leave the minimum, as is well-known, with a thermal energy distribution given by equation (1) above.

Thus

$$S_\tau = \sin \omega t \left\{1 - a\int_0^\infty \epsilon^{-x^2} \sin ax\,dx\right\} + \cos \omega t \left\{a\int_0^\infty \epsilon^{-x^2} \cos ax\,dx\right\} \quad . \quad (9)$$

where $a = \omega\tau(k\theta/eV_0)^{1/2}$ now.

$$= \sin \omega t \left\{1 - a\epsilon^{-a^2/4}\int_0^{a/2} \epsilon^{t^2}\,dt\right\} + \cos \omega t \left\{\frac{a\sqrt{\pi}}{2}\epsilon^{-a^2/4}\right\}. \quad . \quad . \quad . \quad . \quad (10)$$

Hence $$\Gamma^2 = 1 - \left\{\left(1 - a\epsilon^{-a^2/4}\int_0^{a/2} \epsilon^{t^2}\,dt\right)^2 + \frac{a^2\pi}{4}\epsilon^{-a^2/2}\right\}. \quad . \quad . \quad (11\,a)$$

The function $\int_0^x \epsilon^{t^2}\,dt$ is tabulated (*e. g.* Jahnke and Emde (1933), p. 32), or Lash Miller and Gordon (1931) tabulate $\epsilon^{-x^2}\int_0^x \epsilon^{t^2}\,dt$. One may also usefully use expansion in powers of $a$, showing in particular that for small $a$

$$\left.\begin{aligned}\Gamma^2 &\doteq a^2\left(1 - \frac{\pi}{4}\right) + \frac{a^4}{24}(10 - 3\pi) + \ldots . \\ &= 0{\cdot}215a^2 + 0{\cdot}024a^4 + \ldots .\end{aligned}\right\} . \quad . \quad . \quad . \quad (11\,b)$$

The relevant functions in (10) and (11*a*) are plotted in fig. 2, with $a$ as abscissa. We observe now that a phase change of $\pi$ in the signal occurs as $\tau \to \infty$.

In comparison with experiment, we may take the following values for a typical electron gun used at very high frequencies :

$$f\tau \text{ (number of transit cycles)} \approx 3$$

$$V_0 = 4 \times 10^2 \text{ volts}$$

$$\theta \simeq 10^3 \text{ °K.} \quad \therefore \quad \frac{k\theta}{e} \simeq 8{\cdot}6 \times 10^{-2} \text{ volts.}$$

Hence, in this case, $a = 6\pi\sqrt{(2{\cdot}15)} \times 10^{-2} \simeq 0{\cdot}28$, and therefore

$$\Gamma^2 = 0{\cdot}016_5. \quad . \quad . \quad . \quad . \quad . \quad . \quad . \quad . \quad . \quad (12)$$

Since experimental work based on the beam derived from such a gun (*cf.* Robinson and Kompfner 1950) indicates $\Gamma^2 \sim 0{\cdot}02$ this theoretical result might be considered most satisfactory, suggesting that the conditions postulated ($\Gamma^2 \to 0$ at $x=0$, etc.) could be regarded as providing an acceptable model for the fluctuational behaviour at high frequencies.

Before accepting this indication, however, it appears essential to consider the effect of closer approximation to the true potential distribution in the valve " gun ".

Fig. 2.

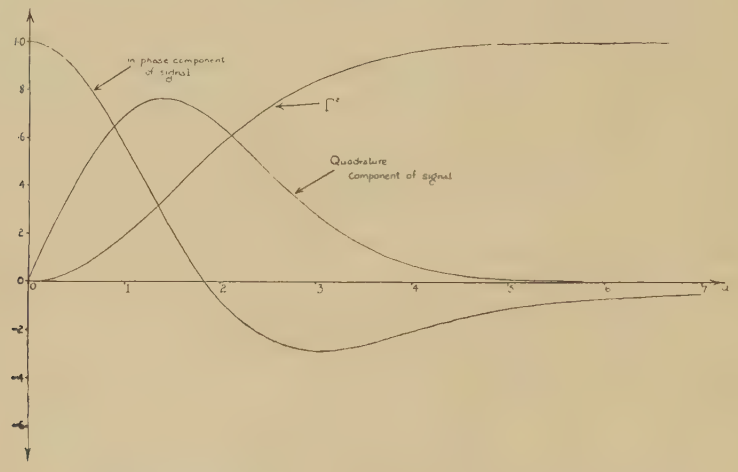


Variation of signal components and $\Gamma^2$ when $V=Cx$.

(*b*) *The Langmuir–Child Potential Law.*

Child (1911) and Langmuir (1913) showed that the current, I, in an idealized parallel-plane diode, limited solely by space-charge, initial cathode emission velocities being neglected, is given by the now classical expression

$$I=\frac{1}{9\pi}\sqrt{\left(\frac{2e}{m}\right)}\frac{V_a^{3/2}}{d^2}, \quad \ldots\ldots\ldots \quad (13)$$

where $d$ : anode-cathode distance.

$V_a$ : anode-cathode potential difference.

We adopt this diode as a second model for the potential-minimum anode region in the electron gun structure, where the minimum is now considered as a virtual cathode at $x=0$. The law of potential variation with $x$ corresponding to (13) is then

$$V \propto Cx^{4/3}, \quad \ldots\ldots\ldots \quad (14)$$

where C is a constant for the structure under a particular current.

The transit-time law with initial energy E (*cf.* equation (6) above) is then

$$\tau_E = \sqrt{\left(\frac{m}{2e}\right)}\int_0^{x_0}\frac{dx}{(Cx^{4/3}+v)^{1/2}}, \quad \ldots\ldots \quad (15)$$

where $v=E/e$, the equivalent initial voltage.

Simple substitution transforms (15) to

$$\tau_E = \frac{2}{3}\left(\frac{v}{c}\right)^{1/4}\sqrt{\left(\frac{m}{2eC}\right)}\int_0^{\sinh^{-1}(x_0^{3/2}\sqrt{(c/v)})} \sinh^{1/2}\phi\, d\phi,$$

which after expansion, integration and some reduction yields

$$\tau_E = \tau_0\{1-0{\cdot}85(v/V_0)^{1/4}+0{\cdot}167(v/V_0)-0{\cdot}038(v/V_0)^2+\ldots.\}. \quad . \quad (16)$$

An alternative, more perspicuous, approach is to split the range of integration in (15) at $x=\xi$, where $\xi$ is the value of $x$ for $V=v$. The two integrals may then be expanded and we obtain

$$\left.\begin{aligned}\tau_E(1) &\approx \tau_0(0{\cdot}28(v/V_0)^{1\cdot4}),\\ \tau_E(2) &\approx \tau_0(1-1{\cdot}13(v/V_0)^{1\cdot4}-0{\cdot}167(v/V_0)\ldots.).\end{aligned}\right\} \quad . \quad . \quad . \quad (17)$$

These expressions themselves seem not without interest in view particularly of a recent discussion by Pierce (1948) of transit-time variation with initial energy in a valve with a potential minimum due to space charge. He measures time, $t$, as we do, from the place of zero field (minimum of potential) and then uses the equation

$$\frac{\partial V}{\partial x} = 4\pi It, \quad . \quad . \quad . \quad . \quad . \quad . \quad . \quad . \quad . \quad (18)$$

(his equation (43)

to determine the transit time.

Where I is the diode current, and $t$ the transit time of an electron to $x$. This equation, however, as an application of Poisson's law—remembering $\partial V/\partial x \equiv 0$ at the minimum—is only valid where all electrons (producing I) have the *same* velocity and $t$ is the transit time of one of them and it is thus quite inappropriate in the present situation. If, indeed, I be supposed produced by a stream of electrons leaving the minimum with zero velocity and $t$ be the transit time of a "perturbed" electron with positive initial velocity then it is obvious that the error in (18) is gross indicating in fact a variation of $\partial V/\partial x$ in the wrong sense.

Equations (16) and (17) are also interesting in view of the common assumption (*e.g.* Rack (1938, p. 613)) that *thermal* energies produce negligible transit time variation in a valve except under extreme conditions. If, however, we set

$$V_0 \sim 10^2 \text{ volts}; \qquad v = k\theta/e \sim 10^{-1} \text{ volts},$$

then from (16): $\tau_E = \tau_0(1-0{\cdot}15)$, showing that in only 3 cycles transit time the difference would already amount to $\sim \frac{1}{2}$ cycle.

Returning to our analysis we proceed as in (*a*), using now

$$\tau_E \approx \tau_0(1-0{\cdot}85(v/V_0)^{1\cdot4}), \quad . \quad . \quad . \quad . \quad . \quad (16a)$$

in place of (6),

remembering also $(v/V_0) \ll 1$. In this case we find that the relative signal is now

$$S_\tau = \sin\omega t\left(1-a\int_0^\infty \epsilon^{-x^4}\sin ax\, dx\right)+\cos\omega t\left(a\int_0^\infty \epsilon^{-x^4}\cos ax\, dx\right) \quad . \quad (19)$$

and

$$\Gamma^2=1-\left\{\left(1-a\int_0^\infty \epsilon^{-x^4}\sin ax\,dx\right)^2+\left(a\int_0^\infty \epsilon^{-x^4}\cos ax\,dx\right)^2\right\} \quad (20)$$

where now $a=\omega\tau\,0{\cdot}85(k\theta/eV_0)^{1/4}$.

The integrals in (19) may again be expanded and we have

$$S_\tau=\sin\omega t\left(1-\frac{a^2\sqrt{\pi}}{4}+\frac{a^4}{4{\cdot}3\,!}\ldots.\right)+\cos\omega t\left(\Gamma(5/4)\,.\,a-\frac{\Gamma(7/4)}{3{\cdot}2\,!}a^3\ldots.\right), \quad (21a)$$

whence for small $a$

$$\Gamma^2=a^2\left(\frac{\sqrt{\pi}}{2}-(\Gamma(5/4))^2\right)-a^4\left(\frac{\pi}{16}+\frac{1}{12}-\frac{\Gamma(5/4)\Gamma(7/4)}{3}\right)\ldots.$$

$$\approx 0{\cdot}066a^2-0{\cdot}002a^4 \quad (21b)$$

$S_\tau$ and $\Gamma^2$ could be calculated in fact as far as $a=2$ using such expansions but the work quickly becomes lengthy. For very large $a$, asymptotic expansions may be sought, but are not of great value here. It was, however, found on plotting accurately $\epsilon^{-x^4}$ that a very close approximation to this function can be found through the formula

$$\left.\begin{aligned} f(x)&=1, && 0\leqslant x\leqslant 0{\cdot}3\\ &=1-1{\cdot}36(x-0{\cdot}3)^2, && 0{\cdot}3<x<0{\cdot}91\\ &=1{\cdot}36(1{\cdot}52-x)^2, && 0{\cdot}91<x<1{\cdot}52\\ &=0. && 1{\cdot}52\leqslant x \end{aligned}\right\} \quad (22)$$

Thus an explicit integration of (19) and (20) could be obtained :

$$S_\tau=\sin\omega t\left\{\cos 0{\cdot}91a\left(-0{\cdot}011+\frac{5{\cdot}44}{a^2}(1-\cos 0{\cdot}61a)\right)\right\}$$

$$+\cos\omega t\left\{\sin 0{\cdot}91a\left(-0{\cdot}011+\frac{5{\cdot}44}{a^2}(1-\cos 0{\cdot}61a)\right)\right\} \quad (23a)$$

$$\Gamma^2=1-\left\{-0{\cdot}011+\frac{5{\cdot}44}{a^2}(1-\cos 0{\cdot}61a)\right\}^2$$

$$\doteqdot 1+\frac{0{\cdot}120}{a^2}(1-\cos 0{\cdot}61a)-\frac{29{\cdot}57}{a^4}(1-\cos 0{\cdot}61a)^2. \quad (23b)$$

The values given by (23$a$, $b$) agree excellently with those derived from (21$a$, $b$) in the common region calculated ($a\leqslant 2$) and the relevant functions are plotted in fig. 3.

Turning to the numerical example quoted above, we now have $a=2{\cdot}175$, whence from fig. 3, $\Gamma^2=0{\cdot}26$. This figure is now greatly in excesss of the experimental value and it is further evident from the lemma of §4 that if $\Gamma_0^2\neq 0$ the situation is merely aggravated.

(*c*) *Discussion.*

It appears clear that this disagreement arises at least in part from our assumption that the smoothed current "emerges" from precisely $x=0$; $V=0$. In fact it is evident that the dynamical smoothing process cannot be *entirely* localized, while a glance at equation (17) shows clearly the important contribution to the above value for $\Gamma^2$ played by the potential in the immediate neighbourhood of the minimum. This feature is evinced even more strongly when we recollect that with the true velocity spectrum the potential *initially* rises with a square law (*cf. e. g.* Langmuir and Compton 1931), since in that case if we again postulate a smooth current from $x=0$, the initial rise of $\Gamma^2$ may be shown to be exceedingly rapid following a law

$$\Gamma^2 \sim \omega^2\tau^2 \log \frac{1}{\gamma\omega^2\tau^2}, \quad \ldots\ldots\ldots \quad (24)$$

($\gamma$, $\equiv e^C$ (where C is Euler's constant), $=1{\cdot}781\ldots.$).

Fig. 3.

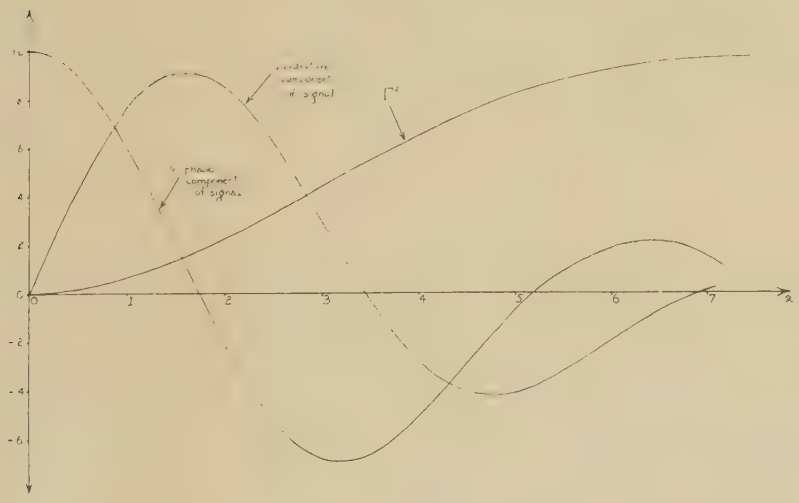


Variation of signal components and $\Gamma^2$ when $V=Cx^{4/3}$.

On the other hand in such a vital region it then becomes imperative to consider other factors in the physics of the fluctuation problem such as the Coulomb repulsion of the electrons; at this point we recollect the lack of a detailed theory of space-charge interaction mentioned previously.

Returning, however, to the Langmuir Child law the *significance* of this region may be readily assessed from fig. 4. The variation of $\Gamma^2$ for the numerical values previously laid down has been computed when it is assumed that the smooth beam "emerges" from a potential value *greater* than zero up to "thermal" potential, $k\theta/e$. In particular we find that in the latter case, $\Gamma^2$ has fallen as low as $\sim 0{\cdot}006$, well below the experimental value, restoring some reasonable confidence in the postulated model. It is probably significant also to notice that the transition from the quadratic potential law to a 4/3 power law occurs in the region $(1\rightarrow 10)\times k\theta/e$.

It is clear that in the linear approximation of ($a$) small weight attached to the very initial region and consequently the condition $\Gamma^2 \approx 0$ at $x=0$ was adequate.

## § 6. Conclusion.

The analysis presented above cannot be regarded as necessarily final in nature, but it is offered in conjunction with the models discussed as a contribution to the study of the behaviour of electron streams.

## § 7. Acknowledgments.

It is a pleasure to thank Mr. R. Kompfner for many stimulating discussions, Dr. Kathleen Sarginson for her help, and Professor M. H. L. Pryce for his interest in the work.

Fig. 4.

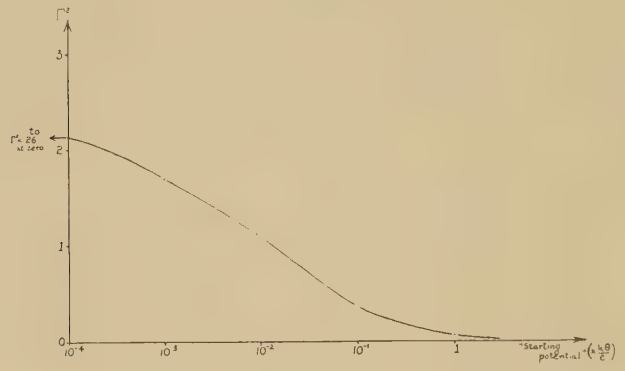


Variation of $\Gamma^2$ with " starting potential ", when $V=Cx^{4/3}$.

## References.

Child, C. D., 1911, *Phys. Rev.*, **32**, 492.
Jahnke, E., and Emde, F., 1933, *Funktiontafeln*, Teubner, Leipzig.
Kompfner, R., 1947, *Jour. Brit. Inst. Rad. Eng.*, **7**, 117.
Kompfner, R., *et al.*, 1946, *Jour. Inst. Elec. Eng.*, **93** (IIIA), 225.
Langmuir, I., 1913, *Phys. Rev.*, **2**, 450.
Langmuir, I., and Compton, K., 1931, *Rev. Mod. Phys.*, **3**, 244.
Lash Miller, W., and Gordon, A. R., 1931, *Jour. Phys. Chem.*, **35**, 2878.
MacDonald, D. K. C., 1949 a, *Phil. Mag.*, (7), **40**, 561 ; 1949 b, Unpublished SERL Memo : " Reduction of signal amplitude due to thermal fluctuation in long electron beams " (October 1949).
North, D. O., 1940, *R.C.A. Review*, **4**, 269, 441.
Pierce, R., 1948, *Bell Syst. Tech. Jour.*, **27**, 159.
Rack, A. J., 1938, *Bell Syst. Tech. Jour.*, **17**, 613.
Robinson, N., and Kompfner, R., 1950, In course of publication.
Schottky, W., and Spenke, S., 1937, *Wiss. Veröff. Siemenswerken*, **16**, 1.
v. d. Ziel, A., 1949, *Proc. Inst. Rad. Eng.*, **37**, 1447 (Letter to Editor).

# LXXX. *Proportional Counters in a Magnetic Field: an Investigation of the Isomerism of $Br^{80}$ and a Measurement of the Fluorescence Yield of Krypton*.*

By D. West and Miss P. Rothwell,
Atomic Energy Research Establishment, Harwell †.

[Received May 17, 1950].

Summary.

The proportional counter technique for measuring the energy of soft electrons has been extended to include higher energy radiations by placing the counter in a strong magnetic field. Suitable X-ray calibration sources consisting of long lived K-capture bodies which give lines at energies up to 50 keV. have been developed.

In an application of the technique to a study of the isomerism of $Br^{80}$, the conversion coefficient of the 37 keV. gamma ray was found to be 1·2, which is close to the calculated value for an electric dipole transition.

In a second application, the fluorescence yield of the K shell of Krypton was measured. The value obtained was 0·67.

## § 1. Introduction

The use of proportional counters for studying the energies of soft radiations has been described recently in a series of papers by Kirkwoood, Pontecorvo and Hanna, and by Curran, Augus and Cockroft. For accurate measurements the great majority of ionizing particles must spend all their energy in the active volume of the counter; if a particle escapes from the counter before coming to rest, the size of pulse it produces will not correspond to its energy and a distorted energy spectrum will be obtained. The limit to the energy which can be measured with a proportional counter is therefore set by the dimensions of the counter and the pressure of gas inside it. In this paper it will be shown that this limit may be extended to higher energies for any particular counter by placing it in a strong magnetic field with its axis parallel to the field. The escape of particles through the side wall of the counter is reduced, since the track is coiled about an axis parallel to the field direction. By using a strong magnetic field, the diameter of a coiled track (for an electron moving perpendicular to the field) can be made much smaller than the range, as can be seen from Table I. in which electron scattering is neglected.

* Some of the results given here have already been reported briefly (Rothwell and West 1950.)

† Communicated by the Authors.

Of course, particles having a small velocity component perpendicular to the axis will escape through the ends of the counter even when the magnetic field is strong enough to prevent escape from the side walls. The escape from the ends, however, is always much less important than escape through the side walls. The effect of Coulomb scattering along the electron track complicates the situation. As far as escape through the side walls is concerned, the scattering will tend to make the lateral spread of any track somewhat greater than the radius of curvature given in the table and so will reduce the efficacy of the field slightly. Scattering will, however, assist in reducing escape of particles along the axis since it prevents any particles from moving nearly parallel to the field for long and as a result being uninfluenced by the field. Considerable reduction in the number of electrons escaping is therefore to be expected when a magnetic field is applied.

Table I.

| Electron energy | Range in air in N.T.P. | Radius of curvature in magnetic field of 7500 gauss. (for an electron moving perpendicular to the field) |
|---|---|---|
| 50 keV. | 4 cm. | 0.1 cm. |
| 100 keV. | 12 cm. | 0·15 cm. |
| 500 keV. | 140 cm. | 0·39 cm. |

The possiblity that the multiplication properties of a counter might be affected by a strong magnetic field was considered. As discussed below it was found experimentally that the multiplication properties were only slightly affected by the magnetic field, in a way which did not invalidate the technique.

The technique has been tested in conditions where, in absence of the field, the electron escape would prevent energy measurements, Electrons of energies up to 50 keV. have so far been studied with this technique in investigations of the nuclear isomerism of $Br^{80}$ and of the Auger effect in krypton.

## § 2. Description of Apparatus.

The counters used in this work were made of soft glass with an aqua-dag cathode painted on the outside (Maze 1946). The wall thickness was 1 mm., the diameter 5 cm., and the active length was 34 cm. The central wire was tungsten 0·005 in., in diameter. This type of counter was used in preference to the conventional metal walled counter to reduce the chance of active gas being adsorbed on the walls. Each counter was fitted with a glass tap and a ground glass joint by means of which it could readily be

connected to a filling apparatus for evacuation and refilling. Pulses were taken off the wire and fed through a head amplifier and a linear amplifier to a four channel electronic pulse analyser. (Cooke-Yarborough, Bradwell, Florida and Howells 1950.) The counter was placed in the horizontal gap of a large electromagnet. The pulses from the counter were fed through a long cable to the head amplifier which, with the rest of the electronic equipment, was removed as far as possible from the influence of stray magnetic fields. Several types of counter fillings were tried. To test their relative merits, a small quantity of $A^{37}$ was admitted to the counter at each filling and the pulse distribution from it was measured. The width of the peak in the distribution is very sensitive to the presence of impurities. The percentage half width at half height of the $A^{37}$ K capture peak was found to be 10·5 per cent by Hanna, Kirkwood and Pontecorvo. With argon and methane fillings, measured values of the half width were usually as high as 13–14 per cent, because the commercial methane used contained a considerable amount of impurities. Since methane cannot be purified very easily, carbon dioxide was tried instead. With argon and carbon dioxide fillings, values of the half width were reduced to 12–13 per cent; the carbon dioxide was purified by freezing, and pumping off any residual gas, repeating the process several times. When, in addition, the argon was purified by allowing it to circulate over heated calcium for several hours the half widths were reduced further in value to between 10·5 per cent, and 11·5 per cent. The best mixture was found to be about 10 parts of argon to 1 part of carbon dioxide; too great a quantity of carbon dioxide gives a greater half width, too small a quantity causes instability of the multiplication factor.

## § 3. Effect of Magnetic Field on the Counter Multiplication Properties.

It was thought that the influence of the magnetic field on the motion of the avalanche electrons and the electrons produced by the ionizing particle might affect the multiplication properties of the counter, so the following experiment was performed in order to test this point. A small quantity of $A^{37}$ was admitted into a counter, of 2 cm. diameter and 22 cm. active length, which was filled with a mixture of argon (21·8 cm. pressure) and methane (7·6 cm. pressure). The pulse distribution due to electrons emitted following the K capture process in $A^{37}$ has a peak at an energy of 2·8 keV. The range of these electrons is very small, so that virtually none escape from the counter. Any change in the pulse distribution when the counter is placed in a magnetic field must therefore indicate that the multiplication properties of the counter have been affected in some way. Fig. 1 shows the pulse size distributions measured with the counter axis parallel and perpendicular to a magnetic field of 7500 gauss and without the field. The points all lie on the same curve indicating that in this case the magnetic field does not influence the counter properties. Later in the work the experiment was repeated with a counter having a larger

diameter, and in this case a slight reduction in pulse size was observed in the presence of the field. Fig. 2 shows the distributions obtained with this counter which had a diameter of 5 cm. and an active length of 34 cm. It was filled with a mixture of argon (24·4 cm. pressure) and carbon dioxide (2·4 cm. pressure). The effect of the magnetic field is quite small and since the shape of the distribution is unaltered it is unimportant for many applications of the technique.

Fig. 1.

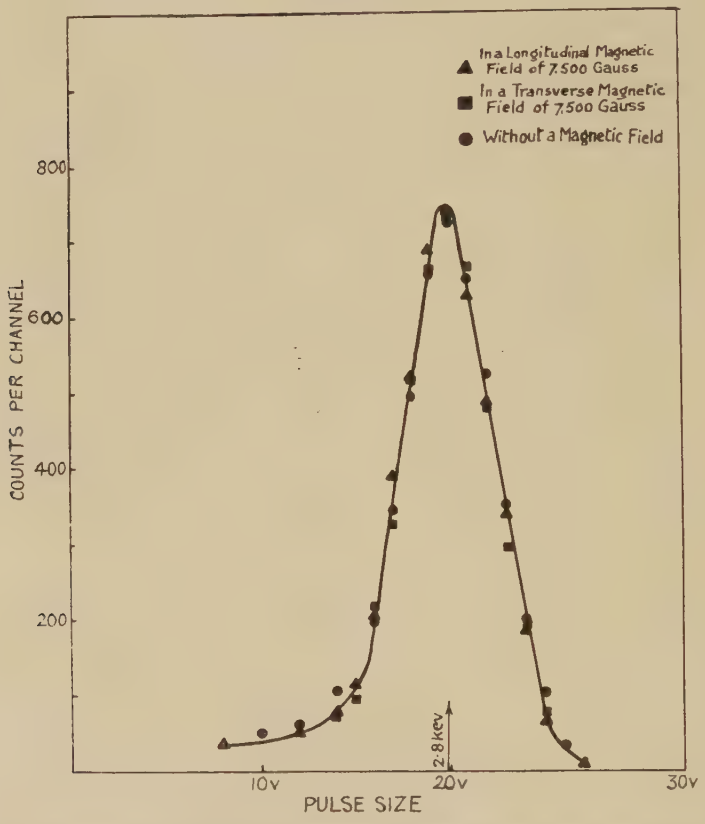


Effect of a magnetic field (7,500 gauss) on the pulse size distribution from $A^{37}$ in the 2cm. diameter counter.

## § 4. Energy Calibration of the Counters.

Some means of calibrating the counters had to be devised before any measurements could be carried out. The usual method employs characteristic X-rays for this purpose. Since it is inconvenient to use an X-ray machine near a large magnet, long-lived radioactive isotopes which decay by K electron capture may be used as an alternative source of X-rays. $A^{37}$ (2·8 keV.) has been used by Pontecorvo, Kirkwood and Hanna, and $Fe^{55}$ (5·9 keV.) by Maeder but X-ray lines of higher energies than these are needed.

K-capture isotopes which can be prepared by thermal neutron irradiation, relatively free from long period $\beta$ activities, were used. Specific activities of a few milli-curies per gm. gave adequate intensity. Table II. lists the K-capture activities which were obtained by irradiation in the Harwell pile.

Fig. 2.

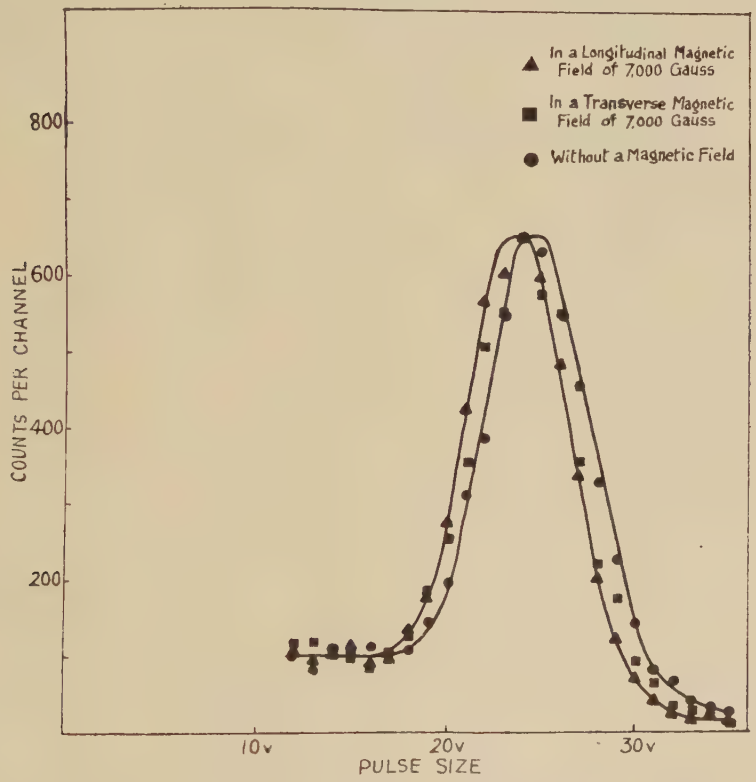


Effect of a magnetic field (7,000 gauss) on the pulse size distribution from $A^{37}$ in the 5cm. diameter counter.

TABLE II.

| Isotope | Half period (days) | Energy of K$\alpha$ X-ray (keV.) |
|---|---|---|
| $Cr^{51}$ | 26·5 | 5·0 |
| $Zn^{65}$ | 250 | 8·1 |
| $Se^{75}$ | 127 | 10·5 |
| $Pd^{103}$ | 17 | 20·2 |
| $Sn^{113}$ | 105 | 24·1 |
| $Gd^{153}$ | 155 | 41·6 |
| $Yb^{169}$ | 33 | 50·8 |

With the lower energy X-rays from Cr, Zn and Se, it was essential to use thin sources and to provide a thin window in the counter wall to admit the radiation. With thick sources, the X-rays emerge only from a thin surface layer and are masked by gamma rays accompanying the K-capture, process, which can emerge from the body of the source. Thin sources were prepared by dissolving the irradiated element in acid and then evaporating a few drops of the solution on a mica foil. The sources were tested with a counter filled to a pressure of about 30 cm. of mercury with argon and carbon dioxide.

Fig. 3.

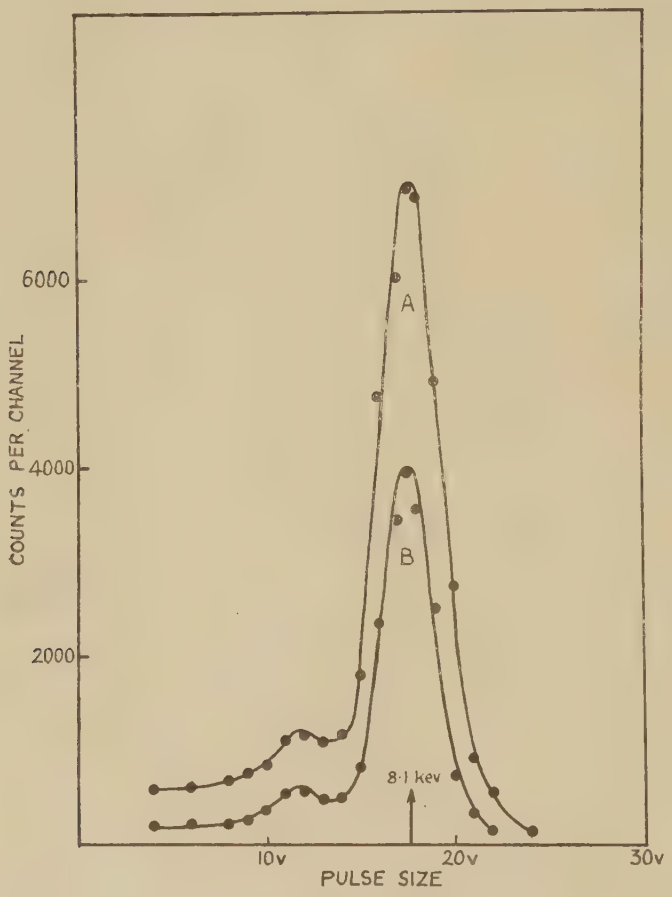


Pulse size distribution from $Zn^{65}$ source.
Curve A: without critical absorber.
Curve B: with critical absorber (·0005″ Ni).

Fig. 3 curve A shows the pulse size distribution obtained with a $Zn^{65}$ source (8·1 keV.). Curve B shows the distribution when a critical absorber (0·0005 in., nickel) which removes the K$\beta$ radiation is placed between the

source and the counter window. The K$\beta$ radiation has an energy of 8·9 keV. and an initial intensity of about one eighth that of the K$\alpha$ radiation. As expected the K$\alpha$ and K$\beta$ radiations are not resolved in curve A and the effect of the critical absorber is merely to reduce the width of the distribution slightly. The small peak on the low energy side of the main peak is due to the escape of the K radiation of argon (2·9 keV.) from the counter following the photoelectric absorption of the incident X-rays in the K shell of argon. Similar distributions having well defined peaks are obtained from the $Cr^{51}$ and $Se^{75}$ sources.

Fig. 4.

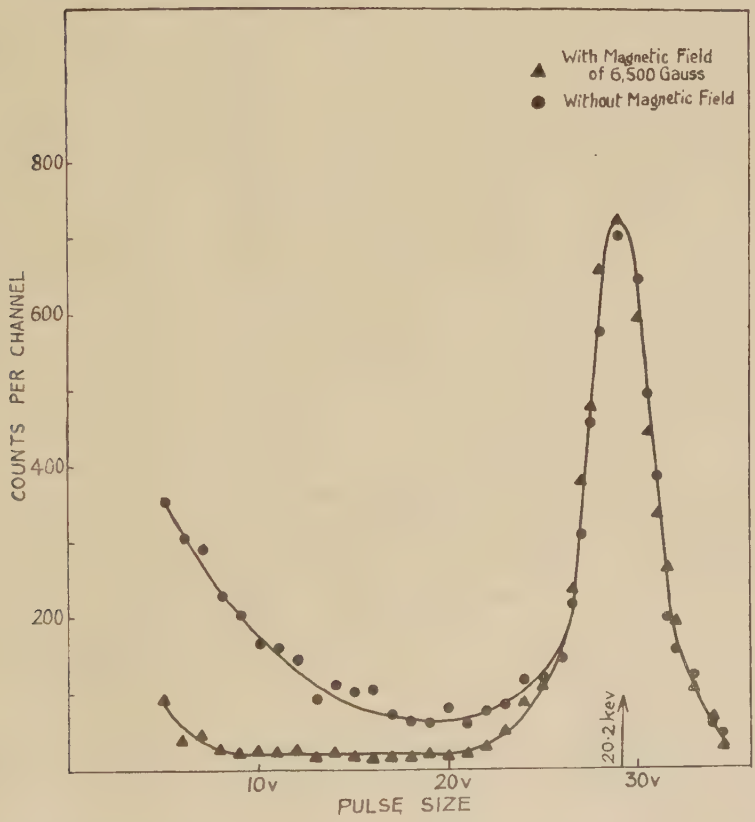


Pulse size distribution from $Pd^{103}$ source with, and without, a magnetic field (6,500 gauss).

With the higher energy X-rays from $Pd^{103}$, $Sn^{113}$, $Gd^{153}$ and $Yb^{169}$, it is not necessary to use very thin sources and the radiations are sufficiently hard to penetrate the glass wall of the counter (1 mm. thickness) without suffering too much attenuation.

Background radiations, consisting of $\beta$ rays or electrons emitted by the source, or electrons generated in the walls by quanta, give rise to a continuous distribution of pulse sizes; these are greatly reduced by a magnetic field. An electron which originates in the cylindrical wall is rapidly bent back into the wall by the field and spends only a very small amount of energy in the counter. Fig. 4 shows the distribution from a $Pd^{103}$ source (20·2 keV.) with and without a magnetic field and demonstrates

Fig. 5.

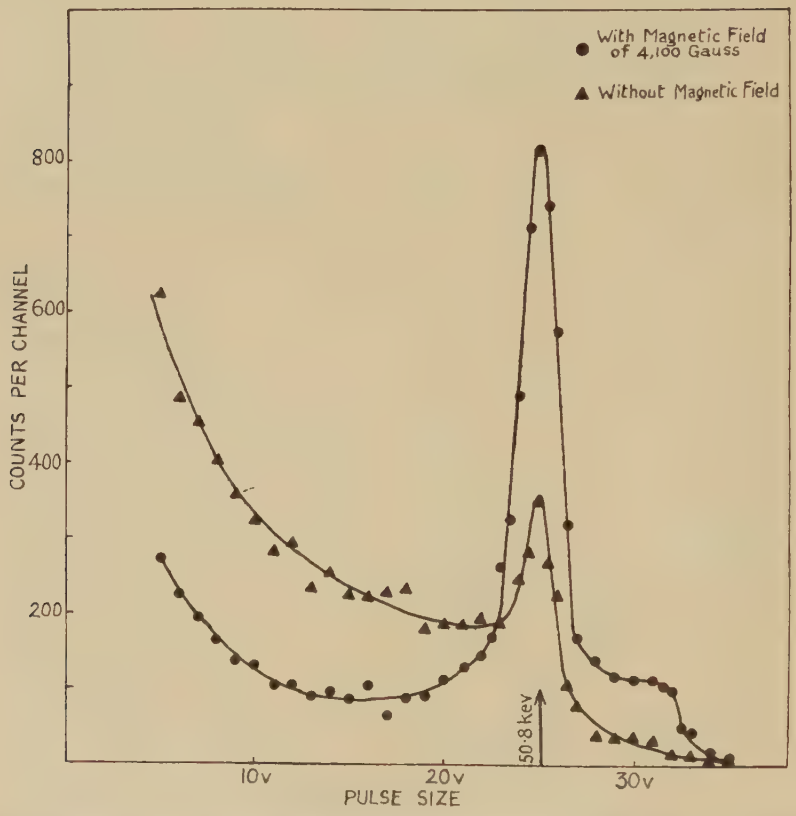


Pulse size distribution from $Yb^{169}$ source with, and without, a magnetic field (4,100 gauss).

this effect very clearly. A similar distribution is obtained from a $Sn^{113}$ source. With the $Gd^{153}$ and $Yb^{169}$ sources, the photoelectrons generated by the X-rays are of sufficiently high energy for a significant fraction of them to escape from the counter at the pressure used. Fig. 5 shows the pulse distribution obtained from a $Yb^{169}$ source (50·8 keV.) with and without a magnetic field. It can be seen that the magnetic field greatly increases the intensity in the peak, as well as decreasing the background intensity.

## §5. Isomerism of $Br^{80}$.

An investigation has been made of the well known case of isomerism in $Br^{80}$, by admitting a small quantity of carrier free methyl-bromide into a counter and measuring the pulse distribution from it. It is known that the 4·4 hr. isomer of $Br^{80}$ decays into the lower state, an 18 min. $\beta$ active body, with the emission of a 49 keV. $\gamma$-ray and a 37 keV. $\gamma$-ray in cascade (Grinberg and Roussinow 1940, Berthelot 1944). The 49 keV. $\gamma$-ray is totally internally converted, but there is still some doubt about the value of the conversion coefficient of the 37 keV. $\gamma$-ray and the type of transition. Berthelot has obtained a value of 0·64 for this conversion coefficient, by coincidence absorption measurements, and concludes that the transition is magnetic dipole. Segrè and Helmholtz (1949) suggest from parity considerations that it is more likely to be electric dipole, in which case the internal conversion coefficient should have a value different from that found by Berthelot.

The method used for producing the active methyl bromide was suggested by Dr. Glueckauf (Glueckauf, Jacobi and Kitt, 1949). A solution of potassium bromide in acetic acid was irradiated for a short period in the Harwell pile. Argon was bubbled through the solution, carrying active methyl bromide, generated during the irradiation, with it. The argon was then passed through a solution of caustic potash and then over phosphorus pentoxide to remove free bromine and water vapour. It then passed into a container cooled by liquid oxygen, where the methyl bromide was frozen down while the argon passed through. The container, still cooled by the liquid oxygen was transferred to the counter filling system and pumped free from air and other gases. The liquid oxygen was then removed and the methyl bromide allowed to evaporate into the counter.

Curves A and B in fig. 6 show the pulse size distribution from the active methyl bromide in an argon filled counter (containing about 30 cm. pressure of argon and carbon dioxide), with and without a magnetic field of 7000 gauss. This demonstrates very clearly the effect the magnetic field has in reducing electron escape.

The five peaks in the distribution arise in the following way. the 49 keV. gamma ray is totally internally converted, but the 37 gamma ray only partially, there are peaks in the distribution at $(37+49)=86$ keV., when both gamma rays are internally converted, and at 49 keV., when the 37 keV. gamma ray is unconverted and escapes from the counter. The chance of a 37 keV. $\gamma$-ray being absorbed in the counter is very small and can be neglected in our counter for pressures of argon less than 1 atmosphere. Both the peaks are modified by the escape from the counter of a 12 keV. Bromine K X-ray which is emitted in some cases during the filling of the vacancy created in the K shell of Bromine when a gamma ray is internally converted. Additional peaks will therefore be produced at $(49-12)=37$ keV. and at $(49-12+37)=(49+37-12)=74$ keV. when one Bromine K X-ray escapes, and at $(49-12+37-12)$ when two Bromine K X-rays escape. Peaks are therefore expected at 37, 49, 62,

74 and 86 keV. The counter was calibrated with 20·2 keV. X-rays from a $Pd^{103}$ source, the position of the calibration peak is indicated in fig. 6 and it can be seen that the five peaks occur at about the expected energies. Fig. 7 shows the pulse size distribution from the active methyl bromide in the same counter filled with krypton at a pressure of 66·5 cm. and carbon dioxide (4 cm.). The escape probability of the bromine K X-ray is 99 per cent in the argon counter, but only 45 per cent in the krypton counter; it

Fig. 6.

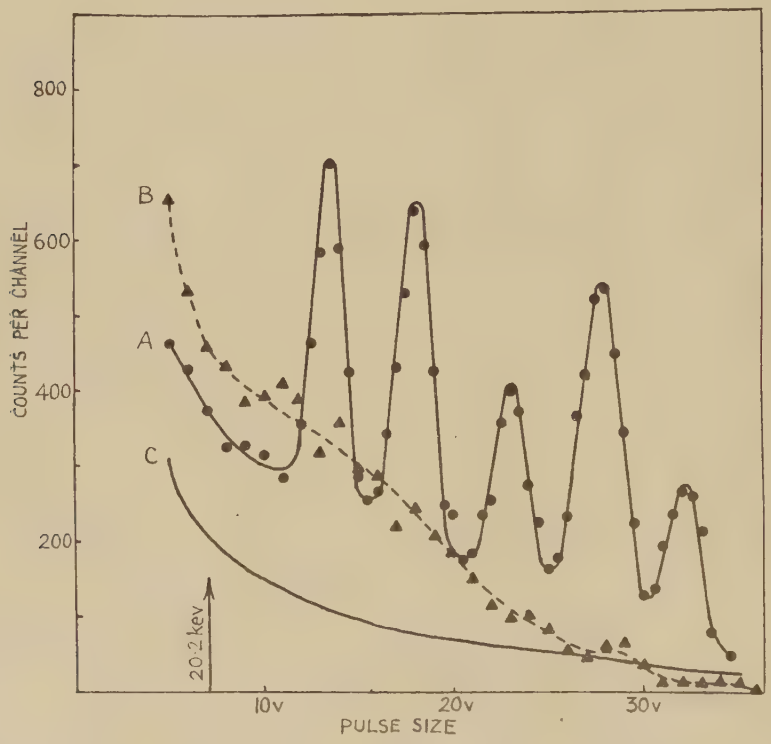


Pulse size distribution from $Br^{80}$ in an argon filled counter.
Curve A: with counter in a magnetic field of 7,000 gauss.
Curve B: without magnetic field.
Curve C: background from $Br^{82}$ (corrected for decay) with counter in a magnetic field of 7,000 gauss.

can be seen that the relative intensities of all the "K escapes" peaks have been reduced in the distribution obtained with krypton. Conversion coefficients can be calculated from these curves. The 49 keV. $\gamma$-ray is totally converted, which is verified by the absence of a peak at (37−12)=25 keV., so the conversion coefficient of the 37 keV. $\gamma$-ray is given by

$$\alpha_{37}=\frac{\text{no. of converted 37 keV. } \gamma\text{-rays}}{\text{no. of unconverted 37 keV. } \gamma\text{-rays}}=\frac{I_{62}+I_{74}+I_{86}}{I_{49}+I_{37}},$$

where $I_{62}$ represents intensity in the 62 keV. (peak), etc.

Table III. gives values of the conversion coefficient obtained in this way for various runs with several different counter fillings and bromine samples. In the case of the measurement with krypton a correction must be applied for reabsorption in the counter of the 37 keV. $\gamma$-ray. The probability of escape is calculated to be 0·92 for a 37 keV. $\gamma$-ray in the krypton filled counter.

TABLE III.

| Counter filling | Conversion coefficient |
|---|---|
| $A+CO_2$ | 1·3 |
| $A+CO_2$ | 1·1 |
| $A+CO_2$ | 1·2 |
| $A+CO_2$ | 1·4 |
| $Kr+CO_2$ | 1·2 |
| | av. 1·2 |

Fig. 7.

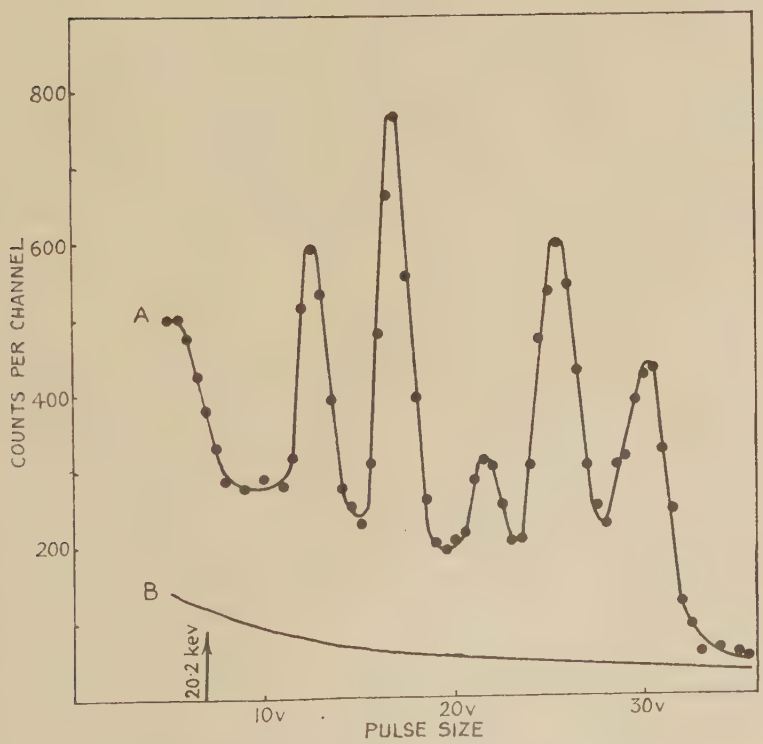


Pulse size distribution from $Br^{80}$ in a krypton filled counter.
Curve A: distribution in a magnetic field of 7000 gauss.
Curve B: background distribution from $Br^{82}$ (corrected for decay) in a magnetic field of 7000 gauss.

The main error in these determinations arises from the background, composed partly of 34 hour $Br^{82}$, which can be measured when the 4·4 hour activity has decayed, and partly of 18 min. $Br^{80}$ in equilibrium with

the 4·4 hour $Br^{80}$ activity, which cannot be separated from it. Curve C, fig. 6, represents the 34 hour background, corrected for decay. The conversion coefficients were evaluated

(1) taking a curve close to C as the true background;

(2) taking a curve drawn close to the troughs between the peaks as the background.

There is a difference of about 14 per cent between these two extreme values of the measured conversion coefficient, and it is the mean which has been tabulated in each case in Table III.

The value of the conversion coefficient calculated for (*a*) a magnetic dipole transition, (*b*) an electric dipole transition, is 0·60 and 1·55 respectively. (Hebb and Nelson 1940). Our value of 1·2 for the conversion coefficient proves that the transition is electric dipole rather than magnetic dipole. This conclusion is in contradiction with the results of Berthelot but agrees with a result of Lidofsky, Macklin and Wu (1950) which has just been briefly reported.

## § 6. Fluorescence Yield of Krypton.

There are two different ways in which a vacancy in an inner shell of the electron structure of an atom may be filled; either a characteristic X-ray is emitted when an electron falls in from a higher level or the corresponding energy is shared between several electrons (Auger electrons), ejected from higher electronic levels. The fluorescence yield is defined for a vacancy in a particular shell of the atom in the following way.

$$\text{Fluorescent yield} = W_{K,(LM,\ldots.)} = \frac{\text{No. of K, (L,M . . . .) X-ray photons emitted}}{\text{No. of vacancies in K, (L,M . . . .) shell.}}.$$

Fluorescence yields were first measured by Auger in 1926. He investigated gaseous materials in a cloud chamber using X-rays to excite the atoms. When the incident X-ray is absorbed in the K shell a photoelectron of energy $E_0 - E_K$ (where $E_0$ = energy of incident X-rays and $E_K$ = binding energy of the K shell of the absorbing atom) is observed. It is accompanied in $W_K$ cases, *i.e.* when a K X-ray is emitted, only by several low energy Auger electrons from vacancies in the L,M . . . . shells. (The fluorescence yield is much smaller for the L,M . . . . shells than for the K shell so that the probability of emission of one or more Auger electrons during the cascade process of filling a vacancy in the L,M . . . . shells is very high). In the remaining $(1-W_K)$ cases a moderately energetic electron of energy $X_K - E_{L,M} \ldots .$ ($X_K$ = energy of K radiation, $E_{L,M} \ldots .$ = binding energy of L.M . . . . shells) is observed as well. The fluorescence yield was obtained from the ratio of the number of events of each type.

A method for measuring fluorescence yields of solid materials was devised by Compton (1929). An ionization chamber is used to measure the number of X-rays (whose energy must be greater than the K binding

energy of the element being examined) absorbed in a block of the material; the intensity of the fluorescent X-rays excited in the material is measured at the same time. After correcting for absorption of the incident X-rays in the L,M . . . . shells the fluorescence yield is obtained directly.

The proportional counter, as pointed out by Kirkwood, Pontecorvo and Hanna, provides an alternative method of measuring the fluorescence yields of gases. When an X-ray is absorbed by the K shell of the counter gas, and the vacancy caused by the emission of the photo-electron is filled with emission of Auger electrons, the full energy of the incident X-rays is spent in the counter. When the vacancy is filled with emission of a K X-ray, however, there is a good chance that this X-ray will escape from the counter, provided the pressure in the counter is low. In this case an energy $E_0 - X_K$ (where $E_0$ is the energy of the incident X-rays and $X_K$ is the energy of the *K radiation*) is spent in the counter. Thus, two peaks are observed in the pulse size distribution and the fluorescence yield can be determined from their relative intensities.

Fig. 8 shows a typical pulse size distribution obtained by irradiating a counter containing krypton and carbon dioxide (16 parts krypton: 1 part carbon dioxide) with characteristic X-rays (24·2 keV.) from a $Sn^{113}$ K capture source. A magnetic field was applied to reduce the escape of photo-electrons from the counter and to reduce background radiations from the source. The energy of the $K_\alpha$ X-ray of krypton is 12·7 keV. so when this radiation escapes a peak is obtained at $24{\cdot}2 - 12{\cdot}7 = 11{\cdot}5$ keV. An unresolved peak due to the escape of the $K_\beta$ radiation of Kr (14·1 keV.) is also apparent. The $K_\beta$ radiation from the source was removed by a critical absorber (0·005 silver) placed between the source and the counter.

Two corrections must be applied in order to evaluate the fluorescence yield, $W_K$, from the relative intensity of these two peaks. First, the intensity of the "escape" peak is reduced by reabsorption of the K X-rays of krypton in the counter gas. The probability of reabso ption was computed from the known absorption coefficients using unpublished calculations of B. Pontecorvo. This correction can be made small by using low pressures of gas and did not exceed 5 per cent in any of the measurements. A second correction was necessary to take account of the incident radiation absorbed in the L,M . . . . shells. Since the total energy of the incident X-ray is then spent in the counter, this process cannot be distinguished from K absorption without subsequent emission of a K X-ray. The ratio of the absorption in the K shell to that in the L,M . . . . shells is known at the K absorption edge for any element and it is assumed that the ratio is the same for energies not much greater than the K binding energy. The ratio for Kr was taken to be 6·4. This value had to be calculated from an empirical formula due to Jönsson (see Compton and Allison) since there are very few measurements of the X-ray absorption coefficient of krypton reported in the literature. It follows, therefore, that absorption in the L,M . . . . shells constitutes a fraction 1/7·4 of the total absorption in krypton. A similar correction had to be applied in the technique

used with solid materials mentioned above. The possiblity of an error due to escape of energetic photo-electrons from the counter was checked by measurements taken with magnetic fields of 3000, 4600, and 5900 gauss with a $Sn^{113}$ source. The relative intensities of the escape peak were 0·55, 0·56 and 0·56 respectively, which shows that the escape is small.

Fig. 8.

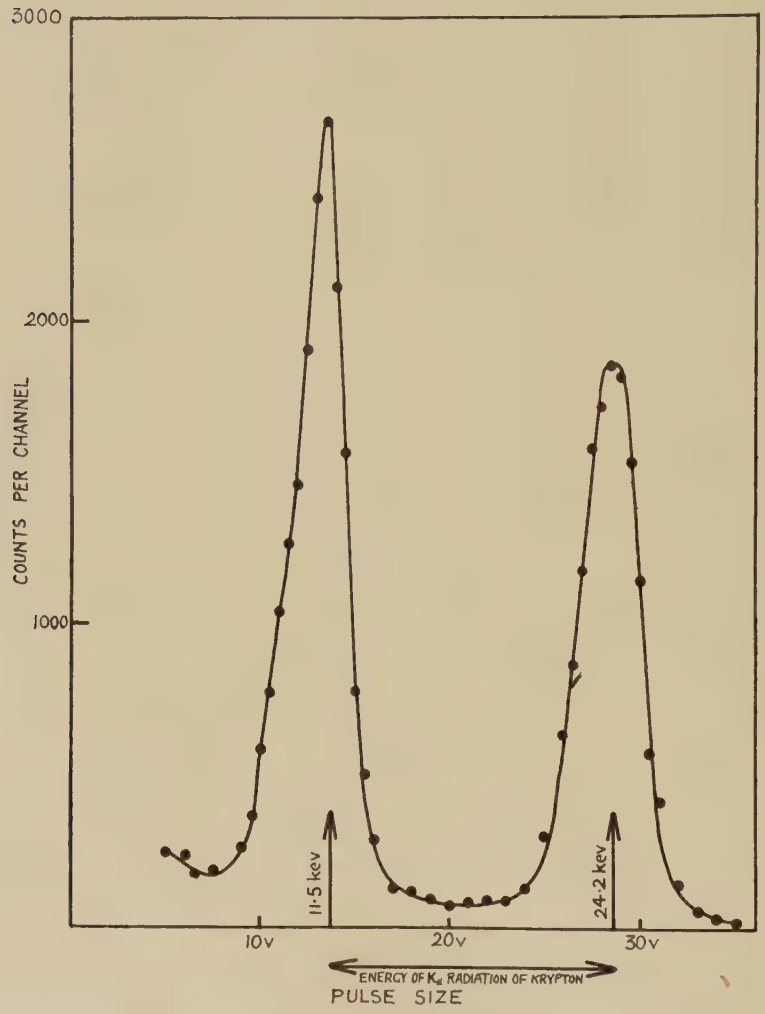


Pulse size distribution from $Sn^{113}$ source (24·2 keV) in a krypton filled counter (magnetic field 4300 gauss).

Absorption of X-rays in the $CO_2$ was neglected since it is very small compared with that in krypton.

The areas under the " escape " and " normal " peaks were measured by planimeter from graphs of the pulse size distribution. The total

number of counts recorded in each peak exceeded 6000 counts in every case. The results obtained with different pressures and using $Pd^{103}$ (20·2 keV.) and $Sn^{113}$ (24·2 keV.) sources are given in Table IV.

The mean value of the fluorescence yield from these results is 0·67. The probable error of the average is only 0·005, but the systematic error, which is mostly due to the L absorption correction, is certainly larger than this.

Values given in the literature for the fluorescence yield of krypton are 0·51 (Auger 1926) and 0·615 (Harms 1927). Locher (1932) gives a value of 0·585 obtained by interpolation from data for neighbouring elements. The value obtained by the proportional counter technique is therefore considerably higher than that obtained by previous measurements.

Table IV.

| Energy of incident X-rays (keV.) | Magnetic field (Gauss) | Pressure of krypton (cm. of mercury) | Fraction of pulses in "escape" peak | Fraction of pulses in "escape" peak | | Mean fluorescence yield |
|---|---|---|---|---|---|---|
| | | | | Corrected for re-absorption of K radiation | And corrected for L,M..... absorption | |
| 24·2 | 3,800 | 5·4 | 0·59 | 0·60 | 0·70 | |
| 24·2 | 3,000 | 7·4 | 0·55 | 0·56 | 0·65 | |
| 24·2 | 4,600 | 7·4 | 0·56 | 0·57 | 0·66 | 0·66 |
| 24·2 | 5,900 | 7·4 | 0·56 | 0·57 | 0·66 | |
| 24·2 | 4,400 | 13·8 | 0·52 | 0·55 | 0·63 | |
| 20·2 | 3,800 | 2·9 | 0·59 | 0·60 | 0·69 | |
| 20·2 | 7,100 | 2·9 | 0·60 | 0·60 | 0·70 | |
| 20·2 | 3,800 | 5·4 | 0·57 | 0·59 | 0·68 | 0·68 |
| 20·2 | 3,800 | 7·4 | 0·57 | 0·59 | 0·68 | |
| 20·2 | 4,400 | 13·8 | 0·55 | 0·58 | 0·67 | |

A measurement of the fluorescences yield of xenon was also attempted, but in this case the accuracy is greatly limited by background radiations from the K capture source used. Fig. 9 shows the distribution from a $Yb^{169}$ source (50·8 keV.) in a xenon filled counter. The main "escape" peak is at 50·8—29·7=21·1 keV. (since the energy of the $K_\alpha$ ray of xenon is 29·7 keV.), and is much more intense than the full energy peak. The subsidiary peak at 16·4 keV. is due to escape of the $K_\beta$ radiation of xenon (34·4 keV.). This was shown to be resolved when the escape peak was investigated in greater detail than in fig. 9. The $K_\beta$ radiation from the source, of energy 57·7 keV. cannot be distinguished in the main peak, but is easily seen in the "escape" peak, at 57·7—29·7=28·0 keV. This suggests that escape peaks may be useful in investigating radiations.

whose total energies are too close to be resolved directly. The remaining peak probably arises from some impurities in the Yb. The value of the fluorescence yield of xenon obtained was 0·81. In view of the background and the fact that only a single measurement was taken, the accuracy is much smaller than in the case of krypton.

Fig. 9.

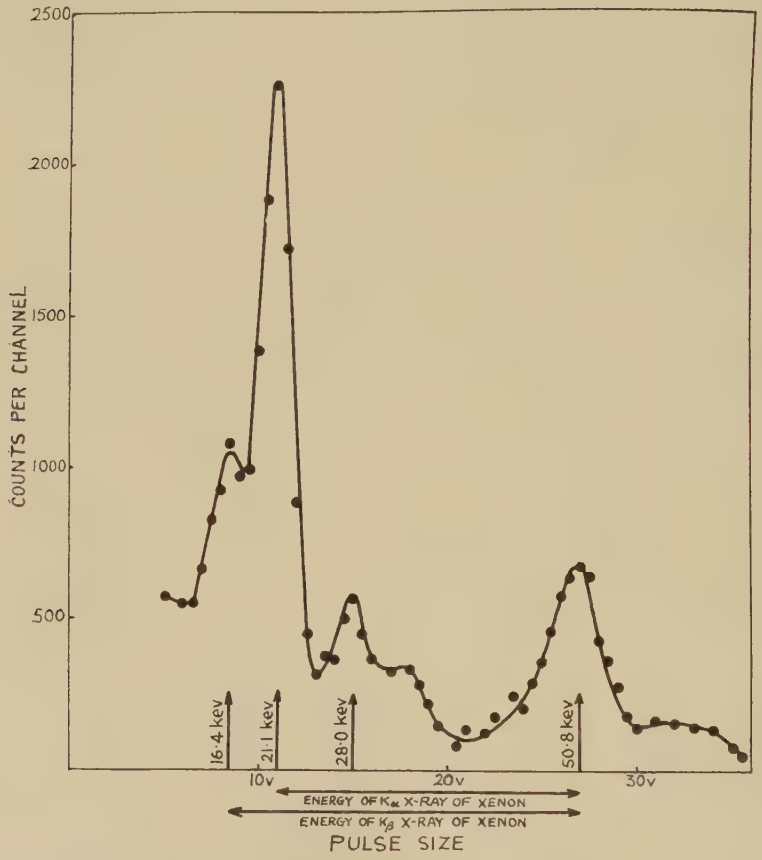


Pulse size distribution from $Yb^{169}$ (50·8 keV) in a xenon filled counter (magnetic field 7,000 gauss).

Acknowledgments.

We are grateful to Dr. B. Pontecorvo for his valuable advice and help in this work, and to Drs. W. D. Allen and R. H. V. M. Dawton who kindly allowed us to use a large electromagnet. Thanks are also due to Mr. F. Bradley for his assistance on many occasions.

The work was done in the Nuclear Physics Division at Harwell and acknowledgment is made to the Director, A. E. R. E., Harwell, for permission to publish these results.

## References


Angus, J., Cockroft, A. L., and Curran, S.C., 1949, *Phil. Mag.*, **40**, 522.

Auger, P., 1926, *Ann. Phys., Paris*, **6**, 183.

Berthelot, A., 1944, *Ann. Phys., Paris*, **19**, 219.

Compton, A. H., 1929, *Phil. Mag.*, **8**, 961.

Compton, A. H., and Allison, S.K., 1935, *X-rays in Theory and Experiment* (New York: D. Van Nostrand Co., Inc.).

Cooke-Yarborough, E. H., Bradwell, J., Florida, C. D., and Howells, G. A., 1950, *Proc. Instn. Elect. Engrs.*, **97**, 108.

Curran, S. C., Angus, J., and Cockroft, A. L., 1948, *Nature, Lond.*, **162**, 302; 1949, *Phil. Mag.* **40**, 36, 53, 305, 929.

Glueckauf, E., Jacobi, R. B., Kitt, G. P., 1949, J. *Chem. Soc.*, S.330.

Grinberg, A. P., and Roussinow, L. I., 1940, *Phys. Rev.*, **58**, 181.

Harms, M. I., 1927, *Ann. d. Physik*, **82**, 87.

Hanna, G. C., Kirkwood, D. H. W., and Pontecorvo, B., 1949, *Phys. Rev.*, **75**, 985.

Hanna, G. C., Pontecorvo, B., 1949, *Phys. Rev.*, **75**, 983.

Hebb, M. H., and Nelson, E., 1940, *Phys. Rev.*, **58**, 486.

Kirkwood, D. H. W., Pontecorvo, B., Hanna, G. C., 1948, *Phys. Rev.*, **74**, 497.

Lidofsky, L., Macklin, P., and Wu, C. S., 1950, *Bull. Am. Phys. Soc.*, **25**, 10.

Locher, G. L., 1932, *Phys. Rev.*, **40**, 484.

Maeder, D., Private communciation.

Maze, R., 1946, *J. Phys. Radium*, **6**, 164.

Pontecorvo, B., Kirkwood, D. H. W., Hanna, G. C., 1949, *Phys. Rev.*, **75**, 982.

Rothwell, P., and West, D., 1950, *Proc. Phys. Soc. A*, **63**, 539, 541.

Segrè, E., and Helmholz, A. C., 1949, *Rev. Mod. Phys.*, **21**, 271.

# LXXXI. *The Eddy Viscosity in Turbulent Shear Flow.*

By A. A. Townsend,
Emmanuel College, Cambridge *.

[Received May 26, 1950].

Summary.

The comparative slowness of those processes in the turbulent wake which determine the turbulent energy balance makes it necessary to consider the whole wake flow in attempts to derive local values of such quantities as turbulent intensity and eddy viscosity. If the wake is in a state of moving equilibrium, *i. e.* the development involves processes controlling the intensity and eddy viscosity to values appropriate to the particular stage of development, then the controlling mechanism must be of large scale both in space and time. It is suggested that the large slow eddies responsible for the phenomenon of intermittently turbulent flow form this mechanism, and a plausible control sequence is outlined in which the intensity of the large eddies controls the level of eddy viscosity. The detailed structure of these large eddies has been investigated by measuring the spectrum functions of the velocity fluctuation components in the wake of a circular cylinder. The group of large eddies is distinct, and it is possible to deduce that the large eddies are randomly placed in the mean stream direction, extend over most of one half of the wake, and have their vorticity roughly in the direction of maximum positive mean rate-of-strain. By a rough calculation it is shown that this type are near the state of energy equilibrium necessary for the operation of the suggested control process. Finally, the generation of Reynolds shear stresses by distortion of quasi-stationary turbulent fields is discussed, and possible reasons for the applicability of the eddy viscosity hypothesis are suggested.

## § 1. Introduction.

Recent work by the author on the structure of the turbulent wake of a cylinder has shown that wake development is due to the existence of a group of large-scale eddies whose function is mainly convective (Townsend 1949 and 1950). That is, they convect fully turbulent fluid from near the wake centre to the outer part of the wake, and simultaneously entrain previously undisturbed fluid bringing it into closer contact with the fully turbulent fluid of the wake core. The appearance of intermittently turbulent flow in the wake is a natural consequence of this process, and is the most striking manifestation of the presence of these eddies which contain only a relatively small fraction of the total turbulent energy. The complete

* Communicated by the Author.

turbulent motion can be regarded as the superposition of a small-scale random motion containing most of the turbulent energy on this large-scale convective motion. Detailed measurements show that the intensity, scale and diffusive properties of the fully turbulent fluid are substantially constant at any section of the wake, irrespective of distance from the wake centre, and this is held to be a natural consequence of the mixing action of the large eddies, which causes the instantaneous properties of a sample of turbulent fluid to depend more on its past history of crossing and recrossing the wake than on its present position. This notion that the properties of the turbulent fluid are not directly controlled by the instantaneous shear is contrary to the usual assumptions of mixing-length theory, which are based on the notion of local and instantaneous equilibrium of the turbulent intensity. If the statistical equilibrium of the wake properties is controlled more by the past history of the wake than by its present state, it is not possible to use this notion to determine the equilibrium turbulent intensity, and this paper describes an alternative approach, based on a consideration of the dynamic equilibrium of the large eddies.

## § 2. Notation for the Cylinder Wake.

The usual notation for turbulent flow with two-dimensional mean motion will be used, that is, the components of the mean velocity along the axes $Ox$, $Oy$, $Oz$ are U, V, 0, and the instantaneous components of the fluid velocity are $\mathrm{U}+u$, $\mathrm{V}+v$, $w$. Fluid density is denoted by $\rho$, kinematic viscosity by $\nu$, and the instantaneous pressure by $\mathrm{P}+p$, where $p$ is the mean pressure. All mean values are taken with respect to time at a point fixed in space.

For the cylinder wake, the coordinate system is such that $Oz$ is along the axis of the cylinder, $Ox$ is parallel to the direction of the mean stream, and $Oy$ is perpendicular both to the direction of the mean stream and to the axis of the cylinder. Then, making the usual "boundary layer" approximations (Goldstein 1938), the exact equations of mean motion reduce to one

$$\mathrm{U}\frac{\partial \mathrm{U}}{\partial x}+\frac{\partial \overline{uv}}{\partial y}=\nu\frac{\partial^2 \mathrm{U}}{\partial y^2}. \qquad \ldots\ldots\ldots \quad (1)$$

If it is assumed that the turbulent shear stress $\overline{uv}$ can be described in terms of a coefficient of eddy viscosity $\epsilon$, defined by

$$\overline{uv}=-\epsilon\frac{\partial \mathrm{U}}{\partial y}$$

then

$$\mathrm{U}\frac{\partial \mathrm{U}}{\partial x}=\frac{\partial}{\partial y}\left[(\nu+\epsilon)\frac{\partial \mathrm{U}}{\partial y}\right]. \qquad \ldots\ldots\ldots \quad (2)$$

Using the same assumptions as in (1), the equation for the balance of turbulent energy is found to be

$$\overline{\mathrm{W}}+\tfrac{1}{2}\mathrm{U}_0\frac{\partial}{\partial x}(\overline{u^2}+\overline{v^2}+\overline{w^2})+\overline{uv}\frac{\partial \mathrm{U}}{\partial y}+\frac{1}{2}\frac{\partial}{\partial y}(\overline{u^2v}+\overline{v^3}+\overline{vw^2})+\frac{1}{\rho}\frac{\partial \overline{pv}}{\partial y}=0, \qquad \ldots \quad (3)$$

where $\overline{W}$ is the mean viscous dissipation

$$\overline{W}=\nu(\overline{u\nabla^2 u}+\overline{v\nabla^2 v}+\overline{w\nabla^2 w}).$$

If the flow is at a sufficiently high Reynolds number to permit the application of the theory of local similarity (Townsend 1948), then

$$\overline{W}=15\nu\overline{\left(\frac{\partial u}{\partial x}\right)^2}, \quad . \quad . \quad . \quad . \quad . \quad . \quad . \quad . \quad . \quad (4)$$

and all the terms in equation (3) can be measured directly except $(1/\rho)(\partial\overline{pv}/\partial y)$, which can be obtained by difference.

§ 3. The Mixing-Length Hypothesis of Local Energy Equilibrium.

The equation for the turbulent energy balance (equation (3)) contains terms representing viscous dissipation, convection of energy by the mean flow, production of turbulent energy by working against the turbulent shear stress, energy transport by diffusive movements, and energy transport by flow down pressure gradients, and states that the energy density is constant in time as a result of a balance between the gains and losses of energy from these processes. By assuming that the turbulence is so small in scale that the equilibrium intensity is determined only by the local parameters of the flow, and further, that the motion is dynamically similar everywhere, it is possible to derive the Prandtl relation between turbulent intensity and rate of shear,

$$v'=\mathrm{K}l_1\left|\frac{\partial \mathrm{U}}{\partial y}\right|. \quad . \quad . \quad . \quad . \quad . \quad . \quad . \quad . \quad . \quad (5)$$

This assumption of small scale implies that the terms representing convection of energy by the mean flow, energy transport by diffusive movements and energy transport by pressure flow are negligible compared with those representing production of energy by shear and loss by viscous dissipation. If this assumption is not made, the energy equation produces no definite results and the simplicity of the attack is lost. Several attempts have been made to allow for the effects of convection and diffusion, but it has been shown experimentally that all the terms in the energy equation are of comparable magnitude, and that it is very unlikely that the mixing-length view of the energy balance is even a good approximation. This is most clearly shown by considering the time necessary for a chance fluctuation in turbulent intensity to disappear. Since the local rate of production of turbulent energy is $-\overline{uv}(\partial \mathrm{U}/\partial y)$ and the local energy density is $\frac{1}{2}(\overline{u^2}+\overline{v^2}+\overline{w^2})$ this time must be of order

$$-\tfrac{1}{2}(\overline{u^2}+\overline{v^2}+\overline{w^2})\Big/\overline{uv}\frac{\partial \mathrm{U}}{\partial y},$$

which experimentally is found to have a minimum value of $1{\cdot}5\,x/\mathrm{U}_0$, *i. e.* more than the time necessary for the free stream to pass from the cylinder to the point of observation (Townsend 1950). This estimate of the "relaxation time" is supported by the experimental observation that the setting

up of dynamical similarity in wake flow is a very slow process, and is not complete even at a distance of 500 diameters downstream from the cylinder.

With the knowledge that diffusive and pressure transport of energy are sufficiently large to change the energy balance by a considerable amount, it can only be concluded that energy equilibrium in the wake is a process involving the whole wake, and that the turbulent intensity in a sample of turbulent fluid is determined more by its past history of crossing and re-crossing the wake than by its present position. This conclusion, while it explains very naturally the observed invariance of the mean properties of the turbulent fluid across any wake section as a consequence of the statistically uniform history of all samples of fully turbulent fluid, makes the problem of computing the actual turbulent intensity from the energy equation almost impossible and a new approach is necessary.

§ 4. The Hypothesis of Moving Equilibrium in Wake Flow.

While the kind of absolute local equilibrium considered in mixing-length theory does not exist in free turbulence, a moving equilibrium may be possible, *i. e.* when the wake is in a steady state, the mean rate of production of turbulent energy over a whole section is controlled by the turbulent intensity in such a way that there is a stable equilibrium intensity for any wake section and that chance fluctuations from this intensity distribution will not persist as the wake develops. Considering the history of a small sample of turbulent fluid, it is possible that, when the turbulent intensity is above normal, increased loss of energy by viscous dissipation may outweigh the consequent rate of conversion of mean flow energy into turbulent energy and so tend to the equilibrium intensity sufficiently far down-stream. This may occur as the result of local changes in structure, similar to those implied in the Prandtl equation, or by overall changes caused by the increased turbulent intensity. The homogeneity of the fully turbulent fluid makes it very unlikely that local changes in structure control the equilibrium, but the group of large eddies could form a very effective large-scale controlling mechanism in spite of their comparatively small energy. These large eddies, conveying turbulent fluid from the wake centre into close contact with non-turbulent fluid from outside the wake, are primarily responsible for the lateral spreading of the wake and consequently control the rate of conversion of mean flow energy into turbulent energy. Taking the extreme examples, if they were to stop completely wake development would almost cease and the overall rate of conversion of mean flow energy to turbulent energy would become very small, while a large increase in their intensity would accelerate wake spread and increase the rate of turbulent energy production. This is easily shown by writing down the kinetic energy of the mean flow

$$\int_{-\infty}^{\infty} \tfrac{1}{2}\rho(U_0-U)^2\,dy = \tfrac{1}{2}\rho U_0^2 \frac{d^2}{l},$$

since

$$\int_{-\infty}^{\infty} \rho U_0(U_0-U)\,dy = \tfrac{1}{2}\rho U_0^2 d C_d,$$

where $l$ is a parameter representing the wake width, $d$ is the cylinder diameter, $C_d$ is the drag coefficient of the cylinder.

Then the total rate of production of turbulent energy over the whole wake section is

$$-\mathrm{U}_0 \frac{\partial}{\partial x} \int_{-\infty}^{\infty} \tfrac{1}{2}\rho(\mathrm{U}_0-\mathrm{U})^2 dy = \tfrac{1}{2}\rho \mathrm{U}_0^3 \frac{d^2}{l^2}\frac{dl}{dx},$$

proportional to the rate of increase of wake width.

## § 5. Energy Balance of The Large Eddies.

If the large eddies control the rate of production of turbulent energy, it follows that their equilibrium intensity is itself controlled, and it is simpler to consider the factors in this control process than the factors controlling the intensity of the fully turbulent fluid. It is clear that the large eddies must obtain energy directly from the mean flow, and it seems likely that the loss of energy by friction of such a large scale motion may be described by the same coefficient of eddy viscosity as is effective for the mean flow. Then the control process should lead to a balance in which the large eddies are maintained in a condition of neutral equilbrium, the viscous dissipation only exceeding the energy gain from the mean flow by a sufficient amount to keep the wake in a condition of similarity. Any increase in the intensity of the large eddies leads to a too rapid spread of the wake, to increased production of turbulent energy, and finally to an increased eddy viscosity which decreases the intensity. If this is true, then for any particular mean velocity profile, the equilibrium condition will be of the form

$$\frac{u_1 l_1}{\epsilon} = \mathrm{R}_c',$$

where $\mathrm{R}_c'$ is a pure number, characteristic of the shape of the mean velocity profile, $u_1$, $l_1$ are the velocity and length scales at the particular wake section.

Applying the momentum condition for the cylinder wake, this becomes

$$\frac{\mathrm{U}_0 d}{\epsilon} = \mathrm{R}_c.$$

This implies that the mean motion in a turbulent wake is always taking place at the effective Reynolds number $\mathrm{R}_c$, whatever the cylinder Reynolds number, $\mathrm{R}_d = \mathrm{U}_0 d/\nu$, may be, which is one way of regarding the observed invariance with cylinder Reynolds number of the properties of the mean flow.

Experience with the laminar instability of a boundary layer suggests that the instability represented by the large eddies might be two-dimensional and periodic in space, but the experiments described below show that the large eddies are certainly three-dimensional and aperiodic. The implications of this superficially surprising results will be considered later.

## § 6. Experimental Arrangements.

The measurements were all made in the wake of a circular cylinder of diameter 0·159 cm. placed in an air-stream of velocity 1280 cm. sec.$^{-1}$ and usually at a position 500 cylinder diameters downstream. The air-stream was produced in the small wind-tunnel in the Cavendish Laboratory, of section 38 cm. $\times$ 38 cm.. At the position of observation, the wake flow is very nearly in a state of similarity, and it is believed that the results obtained are substantially independent of the initial flow conditions close to the cylinder (Townsend 1950).

Turbulent velocity fluctuations were observed with the hot-wire anemometer, in both the single-wire and X-wire forms. Since a straight hot-wire responds very nearly to the component of the velocity fluctuation at right angles to its length and in the plane of the hot-wire and the mean flow direction, a single hot-wire at right angles to the mean stream registers fluctuations of $u$, one in the direction $(1/\sqrt{2}, -1/\sqrt{2}, 0)$ registers fluctuations in $(u+v)/\sqrt{2}$, and one in the direction $(1/\sqrt{2}, 1/\sqrt{2}, 0)$ fluctuations in $(u-v)/\sqrt{2}$. In this way the fluctuations components in the directions of the three axes, i. e. $u, v, w$, and also the components $(u+v)/\sqrt{2}$ and $(u-v)/\sqrt{2}$ could be detected and their intensities measured.

To obtain the intensity spectrum of a fluctuating electric signal, several methods are available. For simplicity, a zero-beat heterodyne analyser was used, a circuit in which, by means of a balanced modulator, the amplified turbulence signal is multipled by a sinusoidal signal from a beat-frequency oscillator, and the intensity of the resultant measured after passage through a low-pass filter. Since only the sum and difference frequencies appear in the resultant, the effect is that the original turbulence spectrum is displaced along the frequency axis by the oscillator frequency, and the energy transmitted through the low-pass filter is proportional to the energy originally contained in a band of frequencies, of central frequency the oscillator frequency and of band-width twice the cut-off frequency of the filter. This form of spectrum analyser is believed to have advantages for the study of the low-frequency part of the spectrum.

## § 7. Properties and Structure of the Large Slow Eddies.

From previous work on the structure of the turbulent wake it is known that the large eddies, which are responsible for producing the intermittently turbulent flow in the cylinder wake, contain only about 5 per cent of the total turbulent energy and extend over the whole width of the wake. The spatial extent of the circulation in the down-stream direction appears to be even greater. Using circuits designed to measure intermittency factors directly, it has been shown that the occurrence of fully turbulent flow in one half of the wake is uncorrelated with its occurrence in the outer half (Townsend 1950), and it is likely that the eddies in the two halves are substantially independent. This result makes it unlikely that the large eddies represent a periodic instability similar to the Karman vortex street, but more definite evidence is found in spectrum measurements (figs. 1–4).

Fig. 1.

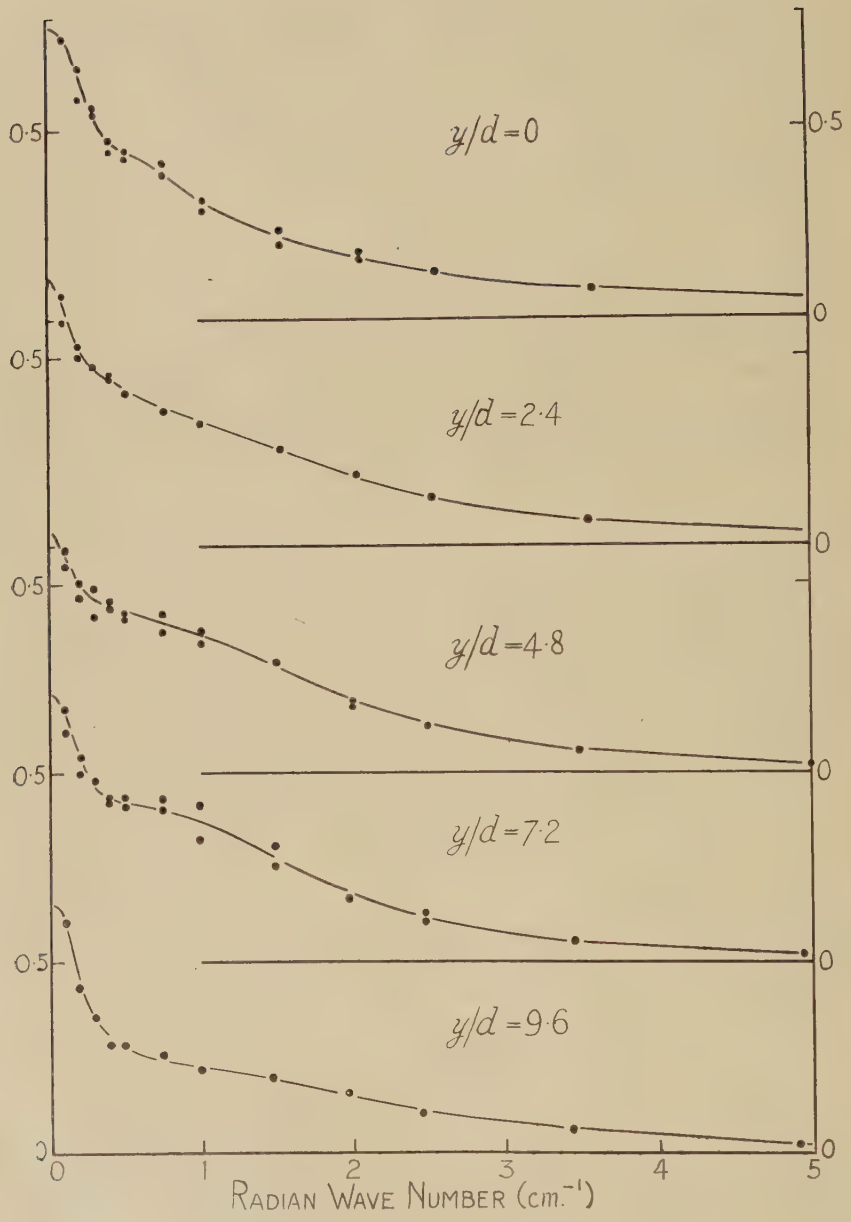


Spectrum functions of $u$-component.

The spectrum of the $u$-component of the velocity fluctuation has a characteristic form, clearly due to the superposition of two groups of turbulence of widely different scales (compare, for example, the spectrum of isotropic turbulence (fig. 5) which may be regarded as the spectrum of a

Fig. 2.

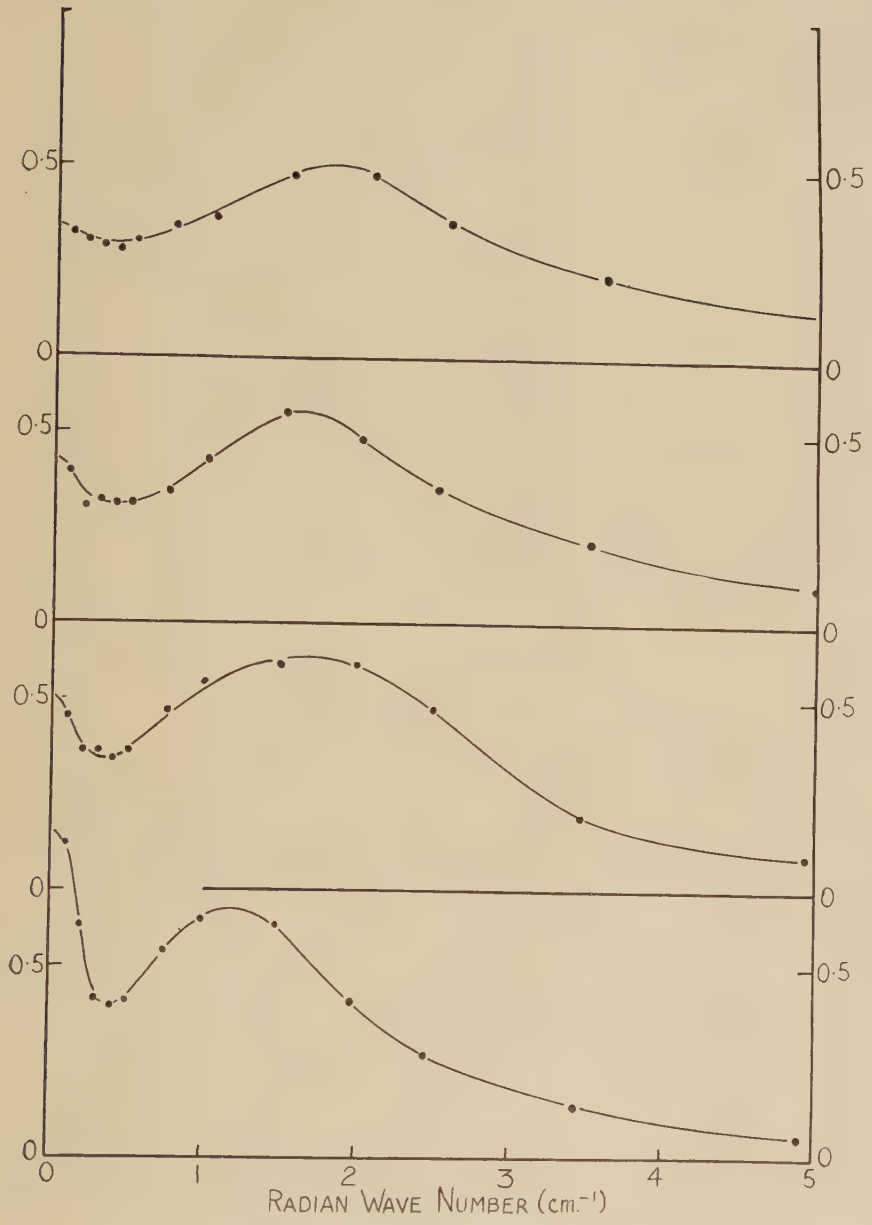


Spectrum functions of $v$-component.

random collection of eddies with a continuous distribution of size), and it is natural to identity the low frequency component of low total energy with the group of large slow eddies previously postulated to explain the experimental observation on diffusion and intermittency. Within the rather large experimental error, the spectrum function of the large slow eddies is a

Fig. 3.

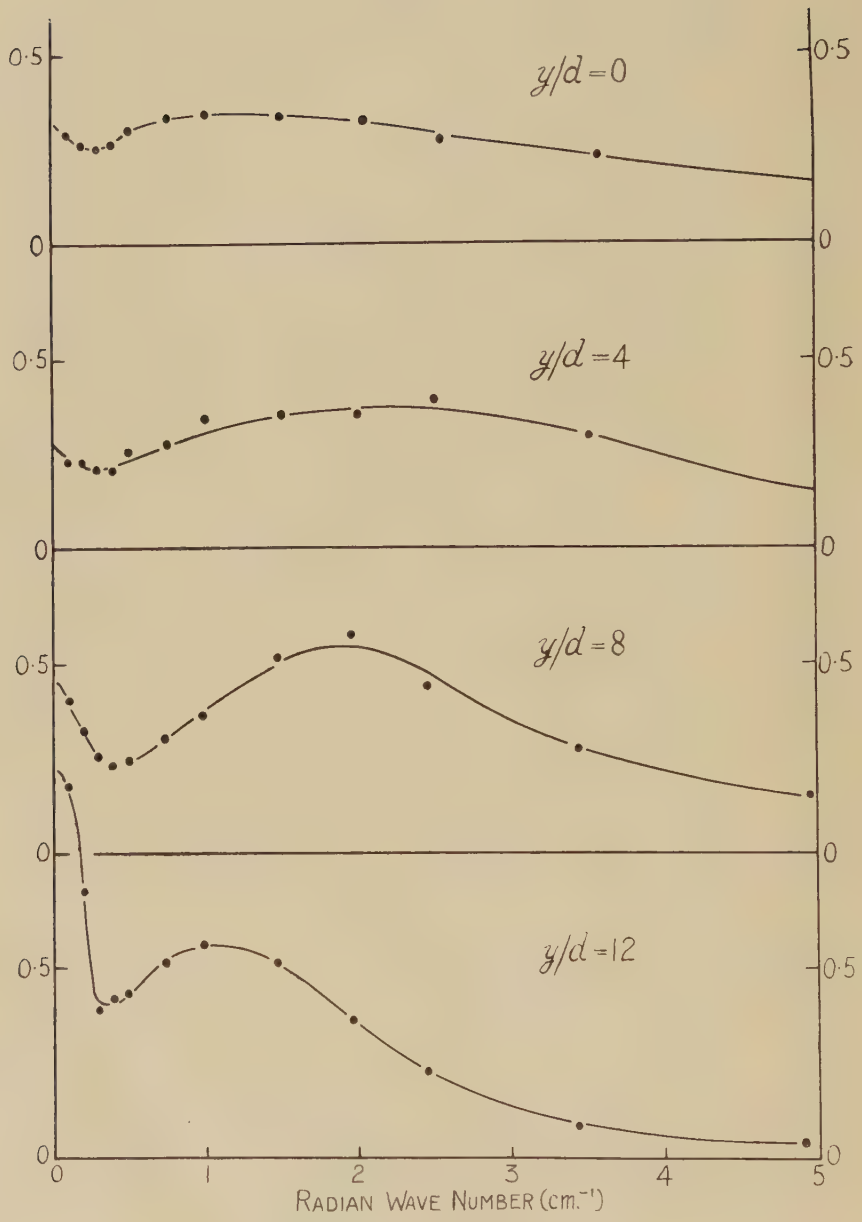


Spectrum functions of $w$-component.

Gaussian error function which is characteristic of an aggregate of similar eddies of simple structure, uncorrelated in position along the $Ox$ axis, and it seems a fair inference that the large eddies are of this general character, *i. e.* are of simple structure and are distributed along the direction of flow

Fig. 4.

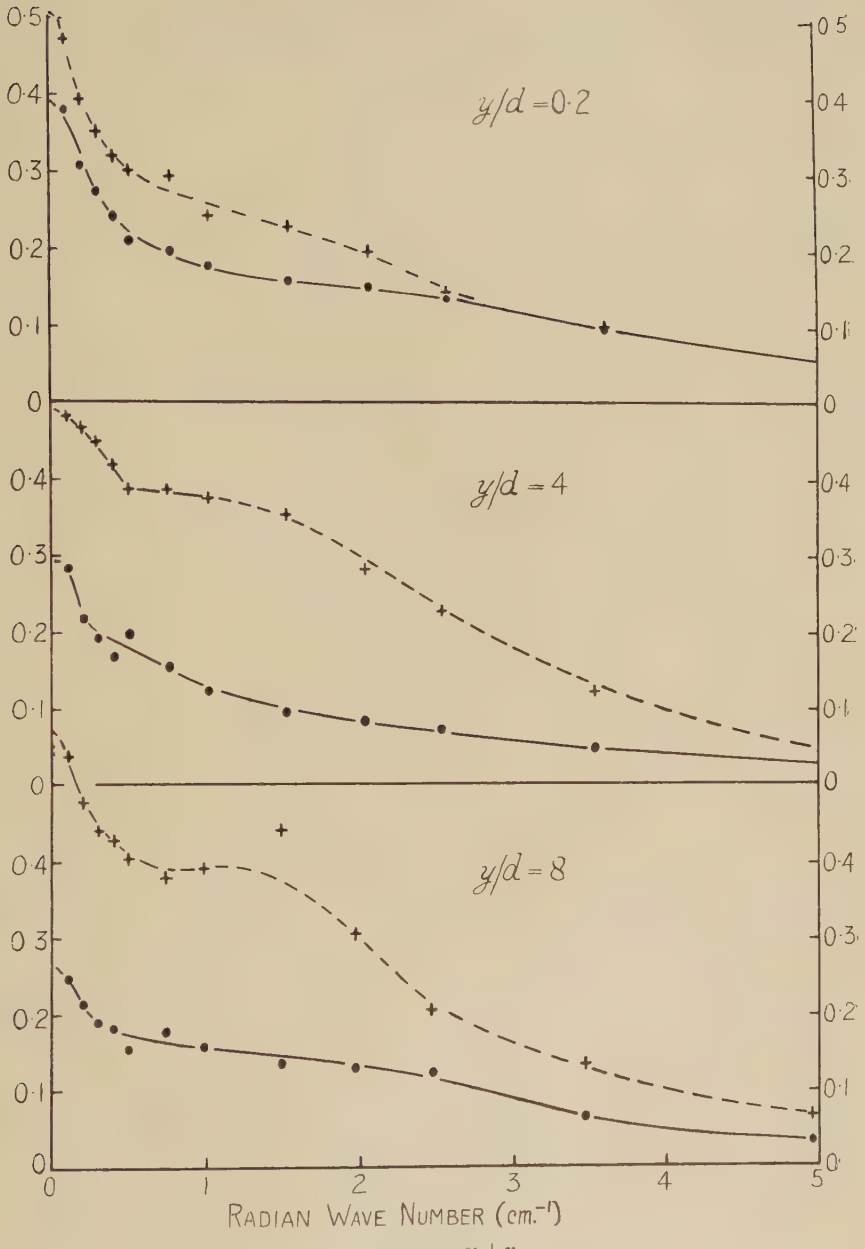


Spectrum functions of $\frac{u \pm v}{\sqrt{(2)}}$ components.

$$\left[\begin{array}{l} \bullet\ \frac{u+v}{\sqrt{(2)}} \\ +\ \frac{u-v}{\sqrt{(2)}} \end{array}\right]$$

randomly and not in a periodic or quasi-periodic manner. The initial surmise that the large eddies might be similar to a vortex-street must be discarded, and it is necessary to study the eddies more closely.

Fig. 5.

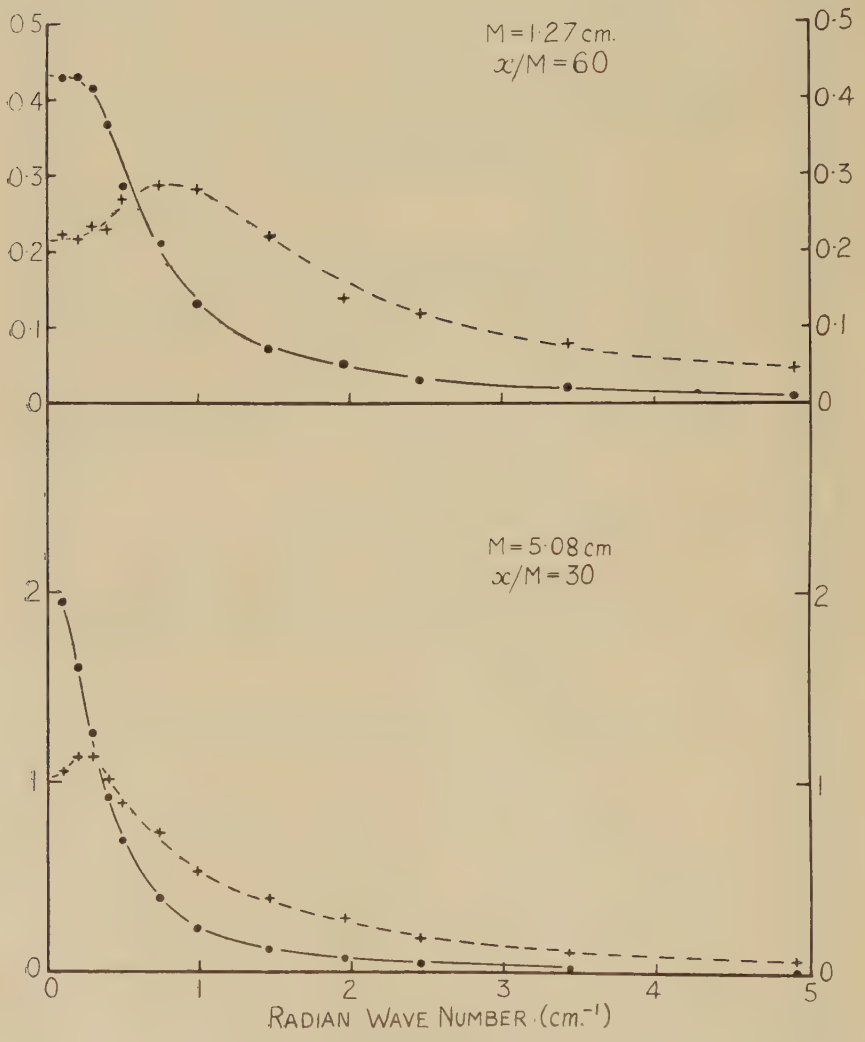


Spectrum Functions in Isotropic Turbulence.

[● *u*-component
+ *v*-component]

Further information can be obtained from the spectrum of the $v$-component of the velocity fluctuation. An assembly of randomly oriented simple eddies has a spectrum function for $v$ which has a maximum at a non-zero

frequency, and this is confirmed both by the spectrum of the $v$-component in isotropic turbulence, and of the large wave-number components of wake spectra. However, the low wave-number components of the wake spectra are again similar in form to a Gaussian error function, and it is concluded that the large eddies must have a preferred orientation. This preferred orientation of the axis of vorticity cannot be in the $yOz$ plane, or the spectrum maxima would be very pronounced, and, since the $u$-component of the large eddies is not small, the preferrred orientation is not along $Ox$. This suggests that one the of principal axes of rate-of-strain of the mean flow (which are at $\pm 45°$ to the $Ox$ and $Oy$ axes) may be the preferred direction, and this hypothesis is confirmed by measuring the spectra of the velocity components in these directions and along $Oz$. Considerable intensity of the low wave-number component is found in the spectra of $w$, and (in the positive half of the wake) of the $(u-v)/\sqrt{2}$ velocity component, while the intensity is much less for $(u+v)/\sqrt{2}$, *i. e.* along the axis of positive rate-of-strain. The preferred direction for the vorticity of the large eddies is approximately the direction of maximum positive rate-of-strain, which suggests that the source of the energy of the large eddies is the stretching they undergo as they are convected by the mean stream.

This examination of the wake spectra shows that the large eddies are of simple structure, are randomly placed in the direction of the free stream, and have a preferred orientation roughly along the principal axis of positive rate-of-strain. By transforming the spectra into the longitudinal correlation function, it can also be shown that the average extent in the $Ox$ direction of a large eddy is considerably larger than the width of the wake, and the typical large eddy must be rather elongated in this direction.

## §8. Mechanism of the Slow Eddies.

Accepting the structure of the large slow eddies that has been outlined above, it is easy to see that such eddies receive energy from the mean flow, and may use it partly in increasing their kinetic energy and partly in working against the shear stresses caused by the smaller eddies of the main body of turbulence. This gain of energy cannot persist indefinitely for, after a sufficient time, the stretching action will cease and the large eddy will be dissipated (fig. 6). The typical history of a large eddy may be something like this. Initially, appreciable circulation occurs by chance in a circuit with normal inclined at a small angle to the $Oy$ axis, and, as the circuit is convected by the mean flow, the energy increases as the area of the circuit decreases. In the early stages of development, it is likely that the dimensions of such an eddy are too great for the effect of eddy viscosity to be appreciable, but, as the circuit area decreases, the velocity gradients tend to increase and loss by eddy viscosity increases in importance. At the intermediate stage of development, it is probable that the energy gain from the mean flow and the energy loss by eddy viscosity are comparable in magnitude, and that the energy is nearly stationary. When the circuit area can no longer decrease, the eddy loses energy and disappears.

The viscosity control mechanism which has been described previously can easily be modified to fit into this scheme. When an eddy reaches an appreciable intensity, its convective action will lead to local spreading of the wake and to increased transfer of energy from the mean flow to the small-scale turbulent motion. The resulting increase in turbulent intensity and eddy viscosity reduces and finally stops the growth of the large eddy, and it may be supposed that, during the intermediate period of the eddy development, it is near a state of equilibrium such that the rate-of-change of total energy is small compared with the gain from the mean flow or the loss by eddy viscosity. The aggregate effect of a succession of these eddies is that the eddy viscosity is maintained continuously at a value such that the mean eddy is in this condition of dynamic equilibrium, the stabilizing process being: increase of energy of large eddy ⟶ increased rate of spread of wake ⟶ increased rate of production of small-scale turbulent energy ⟶ increasing eddy viscosity ⟶ increased energy loss from the large eddy. The time-scales for all these processes are comparable, and it seems very probable that a control process of this kind does operate in the wake.

Fig. 6.

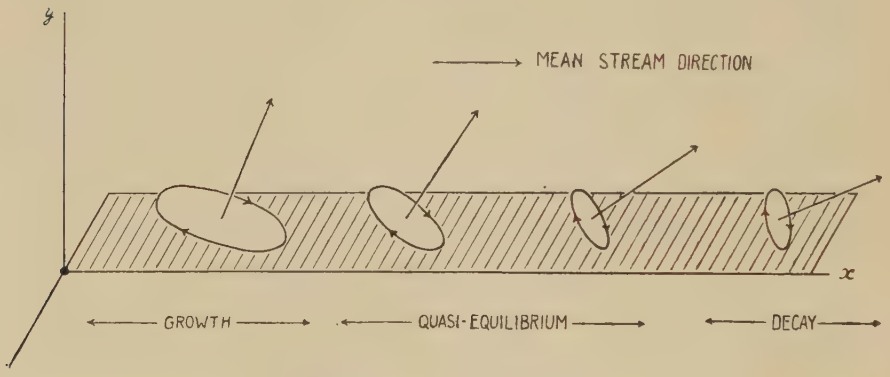


Development of large eddy.

Confirmation of this notion can be obtained by inquiring whether eddies similar to the large eddies of the wake could be in a condition of dynamic equilibrium. Experimentally, the large eddies are found to be long cylindrical structures, generally similar to the eddy described by

$$u=v=Az\exp\{-\tfrac{1}{2}\alpha^2(y^2+z^2)\},$$
$$w=-Ay\exp\{-\tfrac{1}{2}\alpha^2(y^2+z^2)\},$$

which is an eddy with vorticity roughly in the direction $(1/\sqrt{2}, -1/\sqrt{2}, 0)$ and unlimited in the $Ox$ direction. In the absence of better information about the exact structure of a typical large eddy, let us consider the energy balance of such an eddy in a mean velocity field of constant shear $\partial U/\partial y$. Assuming the eddy viscosity $\epsilon$ to be isotropic, the loss of energy by eddy viscosity is

$$D=\int\int_{-\infty}^{\infty} W\,dy\,dz,$$

where

$$W=\rho\epsilon\left[2\left(\frac{\partial u}{\partial x}\right)^2+2\left(\frac{\partial v}{\partial y}\right)^2+2\left(\frac{\partial w}{\partial z}\right)^2+\left(\frac{\partial u}{\partial y}+\frac{\partial v}{\partial x}\right)^2+\left(\frac{\partial v}{\partial z}+\frac{\partial w}{\partial y}\right)^2+\left(\frac{\partial w}{\partial z}\right)+\left(\frac{\partial u}{\partial z}\right)^2\right],$$

and then

$$D=3\pi\rho\epsilon A^2\alpha^2.$$

The rate of production of energy is

$$S=\int\int_{-\infty}^{\infty}\rho uv\frac{\partial U}{\partial y}\,dy\,dz$$

$$=\frac{\pi}{2}\rho A^2\frac{\partial U}{\partial y},$$

If the energy is stationary, S=D, and the equilibrium equation is

$$\frac{\partial U}{\partial y}=6\epsilon\alpha^2.$$

However, it may be argued that in a developing wake the equilibrium condition should be that the ratio of the eddy energy to the wake energy remains constant in the period of dynamic equilibrium. On this hypothesis, the equilibrium equation becomes

$$\frac{\partial U}{\partial y}+\frac{3}{4}\left[\frac{U_0}{x}\right]=6\epsilon\alpha^2,$$

where $U_0/x$ is the time taken for the mean stream to travel from the virtual origin of the wake to the point of observation. From observations on the wake at a cylinder Reynolds number of 1430,

$$\left(\frac{\partial U}{\partial y}\right)_{\max}=3{\cdot}0\left[\frac{U_0}{x}\right]$$

so the two forms of the equilibrium equation are not very different. At the same Reynolds number, it has been found that the mean value of the eddy viscosity is approximately $1/80\ U_0 d$ (Townsend 1950). Under these conditions the equilibrium size of a large eddy is given by

$$\alpha^2 xd=40 \text{ or } 50,$$

depending on which of the two definitions of dynamic equilibrium is used. In fig. 7, the function exp. $(-\alpha^2 y^2)$, representing roughly the distribution of energy in the large eddy, and the mean velocity defect $U_0-U$ are plotted on the same scale, and the equilibrium large eddy is seen to fit very well into one half of the wake.

This very crude calculation shows that eddies of the dimensions necessary to explain the slow mixing processes would be approximately in a state of dynamic equilibrium, and that the suggested viscosity control process is possible. In free turbulence, the occurrence of intermittently turbulent flow makes the existence of the controlling system of eddies especially obvious, but there is quite a possibility that similar processes may be at work in closed flows. The only experimental evidence for a double

Fig. 7.

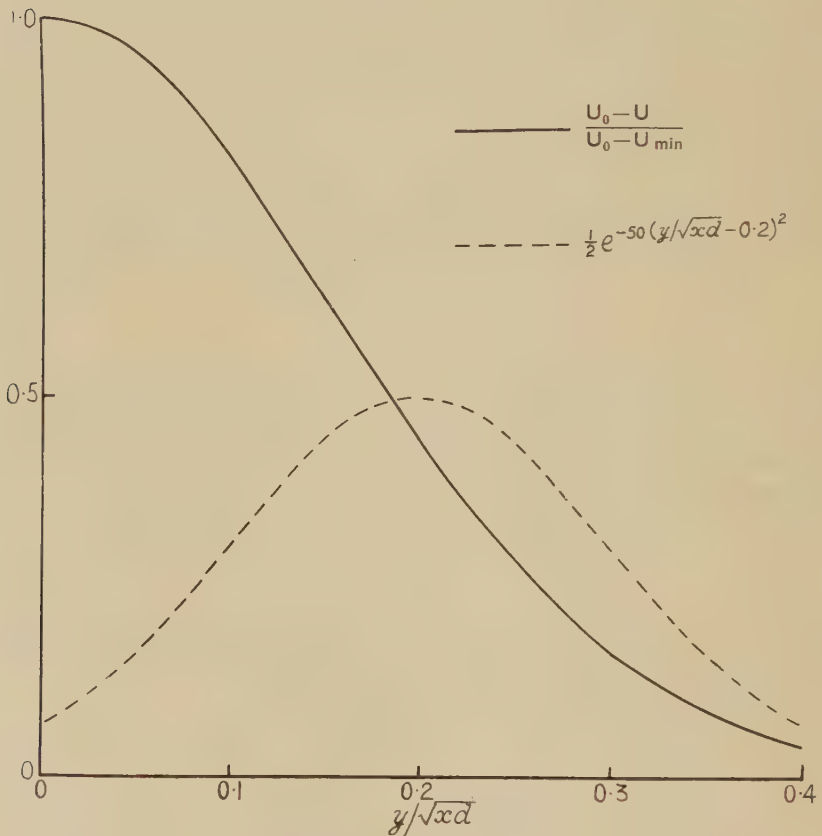


Wake profile and eddy size.

structure of turbulence in a closed flow is the observation of MacPhail (1944) that, in the fully turbulent flow between rotating cylinders, there is superimposed on the small-scale turbulent motion a quasi-periodic velocity variation of scale similar to the original laminar instability described by G. I. Taylor (1923). This velocity variation probably controls the level of eddy viscosity in a similar way to the large eddies of the wake flow. The contrast between the periodicity of the large eddies in cylinder flow and the aperiodic nature of the wake eddies is probably due to the constancy in

time of the cylinder flow which allows the development of a periodic instability. In wake flow, before a periodic instability has developed appreciably, the wake dimensions have increased by too much to permit the continued growth of the original instability.

## § 9. The Concept of Eddy Viscosity.

This description of the turbulent motion in the cylinder wake in terms of an eddy viscosity has the advantage that, assuming the dynamic equilibrium of the large eddies, the exact mechanism of the production of eddy viscosity is irrelevant, and, in principle, it is possible to estimate the equilibrium eddy viscosity without considering the energy balance of the turbulent motion. There is no strong experimental evidence against this use of a coefficient of eddy viscosity to describe the small scale friction, for the scale and intensity of the small-scale turbulent motion are such that "time of flight" and "mixing length" are small compared with times and lengths associated with the mean flow. What is certainly incorrect is the attempt to relate its value to the local parameters of the mean flow, implying local and instantaneous energy equilibrium. The evidence shows that the setting up of Reynolds stresses must be a fairly rapid process compared with the attainment of turbulent energy equilibrium, *i. e.* that transfer of energy from one velocity component to another under the action of the shearing must be rapid. The comparative slowness of energy transfer from the mean flow to the turbulence and then to heat suggests that viscosity is irrelevant to the process of stress production, and, for similar reasons, turbulent transfer between eddies of different sizes also must have little effect on the establishment of the shear stress. The problem then reduces to the distortion of a turbulent field. If the axes of reference are parallel to the principal axes of strain, then the effect of an instantaneous distortion described by contradiction ratios $l$, $m$, $n$, is that

$$\xi_1 = l\xi_0, \quad \eta_1 = m\eta_0, \quad \zeta_1 = n\zeta_0 ,$$

where $lmn=1$ and $\xi_1$, $\eta_1$, $\zeta_1$ are the final vorticity components $\xi_0$, $\eta_0$, $\zeta_0$ are the initial vorticity components.

For the wake, $n=1$, and if $\xi$ is in the direction of positive strain, $\overline{\xi^2}$ increases while $\overline{\eta^2}$ decreases. In terms of the corresponding velocity components, $\overline{u^2}$ decreases and $\overline{v^2}$ increases, leaving $\overline{w^2}$ unchanged, at least for small strains. This results in the production of a Reynolds shear stress, $\rho(\overline{u^2}-\overline{v^2})$, set up instantaneously and proportional to the total strain, and this is probably the first stage in the actual process. When the Reynolds stress developed by straining becomes large, the tendency of ordinary turbulence to isotropy should resist the tendency of the strain, to align the vorticity along the direction of position strain, and the eddy viscosity may represent the balance between the orientating action of the strain and the disorientating effect of the turbulent transfer between the velocity components. That the selective action of the strain acts on

the vorticity rather than on the velocity makes it clear why the turbulent motion in free turbulence is apparently "isotropic." The intensities of the velocity components along the conventional axes of reference are nearly equal, because these axes are at 45° to the principal axes of strain, and transfer between the vorticity components along the principal axes hardly affects the energy in the velocity components along the ordinary axes of reference.

This notion that the eddy viscosity is a parameter describing a balance set up between the orientating effect of the shear and the disorientating effect of turbulent transfer is the last remaining possibility within the "equilibrium" group of theories of the eddy viscosity (after energy equilbrium has been discarded), and its accuracy is dependent on a sufficiently rapid attainment of this equilibrium. Revelant experiments would be on the attainment of isotropy in a uniform field of, say, axisymmetric turbulence, but existing measurements are not sufficiently comprehensive and it is proposed to investigate this matter directly. If the tendency to isotropy is too sluggish to be an effective balance to the straining process, it may be necessary to discard the equilibrium concept of shear stress production altogether, and to suppose that, like the energy, the shear stress is determined mostly by the previous history, probably by the total strain. While it would be premature to consider this hypothesis in detail, it should be mentioned that most of the conclusions concerning the mechanism of control of the large eddies would be equally valid, although the concept of eddy viscosity would then have less physical significance.

## References.

Goldstein, S, 1938, *Modern Developments in Fluid Dynamics* (Oxford : Clarendon Press)

MacPhail, D. C., 1944, *Royal Aircraft Establishment Report* No. 1928

Taylor, G. I., 1923, *Phil. Trans.* A, **223,** 289-343

Townsend, A. A., 1948, *Australian J, Sci. Res.* A, **1,** 161-174 ; 1949, *Proc. Roy, Soc.* A, **197,** 124-140 ; 1950, *Australian J. Sci. Res.* (in the press).

# LXXXII. *The Effect of Eddy Viscosity on Ocean Waves.*

By K. F. Bowden,
Oceanography Department, University of Liverpool *.

[Received May 22, 1950.]

Abstract.

The effect of turbulence on ocean waves appears to call for an eddy viscosity which, while being large compared with the molecular viscosity, is small compared with the eddy viscosity found to apply to currents. A recent suggestion that the eddy viscosity should be taken as proportional to $\lambda^{4/3}$ where $\lambda$ is the wavelength, seems to the author to be unsatisfactory. It is proposed, instead, that the coefficient of eddy viscosity N, applicable to waves, should be of the form $N = Kca$, where $c$ is the speed of propagation, $a$ is the amplitude and K is a constant. This form is indicated on dimensional grounds and is shown to be in conformity with v. Karman's similarity hypothesis for shearing flow. With K of the order of $5 \times 10^{-5}$, the eddy viscosity would be large enough to account entirely for the observed rate of decay of ocean swell, while its effect on the attenuation of waves with depth would still be negligible. In the initial formation of waves, only the molecular viscosity need be considered. A possible effect of eddy viscosity on waves in the generating area would be to limit the steepness of the longer waves to a value less than the breaking steepness, even when the duration and fetch were unlimited.

## § 1. Introduction.

While molecular viscosity appears to be an important factor in the initial formation of surface waves on water, its dissipative effect on the long waves of ocean swell, for example, is negligibly small. If an eddy viscosity of the order of magnitude found to apply to ocean currents, on the other hand, were operative in the case of waves, their loss of energy would be much more rapid than is observed. Since it is well recognized in meteorology and oceanography that the eddy viscosity applicable to a particular motion depends on its scale, the suggestion has been made that waves may be affected by turbulence but that a smaller, and probably variable, eddy viscosity is applicable.

## § 2. Turbulence and Eddy Viscosity.

The first quantitative expression of this idea would appear to be that made recently by Groen and Dorrestein (1950), who assumed an eddy viscosity proportional to $\lambda^{4/3}$, where $\lambda$ is the wavelength. This form was based on a result found by v. Weizsäcker (1948) in the theory of locally

* Communicated by the Author.

isotropic turbulence, and on an empirical law found by Richardson (1926) from diffusion experiments. V. Weizsäcker was considering the transfer of energy from turbulence on a scale characterized by a linear dimension $l$ to turbulence of scales smaller than $l$. By similarity considerations, he found the effective eddy viscosity to be proportional to $l^{4/3}$ for values of $l$ within a certain range. Turbulence on a scale so small that dissipation by molecular viscosity is the dominating factor, or so large that transfer of energy from the mean motion to the turbulence predominates is excluded from the range to which the similarity law applies. In the case of the dissipation of waves, we are dealing with the loss of energy from the mean motion (*i. e.* the wave motion) and it is not clear, therefore, that the eddy viscosity law deduced by v. Weizsäcker's theory will apply to this problem.

Richardson's result, which was obtained originally for the atmosphere and has been found by Richardson and Stommel (1948) to apply also to the ocean in certain conditions, was that the coefficient of diffusion applicable to the dispersal of a group of particles is proportional to $d^{4/3}$, where $d$ is the separation of a pair of particles. The process considered in this case can take place in turbulence which does not necessarily involve shear in the fluid and it is not apparent that the dissipation of energy in a problem involving shearing stresses can be deduced from it.

A further difficulty is that, even if we assume an eddy viscosity proportional to $l^{4/3}$, the question arises: what is the characteristic length $l$ for wave motion: Groen and Dorrestein have taken it to be $\lambda$, but one might expect the amplitude $a$ also to be a characteristic length for a given set of waves.

## § 3. Wave Motion as affected by Molecular and Eddy Viscosity.

Let us consider two-dimensional surface waves in deep water. Let rectangular axes be taken, with $Ox$ and $Oy$ in the undisturbed sea surface and $Oz$ vertically upwards. Let the waves be travelling in the direction of the negative $x$-axis, and U and W be the horizontal and vertical components of the particle velocity at any point. Then for irrotational waves of small amplitude

$$\left.\begin{aligned} \mathrm{U} &= -\omega a e^{kz}\cos(\omega t+kx), \\ \mathrm{W} &= -\omega a e^{kz}\sin(\omega t+kx), \end{aligned}\right\} \quad \ldots\ldots \quad (1)$$

where $\omega=2\pi/\mathrm{T}$, T being the period, $k=2\pi/\lambda$, $\lambda$ being the wavelength and $a$ is the amplitude of the surface elevation. $t$ is the time.

The rate of dissipation of energy by molecular viscosity may be shown to be (Lamb 1932, p. 623)

$$\mathrm{D}=2\mu k^3c^2a^2 \quad \ldots\ldots\ldots \quad (2)$$

where $\mu$ is the coefficient of viscosity and $c=\lambda/\mathrm{T}$ is the velocity of propagation. If no external forces are acting, the amplitude of the waves will decay at a rate given by the factor $\exp(-2\nu kt)$, where $\nu=\mu/\rho$ is the kinematic viscosity, $\rho$ being the density.

To a first approximation, the components of the particle velocity are still given by (1), provided that

$$\theta \equiv \frac{\nu k}{c} \ll 1 \quad . \quad . \quad . \quad . \quad . \quad . \quad . \quad . \quad . \quad . \quad (3)$$

By inserting numerical values in (3), we find that $\theta$ is, in fact, negligibly small, except for very short waves.

To consider the effect of eddy viscosity, we note that a wave motion is specified by the three quantities $\lambda$, T and $a$. We will assume, therefore, that if there exists an eddy viscosity N, applicable to wave motion, it is a function of $\lambda$, T and $a$. If we assume a power law, $N = K\lambda^{\alpha} a^{\beta} T^{\gamma}$ where K is a non-dimensional constant, then, since the dimensions of N are $L^2T^{-1}$, we find

$$\alpha + \beta = 2, \qquad \gamma = -1.$$

Taking $\alpha = \beta = 1$ as the simplest solution including $\lambda$ and $a$,

$$N = K\frac{\lambda a}{T} = Kca. \quad . \quad . \quad . \quad . \quad . \quad . \quad . \quad . \quad . \quad (4)$$

It is suggested that equation (4) gives the appropriate form of eddy viscosity to apply to wave motion. We need not expect K to be an absolute constant but rather a non-dimensional parameter which varies only slowly compared with the other quantities involved. The above treatment is still useful if we can take K as constant over a limited range of the quantities $\lambda$, $a$ and T.

The rate of dissipation of energy by eddy viscosity, replacing $\mu$ by $\rho N$ in equation (2), becomes,

$$W = 2\rho K k^3 c^3 a^3. \quad . \quad . \quad . \quad . \quad . \quad . \quad . \quad . \quad . \quad (5)$$

The particle velocity components will still be given to a first approximation by (1), provided that the criterion (3) is satisfied with N replacing $\nu$, *i. e.*

$$\theta_N \equiv \frac{Nk}{c} = Kka \ll 1. \quad . \quad . \quad . \quad . \quad . \quad . \quad . \quad . \quad (6)$$

It will be shown later that, with a value of K large enough for eddy viscosity to account entirely for the observed rate of decay of ocean swell, the condition (6) is still satisfied.

## § 4. V. Karman's Similarity Hypothesis applied to Wave Motion.

An alternative approach to the problem of the dissipation of wave motion by turbulence may be made by v. Karman's similarity hypothesis for shearing flow, which has found successful application to turbulent flow through pipes and channels. Let $u$, $v$ and $w$ be the components of turbulent velocity and let square brackets [ ] denote values of functions of these components. Then if the mean velocity U is a function of $z$ only, while $V = W = 0$, the rate of dissipation of energy of the mean motion by turbulence is given by

$$\psi = \rho[uw]\frac{dU}{dz}. \quad . \quad . \quad . \quad . \quad . \quad . \quad . \quad . \quad . \quad (7)$$

v. Karman assumed dynamical similarity in the turbulence at various points in the field of motion and deduced that

$$[uw]=l^2\left|\frac{d\mathrm{U}}{dz}\right|\frac{d\mathrm{U}}{dz} \quad . \quad . \quad . \quad . \quad . \quad . \quad . \quad . \quad . \quad (8)$$

where

$$l=\mathrm{K}_1\left|\frac{d\mathrm{U}}{dz}\right| \Big/ \left|\frac{d^2\mathrm{U}}{dz^2}\right| \quad . \quad . \quad . \quad . \quad . \quad . \quad . \quad . \quad . \quad (9)$$

where $\mathrm{K}_1$ is a non-dimensional constant.

In the case of two-dimensional motion, in the $xz$-plane, (7) is replaced by (Lamb, *loc. cit.*, p. 676)

$$\psi=\rho\left\{[u^2]\frac{\partial \mathrm{U}}{\partial x}+[w^2]\frac{\partial \mathrm{W}}{\partial z}+[uw]\left(\frac{\partial \mathrm{U}}{\partial z}+\frac{\partial \mathrm{W}}{\partial x}\right)\right\}. \quad . \quad . \quad (10)$$

In applying this equation to wave motion, we assume that mean values of $\partial \mathrm{U}/\partial x$ etc., as well as $[u^2]$ etc. are taken over an element of volume of dimensions small compared with the wavelength and over a time small compared with the period of the wave motion. If U and W are given by equations (1),

$$\psi=\rho k\omega a e^{kz}\{([u^2]-[w^2])\sin(\omega t+kx)-2[uw]\cos(\omega t+kx)\}. \quad . \quad . \quad (11)$$

By analogy with (8), we should expect $[uw]$ to be a function of $\partial \mathrm{W}/\partial x$ as well as of $\partial \mathrm{U}/\partial z$. In this case, however, $\partial \mathrm{W}/\partial x=\partial \mathrm{U}/\partial z$ so that we may take

$$[uw]=-l_4^2\left|\frac{\partial \mathrm{U}}{\partial z}\right|\frac{\partial \mathrm{U}}{\partial z},$$

where

$$l_4=\mathrm{K}_4\left|\frac{\partial \mathrm{U}}{\partial z}\right| \Big/ \left|\frac{\partial^2 \mathrm{U}}{dz^2}\right|=\frac{\mathrm{K}_4}{k},$$

where $\mathrm{K}_4$ is a constant.

Similarly, we will take

$$[u^2]=\mathrm{C}_2+\frac{\mathrm{K}_2^2}{k^2}\left|\frac{\partial \mathrm{U}}{\partial x}\right|\frac{\partial \mathrm{U}}{\partial x}$$

and

$$[w^2]=\mathrm{C}_3+\frac{\mathrm{K}_3^2}{k^2}\left|\frac{\partial \mathrm{W}}{\partial z}\right|\frac{\partial \mathrm{W}}{\partial z},$$

where $\mathrm{K}_2$ and $\mathrm{K}_3$ are constants, introduced in a way similar to $\mathrm{K}_4$. $\mathrm{C}_2$ and $\mathrm{C}_3$ are positive constants, since $[u^2]$ and $[w^2]$ are essentially positive. From (11), we have, for the mean rate of loss of energy per volume from the wave motion at a given depth $z$,

$$\begin{aligned} d\mathrm{W} &= \frac{1}{\mathrm{T}}\int_0^{\mathrm{T}}\psi\,dt \\ &=\rho k\omega^3 a^3 e^{3kz}\{(\mathrm{K}_2^2-\mathrm{K}_3^2)\overline{|\sin(\omega t+kx)|\sin^2(\omega t+kx)} \\ &\qquad +2\mathrm{K}_4^2\overline{|\cos(\omega t+kx)|\cos^2(\omega t+kx)}\} \\ &=\frac{4}{3\pi}\rho k\omega^3 a^3 e^{3kz}(\mathrm{K}_2^2-\mathrm{K}_3^2+2\mathrm{K}_4^2). \end{aligned}$$

For the rate of dissipation per unit area of the sea surface,

$$W=\int_{-\infty}^{0} dW\,dz=\frac{4}{9\pi}\rho\omega^3a^3(K_2^2-K_3^2+2K_4^2). \quad . \quad . \quad . \quad (12)$$

Hence

$$W=2\rho K k^3c^3a^3$$

as in equation (5) if

$$K=\frac{2}{9\pi}(K_2^2-K_3^2+2K_4^2). \quad . \quad . \quad . \quad . \quad . \quad . \quad . \quad . \quad . \quad (13)$$

The equations of wave motion in the $xz$-plane, in the presence of turbulence are (from Lamb, *loc. cit.*, p. 678)

$$\frac{\partial U}{\partial t}+\frac{1}{\rho}\frac{\partial p}{\partial x}+\frac{\partial}{\partial x}[u^2]+\frac{\partial}{\partial z}[uw]=0,$$

$$\frac{\partial W}{\partial t}+\frac{1}{\rho}\frac{\partial p}{\partial z}+\frac{\partial}{\partial z}[w^2]+\frac{\partial}{\partial x}[uw]=g,$$

where $p$ is the wave pressure. To the first approximation

$$p=\rho g a e^{kz}\cos(\omega t+kx).$$

The condition that equation (1) should still be valid, in the presence of turbulence, to a first approximation, is that terms such as $\partial[uw]/\partial z$ should be small compared with terms such as $(1/\rho)\partial p/\partial x$.

We have $\left|\frac{\partial}{\partial z}[uw]\right|=K_4^2k\omega^2a^2e^{2kz}$ and $\left|\frac{1}{\rho}\frac{\partial p}{\partial x}\right|=gkae^{kz}$. Since $K_4^2$ is of the same order of magnitude as K, we may write the condition as

$$\frac{Kk\omega^2a^2e^{2kz}}{gkae^{kz}}\ll 1$$

and since $kc^2=g$, this becomes

$$Kkae^{kz}\ll 1. \quad . \quad . \quad . \quad . \quad . \quad . \quad . \quad . \quad . \quad (14)$$

Apart from the factor $\exp kz$, condition (14) is the same as that given by (6).

We may therefore derive the equation for the dissipation of wave motion by turbulence from v. Karman's similarity hypothesis without introducing the concept of eddy viscosity or the analogy with molecular viscosity.

## § 5. The Decay of Ocean Swell.

### 5.1. *Waves of a Single Period.*

We will consider waves of constant wave velocity $c$, travelling in the direction $Ox$ and assume a quasi-stationary state, *i. e.* the wave energy varying with distance but constant in time at a given point. Then if E is the energy per area of the waves, the rate of loss of energy with distance, due to eddy viscosity, would be given by

$$\frac{c}{2}\frac{dE}{dx}=-W \quad . \quad . \quad . \quad . \quad . \quad . \quad . \quad . \quad (15)$$

assuming the energy to be propagated with the group velocity $c/2$. Since $E=\frac{1}{2}\rho g a^2$ and taking W from equation (5), we have

$$\frac{da}{dx}=-\frac{4Kg^2a^2}{c^4}$$

using the relation $kc^2=g$. The solution is

$$\frac{1}{a}=\frac{1}{a_0}+\frac{4Kg^2}{c^4}x, \quad . \quad . \quad . \quad . \quad . \quad . \quad . \quad . \quad (16)$$

where $a_0$ is the amplitude at $x=0$. In terms of the period T, since $g\mathrm{T}=2\pi c$,

$$\frac{1}{a}=\frac{1}{a_0}+\frac{64\pi^4K}{g^2T^4}x \quad . \quad . \quad . \quad . \quad . \quad . \quad . \quad . \quad (17)$$

Sverdrup and Munk (1947), in their treatment of the growth and decay of waves, assumed that the effect of eddy viscosity was negligible and attributed the decay of swell to air resistance, the rate of dissipation per area being of the form

$$R=\tfrac{1}{2}s\rho' k^2c^3a^2, \quad . \quad . \quad . \quad . \quad . \quad . \quad . \quad . \quad (18)$$

where $s$ is a coefficient and $\rho'$ the density of the air. If we replace W by R in equation (15), we are led to a solution

$$a=a_0 \exp\{-(s\rho' g/\rho c^2)x\} \quad . \quad . \quad . \quad . \quad . \quad . \quad (19)$$

or in terms of T

$$a=a_0 \exp\{-(4\pi^2 s\rho'/\rho g\mathrm{T}^2)x\}. \quad . \quad . \quad . \quad . \quad . \quad . \quad (20)$$

A comparison of equations (17) and (20) shows the differences to be expected if the decay is due mainly to eddy viscosity or to air resistance. Both equations show that the decay is more rapid for waves of shorter period, the discrimination being greater in the case of eddy viscosity. In either case, therefore, if a spectrum of periods is present in the swell at $x=0$, the maximum amplitude occurring for a period $\mathrm{T}_0$, then at a distance $x$, owing to the selective dissipation, the component of maximum amplitude will occur at a period T where $\mathrm{T}>\mathrm{T}_0$. An increase of effective period with distance usually occurs with ocean swell, but Munk (1947) has shown that such an increase may be explained, in some cases at least, on kinematical grounds without any selective dissipation of energy.

### 5.2. *Effective Period increasing with distance.*

Let us consider the general case of the period T, and thus the velocity $c$, increasing with $x$, without assigning the cause, and follow Sverdrup and Munk by assuming our dissipation equation to apply to the "significant waves". If $c$ varies with $x$, equation (15) is replaced by

$$\frac{1}{2}\left(c\frac{dE}{dx}+E\frac{dc}{dx}\right)=-W. \quad . \quad . \quad . \quad . \quad . \quad . \quad (21)$$

Hence

$$\frac{da}{dx}=-\frac{1}{2}\frac{a}{c}\frac{dc}{dx}-\frac{4Kg^2a^2}{c^4}. \quad . \quad . \quad . \quad . \quad . \quad . \quad (22)$$

Little is known of the way in which $c$ may be expected to increase with $x$, but to obtain a solution we will assume that

$$\frac{dc}{dx} = \sigma \text{ (a constant), so that } c = c_0 + \sigma x.$$

Then the solution of (22) may be shown to be

$$\frac{1}{ac^{1/2}} = \frac{1}{a_0 c_0^{1/2}} + \frac{8\mathrm{K}g^2 x}{7(c-c_0)}\left(\frac{1}{c_0^{7/2}} - \frac{1}{c^{7/2}}\right), \quad . \quad . \quad . \quad . \quad (23)$$

where $a_0$, $c_0$ are values at $x=0$ and $a$, $c$ are values at $x$. Putting $g\mathrm{T} = 2\pi c$,

$$\frac{1}{a\mathrm{T}^{1/2}} = \frac{1}{a_0 \mathrm{T}_0^{1/2}} + \frac{128\pi^4 \mathrm{K}x}{7g^2(\mathrm{T}-\mathrm{T}_0)}\left(\frac{1}{\mathrm{T}_0^{7/2}} - \frac{1}{\mathrm{T}^{7/2}}\right). \quad . \quad . \quad . \quad (24)$$

For dissipation by air resistance, it may be shown that the corresponding solution is

$$a\mathrm{T}^{1/2} = a_0 \mathrm{T}_0^{1/2} \exp\{-(4\pi^2 s\rho'/\rho g \mathrm{T}_0 \mathrm{T})x\}. \quad . \quad . \quad . \quad . \quad (25)$$

### 5.3. *Application to Observations of Swell.*

The above equations have been applied to the examples of swell given by Sverdrup and Munk (*loc. cit.*, Table IV.). $s$ and K have been computed from the recorded values of $x$, $a_0$, $\mathrm{T}_0$, $a$ and T, and are shown in Table I. For the examples of swell Nos. 1, 2, 3 and 5, equations (24) and (25) respectively were used. For Nos. 4 and 6, equations (17) and (20) were used, since T differs little from $\mathrm{T}_0$. The scatter of the values of $s$ and K is about the same and one cannot decide on these data whether the decay law for air resistance or eddy viscosity fits the observations better. It is possible, of course, that both processes operate and are of the same order of magnitude.

Taking the mean value of K, we would have

$$\mathrm{N} = 5{\cdot}6 \times 10^{-5} ca. \quad . \quad . \quad . \quad . \quad . \quad . \quad . \quad . \quad . \quad (26)$$

As an example, for swell of wave velocity 10 m./sec. and amplitude 2 m., $\mathrm{N} = 11{\cdot}2$ cm.$^2$/sec., which does not appear unreasonable. Referring to the condition given by (6), we see that, with this value of K, the condition is easily satisfied. The influence of eddy viscosity on the rate of attenuation of the waves with depth is, therefore, negligible.

## § 6. The Initial Formation of Waves.

Jeffreys (1925) showed that the early stages of the formation of waves could be explained if a transfer of energy from wind to waves took place through normal pressures on the wave profile. The rate of transfer of energy was taken to be of the form

$$\mathrm{A} = \tfrac{1}{2} s\rho'(ka)^2(\mathrm{V}-c)^2 c \quad . \quad . \quad . \quad . \quad . \quad . \quad . \quad . \quad (27)$$

where $\mathrm{V} > c$, $s$ being the "sheltering coefficient" and V the wind speed. Comparing A with D, the rate of dissipation by molecular viscosity, Jeffreys showed the existence of a critical value of V, below which waves

could not be formed. From observations he found $V_{min}=110$ cm./sec. (approximately), which corresponds to $s=0{\cdot}27$. If $V>V_{min}$ this treatment sets no limit to the height the waves may attain and they would grow, presumably, until they reached the breaking steepness of $2a/\lambda=1/7$.

From wind tunnel measurements on wave models of various ratios of $2a/\lambda$, Motzfeld (1937) deduced that A was of the form

$$A=\tfrac{1}{2}s'\rho'(ka)^{3\cdot2}(V-c)^2c \quad . \quad . \quad . \quad . \quad . \quad . \quad . \quad (28)$$

Table I.

*Decrease in Height of Swell.*

| 1 | 2 | 3 | 4 | 5 | 6 | 7 | 8 |
|---|---|---|---|---|---|---|---|
| No. | Decay distance $x$ | At end of fetch | | At distance $x$ | | Air resistance $s$ | Eddy viscosity K |
| | | Ampl. $a_0$ | Period $T_0$ | Ampl. $a$ | Period T | | |
| | km. | m. | sec. | m. | sec. | $\times10^{-2}$ | $\times10^{-5}$ |
| 1 | 2,320 | 3·4 | 7·9 | 0·7 | 11·5 | 1·04 | 4·3 |
| 2 | 1,480 | 2·4 | 8·1 | 1·3 | 17·0 | 0·46 | 2·2 |
| 3 | 1,950 | 3·45 | 8·7 | 1·0 | 17·0 | 1·39 | 7·1 |
| 4 | 1,110 | 2·35 | 10·5 | 1·35 | 11·2 | 1·20 | 6·1 |
| 5 | 1,480 | 2·55 | 12·2 | 1·5 | 9·1 | 1·04 | 4·6 |
| 6 | 185 | 1·25 | 9·0 | 1·05 | 9·5 | 1·84 | 9·3 |
| | | | | | | | |
| | | | | | Mean | 1·16 | 5·6 |

The data in columns 1 to 6 are taken from Table IV. of Sverdrup and Munk's paper (1947). Column 7 gives the value of $s$, computed from equation (20) or (25), assuming the decay to be due to air resistance only. Column 8 gives the value of K, computed from equation (17) or (24), assuming the decay to be due to eddy viscosity only.

with $s'=0{\cdot}014$. Applying this result to the formation of waves, he found no critical wind speed in the region of 100 cm./sec. but for any value of V, $ka$ is a definite function of $c$, which is a maximum when $c=V/3$. For $V<100$ cm./sec., the maximum $ka$ would be negligibly small, but would increase rapidly in the region just above 100 cm./sec.

Neumann (1949), after considering observations of wind stress and wave steepness for various wind speeds, has proposed an equation for A of the form

$$A=\tfrac{1}{2}s''\rho' ka(V-c)^2c \quad . \quad . \quad . \quad . \quad . \quad . \quad . \quad . \quad (29)$$

with $s''=0{\cdot}095$. Like Motzfeld, he found $ka_{max}$ to be a definite function of V and to increase rapidly when V was about 100 cm./sec., but his values of $ka$ were appreciably higher than Motzfeld's.

While differing in detail, therefore, all investigators agree that easily observable waves should first appear when V = 100 cm./sec. approximately, and have a velocity $c=V/3$, *i. e.* 33 cm./sec. approximately. If we take $a=0{\cdot}1$ cm., equation (26) would give $N=1{\cdot}85\times10^{-4}$ cm.$^2$/sec., *i. e.* much less than the kinematic molecular viscosity $\nu$, which is $1{\cdot}8\times10^{-2}$ cm.$^2$/sec. We may conclude that eddy viscosity can play no part in the initial formation of waves and that only dissipation by molecular viscosity need be considered.

It seems unlikely that the relation $N=Kca$ would hold down to values of N comparable with $\nu$. We might, in fact, define a " Reynolds' number for wave motion " by $R_w=ca/\nu$, and expect that turbulence would affect the wave motion only when $R_w$ was above a certain value.

## § 7. The Growth of Waves under the Influence of Wind.

Although Sverdrup and Munk have used an expression for A similar to Jeffreys' (equation (27) for the transfer of energy from wind to waves by normal stresses for $V>6$ m./sec., they found it necessary to take a much lower value of $s$, i. e. $s=0{\cdot}013$. They showed that transfer of energy may also take place by tangential stresses, according to the equation

$$A'=\gamma^2\rho'(ka)^2V^2c, \quad . \quad . \quad . \quad . \quad . \quad . \quad . \quad . \quad (30)$$

where $\gamma^2$ is the resistance coefficient and was taken as $2{\cdot}6\times10^{-3}$. Unlike A, A′ remains finite when $c=V$. Dissipation by molecular viscosity is negligible for waves for which $c$ is several m./sec. If eddy viscosity is also negligible (as assumed by Sverdrup and Munk), the height attainable by waves under the influence of moderate and strong winds is limited only by the breaking steepness, provided the duration and fetch are both sufficiently great. In practice, it is observed that, while the shorter waves may be continually breaking, waves travelling with speeds approaching that of the wind seldom reach the breaking steepness, and usually do not exceed about 1/3 of that steepness. On Sverdrup and Munk's theory, the explanation given is that sufficiently large durations and fetches do not, in fact, occur to enable the long waves to reach a greater steepness.

If eddy viscosity is the limiting factor, we see that the wave steepness cannot exceed an equilibrium value given by

$$A+A'=W.$$

Taking A from equation (27) and A′ from equation (30), we find

$$ka_{\max} = \frac{\rho'[s(1-\beta)^2+2\gamma^2]}{4\rho K\beta^2}, \quad . \quad . \quad . \quad . \quad . \quad . \quad (31)$$

where $\beta=c/V$, and has been termed the " wage age ". Thus if $s$ and $\gamma^2$ are constant, or are functions of $\beta$ only, the equilibrium steepness is a function of the wave age, $\beta$, only. This general result is still true if A is given by either of the alternative equations (28) and (29).

From equation (31) the equilibrium steepness given by $ka_{\max}$ will be less than the breaking steepness, for which $ka=\pi/7$, if

$$\frac{\beta^2 K}{s(1-\beta)^2+2\gamma^2} > \frac{7\rho'}{4\pi\rho} \quad i.e. \quad > 6{\cdot}8\times10^{-4}$$

inserting the numerical values of $\rho'$ and $\rho$. We will consider two special cases of this condition :

(*a*) If $\beta=\frac{1}{3}$ and $\gamma^2$ is negligible,

$$K > 2{\cdot}72\times10^{-3}s.$$

With Jeffreys' value, $s=0{\cdot}27$, $K>7{\cdot}3\times10^{-4}$. With Sverdrup and Munk's value, $s=0{\cdot}013$, $K>3{\cdot}5\times10^{-5}$, but this is hardly valid, since the value $s=0{\cdot}013$ was derived empirically on the assumption that eddy viscosity was negligible.

(*b*) If $\beta=1$, then

$$K > 1{\cdot}36\times10^{-3}\gamma^2.$$

Taking $\gamma^2=2{\cdot}6\times10^{-3}$, $K>3{\cdot}5\times10^{-6}$.

Comparing these inequalities with the value of K deduced in § 5.3, it seems possible that eddy viscosity may limit the steepness of waves travelling with a speed approaching that of the wind, but unlikely that it will limit the steepness of waves travelling at about one-third of that speed.

A relation between wave steepness and wave age was, in fact, found empirically by Sverdrup and Munk. Until we have more data on the rate of transfer of energy from wind to waves, however, we cannot say whether the steepness of the longer waves is limited only by the duration and fetch, or by an eddy viscosity of the form we have been considering.

## § 8 The Effect on Waves of Turbulence due to other Causes.

It has sometimes been assumed that the turbulence affecting waves should be attributed to the effects of wind driven or other currents. Alternatively, it has been suggested that the turbulence affecting currents is derived from wave motion. Neither assumption is made in the present treatment, the turbulence being regarded as inherent in the wave motion itself. The wave motion generates the turbulence and the turbulence reacts on the wave motion. The question still arises, however, whether, in the presence of a shearing current, the increased turbulence would not

greatly increase the effective eddy viscosity for waves. A clue to the answer may be found in equation (10), from which it is seen that for dissipation of energy by turbulence to occur, the mean values of terms such as $[uw]\partial U/\partial z$ must be finite. This implies not only a correlation between $u$ and $w$, but also a correlation between $[uw]$ and $\partial U/\partial z$. It is assumed that, in the case of turbulence associated with the waves themselves, such correlations exist.

If we now consider the turbulence associated with, for example, a wind-driven current, there will undoubtedly be some components in the spectrum of turbulence of scale comparable with, or smaller than, the wavelength of the waves. These components will contribute to $[u^2]$ and $[w^2]$ in equation (10) and may possibly have a finite value of $[uw]$. It is only, however, if the contributions to $[u^2]$—$[w^2]$ and $[uw]$ have components which vary in phase with $\partial U/\partial x$ and $\partial U/\partial z$ respectively, that they will add anything to the dissipation of the waves. There is, therefore, no real discrepancy between the simultaneous existence of a large degree of turbulence due to other causes and a comparatively small eddy viscosity applicable to wave motion.

Acknowledgment.

It is a pleasure to record my thanks to Professor J. Proudman for his helpful criticism and suggestions in preparing this paper.

References.

Groen, P., and Dorrestein, R., 1950, *Nature, Lond.*, **165**, 445.
Jeffreys, H., 1925, *Proc. Roy. Soc.* A, **107**, 189.
v. Karman, Th., 1930, *Proc. 3rd Internat. Congress for Applied Mechanics, Stockholm*, **1**, 85.
Lamb, H., 1932, *Hydrodynamics*, 6th edn. (Cambridge : University Press).
Motzfeld, H., 1937, *Zeits. f. angew. Math. u. Mech.*, **17**, 193.
Munk, W. H., 1947, *Trans. Amer. Geophys. Un.*, **28**, 198.
Neumann, G., 1949, *Deutsche Hydrog. Zeits.*, **2**, 187.
Richardson, L. F., 1926, *Proc. Roy. Soc.* A, **110**, 709.
Richardson, L. F., and Stommel, H., 1948, *J. of Meteorology*, **5**, 238.
Sverdrup, H. U., and Munk, W. H., 1947, U.S. Hydrographic Office, Pub. No. 601.
V. Weizsäcker, C. F., 1948, *Zeits. f. Phys.*, **124**, 614.

## LXXXIII. *Search for the Negative Proton in Fission,*

By J. M. C. Scott * and E. W. Titterton,
Atomic Energy Research Establishment, Harwell, Berks †.

[Received May 17, 1950]

During the 1946 Cambridge Conference a paper was read by Broda, Feather and Wilkinson (1947) describing ionization chamber and chemical experiments designed to test the possibility of emission of a negative proton as an alternative to the emission of a $\beta$-particle and a neutron, which occurs in certain fission products and is responsible for the delayed neutrons. Recently Kuan-Han Sun (1949), who appears unaware of the experiments of Broda *et al.*, has suggested that the delayed neutron emitter $N^{17}$ might undergo negative proton decay. Still more recently, the situation has been reviewed by Feather (1949). The two competing reactions are :

$$X_Z^A \rightarrow Y_{Z+1}^{A-1} + (\beta^- + \nu) + n_0^1 + Q_1 \quad . \quad . \quad . \quad . \quad . \quad (1)$$

$$X_Z^A \rightarrow Y_{Z+1}^{A-1} + P^- + Q_2 \quad . \quad . \quad . \quad . \quad . \quad . \quad . \quad . \quad . \quad (2)$$

If the negative proton has the same mass as the positive proton ($H_1^1 - m_e c^2$), then from the known mass values (*cf.* Stephens 1949)

$$Q_2 = Q_1 + 1{\cdot}79 \text{ MeV}. \quad . \quad . \quad . \quad . \quad . \quad . \quad . \quad (3)$$

Since $Q_1$ is positive for the delayed neutron emitted in fisson, it follows that reaction (2) is energetically possible and non-relativistic negative protons might be emitted.

In the course of an investigation in this laboratory, involving the examination of large numbers of tracks formed by the slow neutron fission of $U^{235}$ in photographic plates, a search has been made for associated events which might furnish evidence of negative proton emission from a fragment. The delayed neutron emitters have lives ranging from about 0·05 to 56 seconds (Hughes *et al.*, 1948) and, as the fragments come to rest in the photographic emulsion in a time less than $10^{-11}$ sec., it might be expected that the negative proton would be emitted after the nucleus has stopped. If a slow negative proton is emitted the question arises as to its ultimate fate.

Among the possibilities are :

(i) annihilation with a proton in the emulsion with emission of two $\gamma$-rays ;

---

* Now at the Cavendish Laboratory, Cambridge.
† Communicated by the Authors.

(ii) capture by a heavy nucleus such as Ag or Br and subsequent annihilation with a proton of the nucleus with a chance that one of the $\gamma$-rays interacts with nucleons of the same nucleus leading to meson production and break-up of the nucleus to produce a " star ";

(iii) capture by a nucleus and conversion of the rest masses of the positive and negative protons into excitation energy of the nucleus in some other way, leading to a high energy nuclear explosion.

(iv) radiative capture by a nucleus which, unlike the first three, does not involve the annihilation of the " rest mass " of the particle.

The idea that negative protons may exist is derived ultimately from analogy with electrons. The hole theory, with its sea of occupied negative energy states, was first introduced as a complement to the Dirac electron theory and the discovery of the positron then fitted in naturally. The application of the same ideas to neutrinos is also generally accepted. In the case of protons, although the Dirac equation does not give the right magnetic moment, it nevertheless appears to be the proper way of describing particles with spin $\frac{1}{2}$. If the true relativistic theory of protons does include a hole theory and negative protons, it seems certain that they must be capable of annihilation with positive protons with emission of two $\gamma$-rays, just like positrons.

An objection to this view is as follows. If negative protons can be produced according to equation (2) which, omitting those nucleons not transformed, can be written :

$$N+N \rightarrow P^{+}+P^{-}+\text{k.e.} \quad . \quad . \quad . \quad . \quad . \quad . \quad . \quad (4)$$

then it might appear that two neutrons in any nucleus can annihilate by way of virtual creation of a negative proton as an intermediate state

$$N+N \rightarrow P^{+}+P^{-} \rightarrow 2\gamma, \quad . \quad . \quad . \quad . \quad . \quad . \quad . \quad (5)$$

and it follows that most known nuclei ought to explode. Thus if negative protons exist and are produced by Feather's process (2), it would seem likely that they cannot annihilate with positive protons, and therefore that they do not bear the same relation to protons as positrons do to electrons. This argument would only rule out the creation by Feather's process of a negative proton analogous to a positron. It is still possible to imagine a negative particle which cannot turn its rest energy into photons in this way. If created by Feather's process, it would then be absorbed by process (iv), *e. g.*

$$Br^{79}+P^{-} \rightarrow Se^{80}+\text{energy} \quad . \quad . \quad . \quad . \quad . \quad . \quad . \quad (6)$$

and gamma rays would be emitted similar to those from neutron capture. However, it does seem reasonable to postulate the existence of the anti-protons demanded by the hole theory, and meet the above objection by supposing that the neutrons occurring in nature can only react with anti-neutrons, and to assume that these (like positrons) do not normally occur in nature.

If we assume, therefore, that a negative proton can undergo annihilation with a proton, we may calculate the probability of the process by regarding it as the dropping of an ordinary proton into a hole. Even if the Dirac equation is not strictly valid for protons (in view of the magnetic moment difficulty) it seems to likely give the correct order of magnitude. The mathematical argument is the same as that for electrons, and gives a cross-section for negative protons (of velocity $v \leqslant c$)

$$\sigma = \pi e^4 / M^2 c^3 v, \quad . \quad . \quad . \quad . \quad . \quad . \quad . \quad . \quad . \quad (7)$$

and a lifetime of the order of $10^{-3}$ seconds in a material containing free protons. This time is much longer than that required for the particle to come to rest in the emulsion, so if the particle escapes from the fission fragment nucleus at all it ought not to be annihilated in flight.

These arguments lead to the view that possibilities (i) and (iv) above would allow a negative proton to be observed in the emulsion as a track of appreciable length emanating from the end of a fission track. Possibilities (ii) and (iii) on the other hand would give rise to a track leaving the end of a fission fragment and terminating in a star of tracks, some of which would be at low energy.

In the experiments which have been carried out in this Establishment some $6{\cdot}5 \times 10^5$ fission tracks representing $1{\cdot}3 \times 10^6$ fission fragments have been examined. About half were in Ilford $C_2$ emulsions sensitive to protons of energy up to 40 MeV and half in $D_1$ emulsions which, under the conditions of the experiment, recorded protons up to a maximum energy of 2·5 MeV. No tracks longer than $3\mu$ (proton energy $\sim$300 kV) were observed associated with the ends of fission tracks though many knocked-on protons (identified from the geometry of the events) were observed along the fragment tracks. One case of a 3-particle star having its origin at the end of a fission track was shown to be a chance juxtaposition of events. It was identified as being similar to many other stars found in the emulsions resulting from the decay of chains of $\alpha$-emitters present as contaminant in the uranium solutions employed for impregnating the plates.

From this result it appears that negative proton emission, if it occurs at all, is an improbable process. Accepting 0·8 per cent (Hughes *et al.*, 1948) as the yield of delayed neutron emitters in the slow neutron fission of $U^{235}$ the experiment allows us to set an upper limit of 1 in $5 \times 10^3$ to the probability of negative proton emission relative to delayed neutron emission from these fragments.

We thank the Director, A.E.R.E., for permission to publish this paper.

## References

Broda, Feather and Wilkinson, 1947, *Report on an International Conference on Fundamental Particles held at the Cavendish Laboratory, Cambridge, in July* 1946. (London: Published by the Physical Society) p. 114.

Feather, 1949, *Edinburgh Conference, November*, 1949.

Hughes, Dabbs, Cahn and Hall, 1948, *Phys. Rev.*, **73**, 111.

Kuan-Han Sun, 1949, *Phys. Rev.*, **76**, 1266.

Stephens, 1949, *Phys. Rev.*, **76**, 181.

# LXXXIV. *The Emission of Short Range Alpha Particles from Light Elements under Proton Bombardment.*—III. *The Reactions* $^{6}Li(p\alpha)^{3}He$ *and* $^{7}Li(p\gamma)^{8}Be^{*}$.

By W. E. Burcham and Joan M. Freeman,
Cavendish Laboratory, Cambridge †.

[Received June 14, 1950.]

Summary.

The emission of short range alpha particles associated with the 14·8 MeV. gamma radiation produced in the $^{7}Li(p\gamma)$ reaction has been established. The energy distribution of these particles can be interpreted as due to a level in the $^{8}Be$ nucleus at $3030\pm100$ keV. energy, with a width of 2000 keV.

Some observations on the energy release ($3{\cdot}97\pm0{\cdot}03$ MeV.), cross section and excitation function for the $^{6}Li(p\alpha)^{3}He$ reaction are also presented.

## §1. Introduction.

The disintegration of $^{7}Li$ by protons is of particular interest since a well known resonance level of the compound nucleus $^{8}Be$ can easily be observed. The properties of this level have been studied in detail by Devons and Hine (1949) by observations on the capture reaction

$$^{7}Li+{}^{1}H \rightarrow {}^{8}Be^{*} \rightarrow {}^{8}Be+\gamma_1. \quad . \quad . \quad . \quad . \quad . \quad . \quad (1)$$

The energy of the gamma radiation emitted by the excited $^{8}Be^{*}$ nucleus formed in this reaction was measured by Walker and McDaniel (1948) and components of 14·8 MeV. and 17·6 MeV. were found. The energy 17·6 MeV. agrees with that expected if the $^{8}Be$ nucleus is left in its (unstable) ground state after the emission of the radiation. The 14·8 MeV. component could be due to a transition to an excited state of energy 2·8 MeV. in the $^{8}Be$ nucleus, in accordance with the reaction

$$^{7}Li+{}^{1}H \rightarrow {}^{8}Be^{*} \rightarrow {}^{8}Be^{**}+\gamma_2. \quad . \quad . \quad . \quad . \quad . \quad . \quad (2)$$

Evidence from other reactions for the existence of such a state is summarized by Wheeler (1941), and a $^{8}Be$ nucleus left in this state is known to break up with the emission of two alpha particles of about 1·4 MeV. energy ‡. It follows that short range alpha particles should be associated

† Communicated by O. R. Frisch.

‡ (*a*) The energy of the alpha particle pair exceeds the energy of the excited state by $89\pm5$ keV., which is the disintegration energy of the ground state of $^{8}Be$ according to the measurements of Tollestrup, Fowler and Lauritsen (1949).

(*b*) Reaction (2) and the subsequent alpha particle emission might be referred to as the $^{7}Li(p\gamma',\alpha)^{4}He$ reaction, in accordance with the terminology adopted by Fowler, Lauritsen and Lauritsen (1948), but in this paper the abbreviation $^{7}Li(p\gamma)^{8}Be^{*}$ will be used.

with the 14·8 MeV. gamma radiation observed in the Li($p\gamma$) reaction, providing that this radiation results from a transition to the alpha-emitting level of $^{8}$Be. In the present work, of which a preliminary account has already been given (Burcham and Freeman 1949 a), such alpha particles were found and their energy distribution was examined and compared with that predicted from the gamma ray spectrum.

In the course of this work a number of check experiments were made on the disintegration of $^{6}$Li by protons, mainly in order to assess the contamination by the lighter isotope of targets of separated $^{7}$Li. The results of these observations are also presented.

## §2. Experimental Method.

### (a) *General.*

The apparatus used in these experiments has been previously described (Burcham and Freeman 1949 b, 1950; subsequently referred to as I, II). In some of the work the analysing magnet was turned on its side so that observations could be made in a horizontal plane and the target could be brought nearer the high voltage accelerating tube; larger currents could so be obtained.

### (b) *Targets.*

Thin lithium targets were prepared by evaporating the metal *in vacuo* on to copper discs. During transference from the evaporator to the target chamber these targets lost their metallic lustre and were presumably converted into lithium hydroxide or carbonate† (*cf.* Bonner and Evans 1948 b). Targets of the $^{7}$Li and $^{6}$Li isotopes (similarly oxidized by exposure to air) were also available. These were deposited on copper, silver or aluminium backings in the small electromagnetic separator at the Atomic Energy Research Establishment, Harwell, and had surface densities, calculated from the ion current, of between 10 and 100 $\mu$gm./cm.$^{2}$ of lithium before exposure to the atmosphere. A fairly satisfactory thin target of $^{7}$Li was also prepared by converting a $^{7}$Li sample into sulphate and evaporating *in vacuo* on to a copper button.

Target thicknesses in keV. equivalent energy for protons and alpha-particles were calculated assuming a stopping power of 400 keV./mgm./cm.$^{2}$ for lithium carbonate for protons of 400 keV. energy. This value is consistent with the results of Warshaw (1949), with the figures given by Bonner and Evans (1948), and also with direct measurements made by comparison of the shape of the $^{7}$Li($p\gamma$) resonance curve with that obtained from a thick target of the same composition (*cf.* Tangen 1946). The targets used were of thickness equivalent to 10–90 keV. energy for protons.

† The surface densities given refer to the oxidized deposit except where it is otherwise stated.

## §3. Results for $^6$Li.

The disintegration of $^6$Li by protons leads to the emission of short range alpha particles and $^3$He nuclei according to the reaction

$$^6\text{Li} + ^1\text{H} \rightarrow ^3\text{He} + ^4\text{He}. \quad \ldots\ldots\ldots \quad (3)$$

Fig. 1.

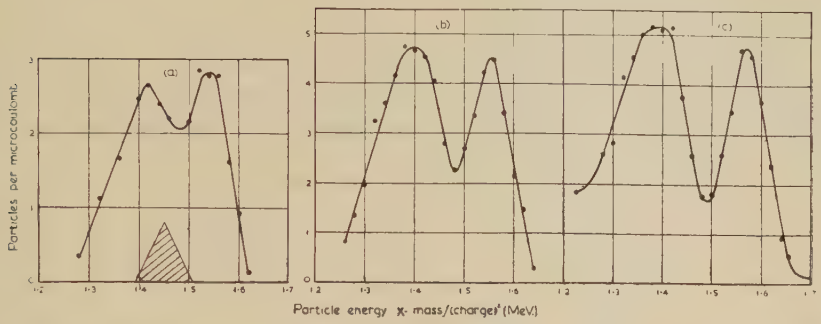


Alpha particles and $^3$He nuclei from the reaction $^6\text{Li}(p\alpha)\,^3\text{He}$. Angle of observation 135°. Proton energy (*a*) 330 keV., (*b*) 630 keV., (*c*) 930 keV. Target thickness 90$\mu$gm./cm.$^2$. The shaded triangle gives the analyser resolution.

Fig. 2.

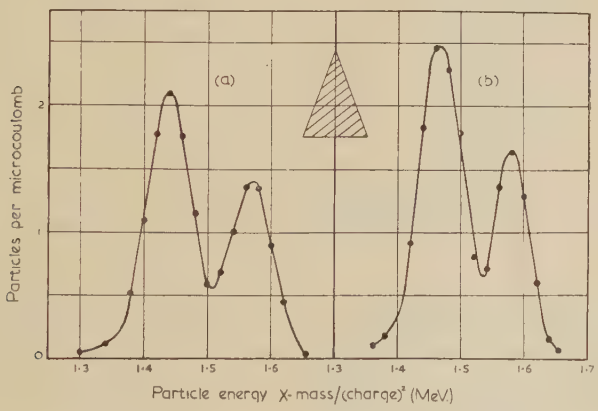


Alpha particles and $^3$He nuclei from the reaction $^6\text{Li}(p\alpha)^3\text{He}$. Angle of observation 135°. Proton energy (*a*) 380 keV., (*b*) 450 keV. Target thickness 15$\mu$gm./cm.$^2$. The shaded triangle gives the analyser resolution.

References to determinations of the energy release in this reaction and to observations on the cross section, excitation function and angular distribution are given by Hornyak and Lauritsen (1948) and a later determination of the enegy release as 4·017±·022 MeV. has been published by Tollestrup, Fowler and Lauritsen (1949).

Fig. 1 (*a*), (*b*), (*c*) shows the spectrum of particles obtained from an ordinary lithium target of surface density 90 $\mu$gm./cm.$^2$. The curves were all taken with an analyser resolving power of 50 (4 per cent resolution in energy) and at an angle of observation of 135° with the proton beam.

Bombarding energies of 930, 630 and 330 keV. were used, and the $^6$Li($p\alpha$) yield was monitored by simultaneous observation of the alpha-particles from the $^7$Li($p\alpha$)$^4$He reaction. Fig. 2 (*a*), (*b*) gives curves taken at the same angle, and with the same resolution, for bombarding energies of 380 and 450 keV. and with a target of surface density 15 $\mu$gm./cm.$^2$; these two curves were used for detailed comparison with the results obtained with thin $^7$Li targets.

The two groups in figs. 1 and 2 are the $^4$He and $^3$He particles emitted in reaction (1). The energy of these particles observed at 135° does not vary greatly for the range of bombarding energies 300–900 keV. This simplified the determination of an excitation function for the reaction

Fig. 3.

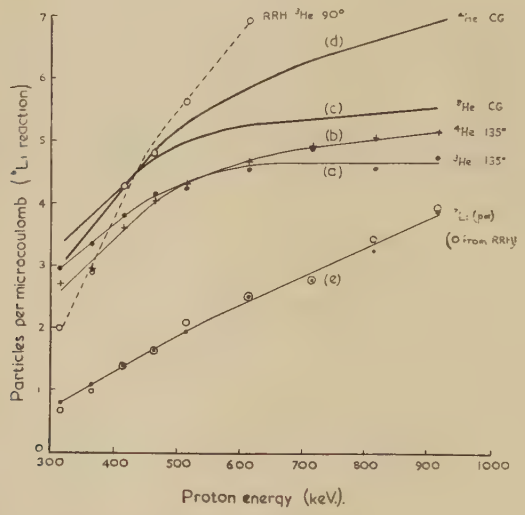


Excitation function for the reaction $^6$Li($p\alpha$)$^3$He; angle of observation 135°. (*a*) $^3$He nuclei, (*b*) $^4$He nuclei, (*c*) $^3$He yield corrected for motion of mass centre, (*d*) $^4$He yield corrected for motion of mass centre, (*e*) yield of $^7$Li($p\alpha$)$^4$He reaction on a different scale; ○ observations of Rumbaugh, Roberts and Hafstad at 90°.

over this range, since it was only necessary to set the analyser field for the peak of either group and to take counts for a series of bombarding energies; checks were made at a number of points to ensure that the analyser field was correctly set. The yield of reaction (1) so observed for the 90 $\mu$gm./cm.$^2$ target is shown in fig. 3; curves (*a*) (*b*) give the actual observations for the $^3$He and $^4$He particles, and curves (*c*) (*d*) are corresponding smoothed curves after correction for centre of mass motion. The angle in the mass-centre system for which the observations are actually made depends on the bombarding energy and varies from 139° to 143° over the energy range studied. The $^3$He particles correspond to alpha particles emitted in the forward direction between angles of 30°

and 38°, and the difference in yields for proton energies above 500 keV. suggests that the angular distribution of reaction (3) is asymmetric, though at lower energies there appears to be isotropy, in agreement with the results of Neuert (1938). The true asymmetry of the angular distribution is probably more than is suggested by fig. 3, since the curves of fig. 2, taken with a very thin target, show an even larger $^4$He/$^3$He ratio at 135°. This is due in part to the fact that the observed yield of a group of particles of given energy increases with target thickness as previously described (II, fig. 2), and the target thickness necessary for the maximum yield of the $^3$He particles (of energy about 2·1 MeV.) is greater than that required for the maximum yield of the $^4$He particles (energy 1·5 MeV.). In the case of the $^6$Li($p\alpha$) reaction the target thicknesses necessary for maximum yield of the $^3$He and $^4$He particles (allowing for the difference in stopping power of the target for the two particles) are about 100 and 60 $\mu$gm./cm.$^2$ respectively for an analyser resolution of 4 per cent. If a rough correction for this effect is made for the 90 $\mu$gm./cm.$^2$ target a $^4$He/$^3$He ratio in agreement with that obtained from the 15 $\mu$gm./cm. target is found.

The observations of Rumbaugh, Roberts and Hafstad (1938) on the yield of this reaction are also plotted (after fitting at the 430 keV. point) in fig. 3; their figures for the $^3$He group at 90° show a much more rapid rise than the present results, although the increase in intensity of the $^7$Li($p\alpha$) reaction used for monitoring (fig. 3 (*e*)) was in agreement with their results. The resolution shown in the curves of fig. 1 is sufficient to make the relative excitation function reliable to about 10 per cent. As an extra check an excitation function was plotted using as detector an electron multiplier in which a mica screen was inserted to prevent the $^4$He particles being detected. The $^3$He particles were thus recorded with uniform efficiency over the energy range studied; the excitation curve obtained agreed well with that shown in fig. 3.

The energy release in reaction (3) was calculated from the curves of fig. 1, using "extrapolated" energies in order to eliminate the target thickness correction (*cf.* II, §2 a). A special analyser calibration for "extrapolated" energies was used to replace that of I, fig. 8, and in this calibration the Q values for the reference reactions $^9$Be($p\alpha$)$^6$Li and $^9$Be($pd$)$^8$Be were changed from the values given in I to the latest values (2·121 MeV. and 0·558 MeV.) published by Tollestrup, Fowler and Lauritsen (1949). A carbon deposit formed on the targets during bombardment and the thickness of this film was found as described in II, §2 (a) to be $8\pm3$ keV. for protons; a correction of $32\pm12$ keV. to the alpha particle energy and $27\pm12$ keV. to the $^3$He energy has therefore been made. The results for the 90 $\mu$gm./cm.$^2$ target are given in Table I.; no estimation of carbon thickness was made for the 15 $\mu$gm./cm.$^2$ target, and energy releases deduced from the curves of fig. 2 have therefore not been included. The error in each of the stated Q values arises chiefly from the correction for carbon thickness and the uncertainties in proton energy ($\pm10$ keV.) and

in calibration of the analyser for extrapolated energies (±15 keV.) and amounts to ±40 keV. Assuming that the observations provide three independent values for Q the mean value for the energy release in the $^6$Li($p\alpha$) reaction is

$$Q = 3{\cdot}97 \pm {\cdot}03 \text{ MeV.}$$

This lies between the older values listed by Hornyak and Lauritsen (1948) and the latest figure given by Tollestrup, Fowler and Lauritsen (1949).

The cross section for reaction (3) was obtained by comparing the yield of the $^6$Li($p\alpha$) reaction with that of the $^{10}$B($p\alpha$) and $^9$Be($p\alpha$) reactions. The $^6$Li target used had a surface density, estimated from the ion current in the electromagnetic separator, of 5·4 μgm./cm.$^2$ of the isotope before oxidation, the $^{10}$B target was the 38 μgm./cm.$^2$ target used in II, and the

Table I.

Energy release in the $^6$Li($p\alpha$)$^3$He reaction.

| Proton energy (keV.) | $^3$He energy (keV.) | $^4$He energy (keV.) | Q(MeV.) | |
|---|---|---|---|---|
| | | | From $^3$He energy | From $^4$He energy |
| 322 | 2122 | — | 3·98 | — |
| 622 | 2152 | 1482 | 4·00 | 3·95 |
| 922 | 2162 | 1482 | 3·96 | 3·95 |

$^9$Be target was deposited by vacuum evaporation and found to have a surface density of 16 μgm./cm.$^2$ by direct weighing. The yields from these targets were assumed to be proportional to the integral $\int \frac{N(E)\,dE}{E}$ taken over the observed alpha-particle group, N(E) being the number of alpha particles recorded when the setting of the analyser corresponded to an energy E. The small variation of yield due to the slowing down of the incident protons in the target was neglected The integrals were evaluated graphically and it was found that, assuming isotropic distributions in the centre of mass system,

$$\frac{\sigma^6\text{Li}\,(p\alpha)(330 \text{ keV.})}{\sigma^{10}\text{B}\,(p\alpha)(330 \text{ keV.})} = 10{\cdot}8,$$

$$\frac{\sigma^6\text{Li}\,(p\alpha)(330 \text{ keV.})}{\sigma^9\text{Be}\,(p\alpha)(530 \text{ keV.})} = 0.65.$$

The cross section for the $^{10}$B($p\alpha$) reaction for a proton energy of 330 keV. was taken to be $4{\cdot}5 \times 10^{-27}$ cm.$^2$ (II), and that for the $^9$Be($p\alpha$) reaction for a proton energy of 530 keV. to be $1{\cdot}3 \times 10^{-25}$ cm.$^2$ (Thomas, Rubin,

Fowler and Lauritsen 1949). The corresponding values for the $^6$Li($p\alpha$) cross section for a proton energy of 330 keV. are $4{\cdot}9\times10^{-26}$ cm.$^2$ and $8{\cdot}5\times10^{-26}$ cm.$^2$. The difference between the two values is probably due to systematic errors in the cross sections assumed : the latter value exceeds the cross section of $5\times10^{-26}$ cm.$^2$ obtained from the results of Bowersox (1939) and both are very much greater than the value of $8{\cdot}5\times10^{-27}$ cm.$^2$ deduced from the curves given by Rumbaugh, Roberts and Hafstad (1938).

## §4. Results for $^7$Li.

A search for the emission of short range alpha particles in reaction (2) was first made by bombarding a thin target of ordinary lithium with protons. Fig. 4 (*a*), (*b*) shows the results obtained with a target of surface

Fig. 4.

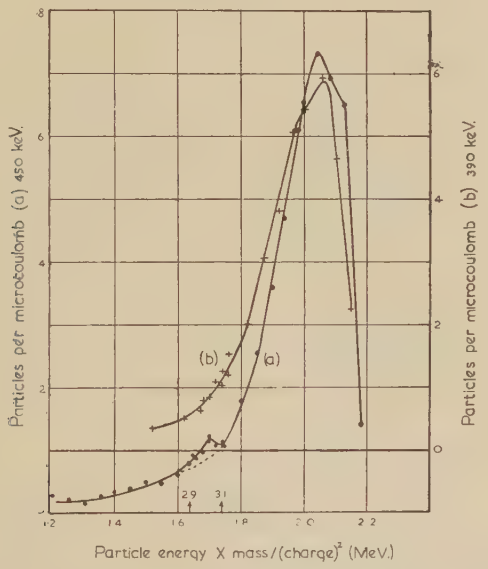


Alpha particles and $^3$He nuclei from ordinary lithium bombarded by protons of energy (*a*) 450 keV. ; (*b*) 390 keV. The arrows show the position in which short range alpha particles emitted in the $^7$Li($p\gamma$)$^8$Be* reaction would be expected for disintegration energies of $^8$Be of 2900 and 3100 keV.

density 17 $\mu$gm./cm.$^2$ (equivalent thickness about 20 keV. at the angle used), an angle of observation of 60° and an analyser resolution of 8 per cent ; curve (*a*) was taken at a bombarding voltage of 450 keV., at which the ($p\gamma$) resonance was observed, and curve (*b*) at 390 keV. for which there should have been very little effect due to the resonance level. The corrections for target thickness and carbon deposit were made by shifting the energy scale until the $^3$He and $^4$He peaks fitted the values expected from the energy release in reaction (3). The position of alpha particles

expected from the disintegration of a $^{8}$Be nucleus with an energy release of 2900 and 3100 keV. is also shown and there is some slight evidence for the appearance of extra particles in this region on curve (*a*). The intensity of the incompletely resolved $^{6}$Li($p\alpha$) group was estimated by integrating over the distribution and was compared with that of the small group which might be due to the $^{7}$Li($p\gamma$)$^{8}$Be* reaction. Using the $^{6}$Li($p\alpha$) cross section given in § 3, the thick target yield of disintegrations leading to the emission of 14·8 MeV. gamma radiation was estimated to be $2{\cdot}1\times10^{-10}$ per incident proton for a target of LiOH. The predicted figure is $1{\cdot}75\times10^{-9}$, derived from the thick target yield of $5{\cdot}35\times10^{-9}$ quanta (14·8+17·6 MeV. radiation) per proton (Fowler, Lauritsen and Lauritsen 1948), and the ratio 0·33 of the intensity of the 14·8 MeV. radiation to that of the total radiation at resonance (Walker and McDaniel 1948). The difference between the observed and predicted yields is probably due to the bad definition of the small alpha-particle group shown in fig. 4.

Fig. 5.

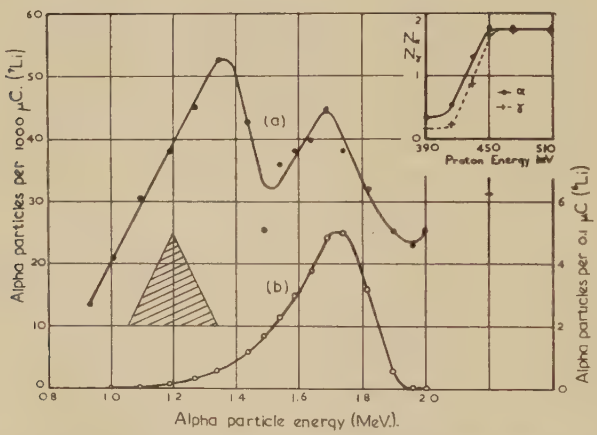


Alpha particles from lithium isotopes bombarded with 440 keV. protons. Angle of observation 104°. (*a*) $^{7}$Li; (*b*) $^{6}$Li. The shaded triangle gives the analyser resolution. Inset: Yield of gamma radiation and of alpha particles from $^{7}$Li as a function of proton energy.

In order to reduce the effect of the $^{6}$Li($p\alpha$) group, targets of the lithium 7 isotope deposited on copper backings were bombarded. The lithium 7 samples were enriched by a factor of about 500 over normal lithium, but owing to the low cross section for reaction (2) and the high cross section for the $^{6}$Li($p\alpha$) process, and to the fact that the first targets used were more than 100 keV. thick, the yields from the two reactions were of the same order of magnitude. In the first experiments with thick targets, the background due to the $^{6}$Li groups had to be subtracted, and the analyser resolution was therefore set at 12 per cent in order to increase the counting rate and improve the statistical accuracy. The curve given in fig. 5 (curve

(*a*)) which is that already published (Burcham and Freeman 1949 a, fig. 2), but transferred to an energy scale, is typical of these results ; a bombarding energy of 440 keV. and an angle of observation of 104° were used. There is clearly a group of particles centred at an energy of 1·38±0·08 MeV., and of width about 0·45 MeV., which cannot be due to contamination of the target by $^6$Li. The group observed from a thick $^6$Li isotopic target is shown in fig. 5 curve (*b*) ; such contamination, in the correct proportion. could evidently account for the higher energy group shown in curve (*a*). In order further to establish the identity of the group of alpha particles of mean energy 1·38 MeV., the excitation function of this group was compared with that of the total gamma radiation over the range 350–700 keV. Part of the two curves is shown in fig. 5 (inset), and the close similarity between them definitely establishes the connection between the 1·38 MeV. alpha particles and the resonant gamma radiation. With certain assumptions, discussed in §5, these results indicate the existence in $^8$Be of a level, unstable with respect to alpha particle emission, at 2900±200 keV. above the ground state and with a width of 900 keV. or less. The work described later in this section, in which the $^6$Li contamination was less important, modifies these conclusions.

In order to see whether the higher energy group of fig. 5 (*a*) could also be attributed in part to the $^7$Li($p\gamma$)$^8$Be* reaction, the contamination of the $^7$Li target by $^6$Li was estimated quantitatively, using the $^6$Li($d\alpha$) reaction as an indicator. The results obtained for the $^7$Li target and a thin $^6$Li target for comparison, were as follows :

$^7$Li target : Intensity of $^6$Li($d\alpha$) group=65±20 alpha particles/1000 $\mu$C.

$^6$Li target : Intensity of $^6$Li($d\alpha$) group=203±10 alpha particles/1000 $\mu$C.

$^6$Li target : Intensity of $^6$Li($p\alpha$) group=115±5 alpha particles/1000 $\mu$C.

From these figures the intensity of the $^6$Li($p\alpha$) group on the $^7$Li target was expected to be 37±11 per 1000 $\mu$C., while the intensity found was 44±5 ; the second group could thus, within the limits of error, be ascribed entirely to $^6$Li contamination.

For a given isotopic enrichment the $^6$Li contamination becomes relatively less important in comparison with the effect from $^7$Li as the target thickness decreases until a target of thickness equal to the width of the ($p\gamma$) resonance (14 keV.) is reached. Experiments were therefore made with thinner targets ; fig. 6 shows the results obtained with an evaporated $^7Li_2SO_4$ target. The thickness of the target is shown by the inset curve, which gives the gamma-ray yield as a function of bombarding voltage with a beam of 20 keV. spread in energy. Curves (*a*) (*b*) (*c*) (*d*) give the alpha-particle yields for bombarding voltages of 390, 450, 550 and 750 kV. taken with the analyser at an angle of 135° with the proton beam. The resonant character of the alpha-particle distribution and the presence of a group which may be ascribed to $^6$Li contamination are again shown. The energy level in $^8$Be deduced from these observations is centred at

3200 keV. above the ground state, and has a width of less than 1100 keV., though both these conclusions are uncertain owing to the presence of the $^6$Li contamination.

Fig. 6.

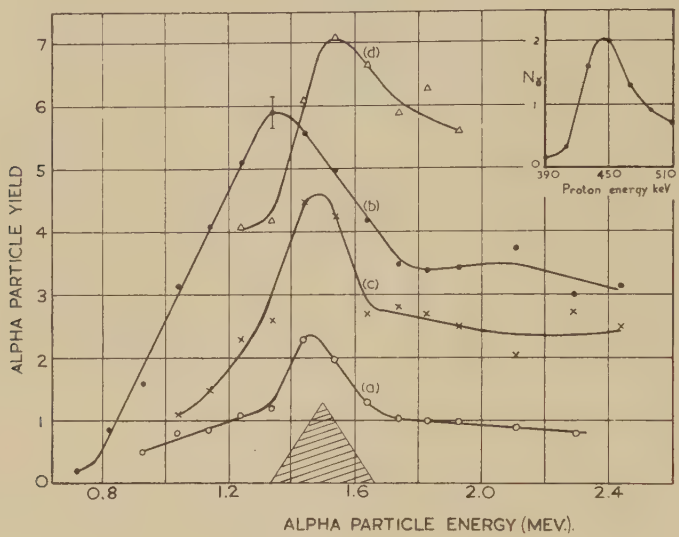


Alpha particles from thin $^7Li_2SO_4$ target bombarded by protons of energy (*a*) 390 keV., (*b*) 450 keV., (*c*) 550 keV., (*d*) 750 kev. Angle of observation 135°. Inset : Yield of gamma radiation as a function of proton energy.

Fig. 7.

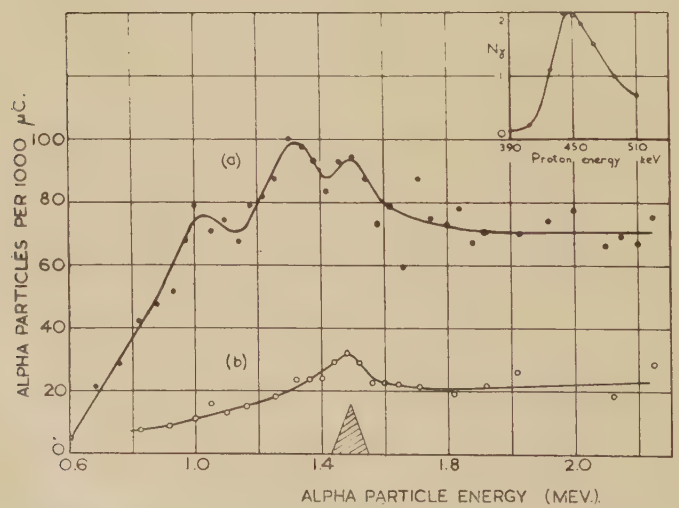


Alpha particles from a thin target containing 50$\mu$gm/cm$^2$ of $^7$Li bombarded by protons of energy (*a*) 450 keV., (*b*) 390 keV. Inset: Yield of gamma radiation as a function of proton energy. The shaded triangle gives the analyser resolution.

At this stage more uniform depositis of $^7$Li of known density became available, and it was then possible to use thin targets with a higher percentage of lithium than in $Li_2SO_4$. Fig. 7 gives the alpha-particle spectrum obtained from an aluminium foil on which 50 $\mu$gm./cm.$^2$ of $^7$Li had been deposited (as estimated from the ion current in the electromagnetic separator). The inset curve gives the gamma ray yield, and the alpha-particle spectra were taken for bombarding voltages of 450 keV. (curve (*a*)) and 390 keV. (curve (*b*)) ; in both cases the angle of observation was 135° and the analyser resolution 4 per cent in energy. The yields for the 450 keV. observations were monitored by simultaneous observation of the total gamma-ray intensity. For a target of this thickness the curves of fig. 2 and the excitation function given in fig. 3 show that the yield of particles from $^6$Li contamination will change by only about 10 per cent between 390 and 450 keV., and the 390 keV. curve of fig. 7 has therefore been used as a background determination and subtracted from the 450 keV. alpha-particle spectrum. Since the resolution width of the analyser (60 keV. at 1500 keV.) is considerably less than the width of the alpha-particle distribution a normalizing factor for intensity must be used to give the true distribution. This factor was obtained by the method used by Thomas, Rubin, Fowler and Lauritsen (1949) in which the analyser was used to study particles scattered elastically at different energies from a thick copper target ; comparison of the observed distribution with that expected from the Rutherford scattering law gives the normalizing factor.

The ordinates of fig. 7, after correction for background, were each multiplied by the observed normalizing factor, and the resulting alpha-particle distribution is plotted in fig. 8 (curve (*a*)). The shape of this distribution may still be distorted at low energy, since the normalizing factor was obtained under conditions of high gain and low bias, while in the observation of the alpha-particle spectrum the bias was increased to discriminate against scattered protons. Similar observations for proton energies of 450 keV. and 390 keV., and an angle of 135° were made with other thin targets containing 30–50 $\mu$gm./cm.$^2$ of $^7$Li ; several of these targets showed no appreciable effect due to $^6$Li contamination. Long counting periods were necessary with the analyser resolution used, and correction had to be made for the gradual growth of carbon deposit on the targets during the experiments. This growth was estimated by periodic observation of the $(p\gamma)$ resonance curve. Fig. 8 (*b*) is the result of adding together all the thin target observations after correction for the carbon deposit, and after normalization and removal of background ; the curve has the same appearance as that of fig. 8 (*a*), although it is shifted in energy owing to the carbon correction. Most of the thin target observations showed the structure which appears in both fig. 8 (*a*) and fig. 8 (*b*), although the statistical errors (indicated in fig. 8 (*b*)) are large, and it would be permissible to draw a curve with a single peak through the points. The interpretation of this curve is discussed in §5 ; by integration over it the number of disintegrations leading to the production of 14·8 MeV. gamma

radiation in the targets used (all of thickness greater than the resonance width) was found to be $1{\cdot}05\times10^{-9}$ per proton, which is to be compared with the predicted figure of $1{\cdot}75\times10^{-9}$ for a thick LiOH target. The difference is probably not significant in view of the uncertainty of target composition, and of the fact that the bias used in the alpha particle observations may have reduced the efficiency of detection below 100 per cent at low energies. The integrated yield was found to be about 20 times the peak yield with the analyser resolution used.

A simultaneous observation of the alpha particle and gamma ray excitation functions was made for one of the 30 $\mu$gm./cm.$^2$ targets for alpha

Fig. 8.

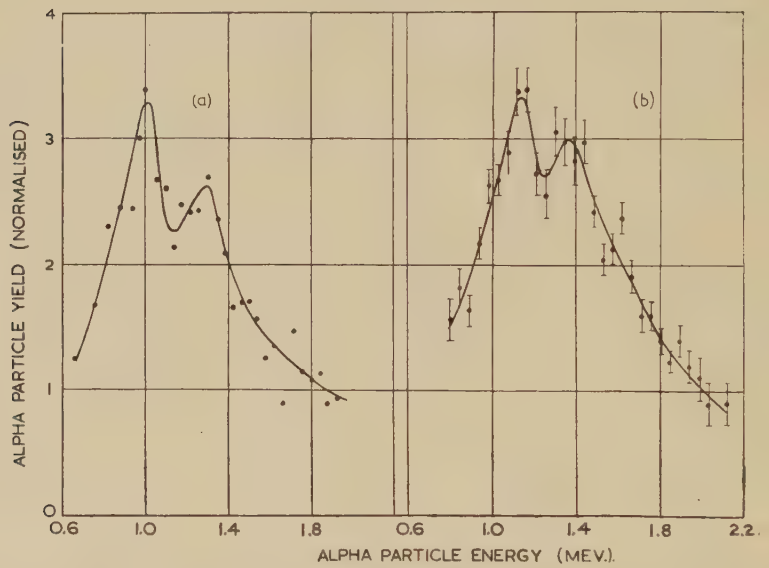


Alpha particles from thin $^7$Li targets bombarded by protons of energy 450 keV. Angle of observation 135°. (*a*) Observations shown in Fig. 7 (*a*), normalized and with background subtracted. (*b*) Combination of all normalized observations.

particles of energy 970, 1235 and 1500 keV.; the curves, of which that for 1500 keV. is shown in fig. 9, were all very similar.

The observation of resonant alpha particles at energies as high as 1500 keV. makes it extremely unlikely that the effects observed can have been in any way due to protons multiply scattered within the analyser: the impluses from the 1500 keV. alpha particles were several times larger than those from the protons of 450 keV.

During the course of this work the alpha particle spectrum was observed at a number of different angles, chiefly with the object, in the case of the thicker targets, of finding the angle at which the separation of the $^7$Li

and $^{6}$Li groups was best. Low resolution observations of this type showed no large differences in yield or spectrum of the resonant alpha particles over the range 45°–135°.

## §5. Discussion

The results presented in §4 make it certain that there is a resonant emission of alpha particles associated with the 14·8 MeV. resonant gamma radiation from the $^{7}$Li($p\gamma$) process. Walker and McDaniel (1948) observed that the energy of the 14·8 MeV. radiation increased with increasing proton energy, and the emission of alpha particles must therefore follow that of the gamma radiation. The approximate agreement between the alpha particle and gamma ray yields makes it unlikely that there is any

Fig. 9.

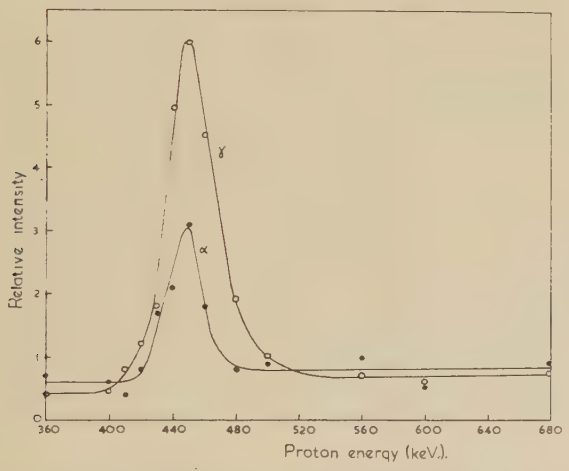


$^{7}$Li($p\gamma$)$^{8}$Be* : simulanteous excitation curves for emission of alpha particles and gamma radiation. Alpha particle energy 1500 keV.

strongly competitive mode of break-up of the excited $^{8}$Be nuclei left after the emission of the 14·8 MeV. radiation in accordance with reaction (2).

The precise interpretation of the results given in fig. 8 (*b*) is difficult, since the alpha particles are emitted from a $^{8}$Be nucleus whose momentum is partly determined by the recoil due to emission of a quantum of 14·8 MeV. radiation. The angular distribution of the 14·8 MeV. radiation with respect to the incident proton is not known in detail, and the velocity distribution of the $^{8}$Be nuclei produced in reaction (2) therefore cannot be calculated. On the assumption of an isotropic distribution of recoil momenta, the single alpha particle spectrum which would be observed at 135° when the $^{8}$Be nuclei are left with an excitation energy of 3000 keV. was calculated and found to be of width about 400 keV. The centre of

the distribution corresponded within 50 keV. with the energy expected if the gamma ray recoil had been neglected. In interpreting the alpha particle spectra obtained in this work, it has therefore been assumed, as a first approximation, that the gamma ray momentum may be neglected for the determination of the position of the energy level involved from the observed maximum yield. The deduction of the true width of the level or levels corresponding to the observed distribution of alpha particles is more difficult, since the relative importance of the recoil effect depends on the actual width of the level. If the width due to recoil (assumed constant over the spectrum) is $\Delta$ and the true width of the level is $\Gamma_0$ the observed width should be given approximately by

$$\Gamma=\sqrt{(\Gamma_0^2+\Delta^2)}.$$

The validity of this formula was checked by graphical construction for a number of assumed values of $\Gamma_0$.

The work of Walker and McDaniel indicates a level of $^8$Be of width about 2100 keV. Neglecting the influence of recoil, in a first approximation, this corresponds to a real width $\Gamma_0$ of 1050 keV. for the energy spectrum of single alpha particles. With $\Delta=400$ keV. the observed width would be $\Gamma=1120$ keV., which is in good agreement with the value of 1100 keV. calculated from fig. 8 (*b*). The $^8$Be level reported by Walker and McDaniel is at an excitation of 2800 keV. above the ground state or 2900 keV. above the state representing two free alpha particles ; there is an uncertainty of about 200 keV. in this figure. Again neglecting recoil, the peak of the alpha-particle spectrum should be at $1450\pm100$ keV., which is in agreement with the value of $1560\pm50$ keV. calculated from the mid-point of the curve of fig. 8 (*b*). The present results are therefore in agreement with the work of Walker and McDaniel within the limits of error of the experiments.

The curve given in fig. 8 (*b*) shows evidence of a structure which was observed in a number of the thin target experiments made with an analyser resolution of 4 per cent. The statistical fluctuations were, however, always large, and it has not so far been possible to obtain reliable evidence for a splitting of the $^8$Be level concerned. Further experiments, with larger intensities, and designed to display the total energy of the alpha particle pair, would be desirable to clarify this point†. The curve

† (*a*) R. M. Littauer and P. Meyer have recently studied the alpha-particle spectrum in this laboratory using an analyser with increased resolution, solid angle, and coverage, and with large bombarding currents. Their results suggest a single level.

(*b*) The possibility that the double peak shown in fig. 8 (*b*) is connected with a strong anisotropy in the emission of the 14·8 MeV gamma radiation is rendered unlikely by recent unpublished measurements by Devons and Lindsey on the angular distribution of this radiation. A study of the correlation between the direction of emission of the 14·8 MeV. gamma radiation and the following alpha particles is being attempted.

of fig. 8 (*b*) is therefore taken to indicate a single level in $^{8}$Be at an excitation energy of $3030 \pm 100$ keV. above the ground state and a real width of about 2000 keV.

A level in the nucleus $^{8}$Be at an excitation energy of about 3000 keV. above the ground state has been observed in the following reactions :

| | |
|---|---|
| $^{11}$B($p\alpha$)$^{8}$Be* | Dee and Gilbert 1936. |
| $^{10}$B($d\alpha$)$^{8}$Be* | Smith and Murrell 1939. |
| $^{4}$He($\alpha\alpha$)$^{4}$He | Devons 1939. |
| $^{7}$Li($dn$)$^{8}$Be* | Green and Gibson 1949. |
| $^{12}$C($\gamma\alpha$)$^{8}$Be* | Goward, Telegdi and Wilkins 1950. |

There is also evidence of a similar level in $^{8}$Be at nearly the same excitation, which takes part in the break-up of $^{8}$Li ; this has been established by observations on the decay of $^{8}$Li produced in the following reactions :

| | |
|---|---|
| $^{7}$Li($dp$)$^{8}$Li | Christy, Cohen, Fowler, Lauritsen and Lauritsen 1947 ; Bonner, Evans, Malich and Risser 1948 ; Baxter, Burcham and Paul 1950. |
| $^{11}$B($n\alpha$)$^{8}$Li | Lawrance 1939. |
| $^{9}$Be($\gamma p$)$^{8}$Li | Titterton 1950. |

None of these reactions, with the possible exception of $^{7}$Li($dn$), suggests a level width of as much as 2000 keV.; most of them are consistent with a width of about 800 keV., and it is therefore not at present possible to identify the level concerned in the $^{7}$Li($p\gamma$)$^{8}$Be* reaction with any previously known level of $^{8}$Be. It is, however, certain that this level lies within about 200 keV. of those deduced from other experiments. In the particular case of the break-up of $^{8}$Li, Baxter, Burcham and Paul (1950) using the same analyser as in the present experiments, found a level at $3130 \pm 50$ keV., which is to be compared with the value of $3030 \pm 100$ keV. found in the present work.

The excitation curves given in fig. 9 suggest that the alpha particle yield at resonance increases less sharply than that of the total gamma radiation. This might be due to an uncertainty in the background levels owing to the low counting rates, but it would be in agreement with the observation of Devons and Hine (1949) that the ratio of the 14·8 to the 17·6 MeV. gamma radiation decreases at the 440 keV. proton resonance energy.

## Acknowledgments

We are grateful to Sir John Cockcroft and to Dr. W. D. Allen and members of his group at the Atomic Energy Research Establishment, Harwell, who provided the separated lithium isotopes. We also wish to thank Messrs W. Birtwhistle and D. D. Stewart for much technical assistance.

## References


Baxter, A. S., Burcham, W. E., and Paul, E. B., 1950, *Phil. Mag.* (to be published).

Bonner, T. W., and Evans, J. E., 1948, *Phys. Rev.*, **73**, 666.

Bonner, T. W., Evans, J. E., Malich, C. W., and Risser, J. R., 1948, *Phys. Rev.*, **73**, 885.

Bowersox, R. B. 1939, *Phys., Rev.*, **55**, 323.

Burcham, W. E., and Freeman, J. M., 1949 a, *Phys. Rev.*, **75**, 1756, **77**, 287; 1949 b, *Phil. Mag.*, **40**, 807; 1950, *Ibid.*, **41**, 337.

Christy, R. F., Cohen, E. R., Fowler, W. A., Lauritsen, C. C., and Lauritsen, T., 1947, *Phys. Rev.*, **72**, 698.

Dee, P. I., and Gilbert, C. W., 1936, *Proc. Roy. Soc.*, A, **154**, 279.

Devons, S., 1939, *Proc. Roy. Soc.*, A, **172**, 564.

Devons, S., and Hine, M. G. N. 1949, *Proc. Roy. Soc.*, A, **199**, 56.

Fowler, W. A., Lauritsen, C. C., and Lauritsen, T., 1948, *Rev. Mod. Phys.*, **20**, 236.

Goward, F. K., Telegdi, V. and Wilkins, F. J., 1950. *Proc. Phys. Soc.*, A, **63**, 402.

Green, L. L., and Gibson, W. M., 1949, *Proc. Phys. Soc.*, **62**, 407

Hornyak, W. F., and Lauritsen, T., 1948, *Rev. Mod. Phys.*, **20**, 191.

Lawrance, A. M., 1939, *Proc. Camb. Phil. Soc.*, **35**, 304.

Neuert, H., 1938, *Phys. Zeits.*, **38**, 618.

Rumbaugh, L. H., Roberts, R. B., and Hafstad, L. R., 1938, *Phys. Rev.*, **54**, 654.

Smith, C. L., and Murrell, E. B. M., 1939, *Proc. Camb. Phil. Soc.*, **35**, 298.

Tangen, R., 1946, *Kgl. Norske Skrifter* No. 1.

Thomas, R. G., Rubin, S., Fowler, W. A., and Lauritsen, C. C., 1949, *Phys. Rev.*, **75**, 1612.

Titterton, E. W., 1950, *Nature, London.*, **165**, 721.

Tollestrup, A. V., Fowler, W. A., and Lauritsen, C. C., 1949, *Phys. Rev.*, **76**, 428.

Walker, R. L., and McDaniel, B. D., 1948, *Phys. Rev.*, **74**, 315.

Warshaw, S. D., 1949, *Phys. Rev.*, **76**, 1759.

Wheeler, J. A., 1941, *Phys. Rev.*, **59**, 27.

# LXXXV. *Short Range Alpha Particles from the Break-up of* $^{8}$Li.

By A. S. Baxter, W. E. Burcham and E. B. Paul†,
Cavendish Laboratory, Cambridge ‡.

[Received June 27, 1950.]

Summary.

The energy spectrum of the alpha particles from the $^{8}$Li–$^{8}$Be* break-up has been studied using a magnetic analyser and thin targets. The most probable energy of the alpha particle pair emitted was found to be $3150 \pm 50$ keV.

## §1. Introduction.

The nucleus $^{8}$Li is an electron emitter of 0·89 sec. half-life which breaks up in accordance with the reaction

$$^{8}\mathrm{Li} \rightarrow {}^{8}\mathrm{Be}^{*} + \beta^{-} \rightarrow 2\,{}^{4}\mathrm{He} + \beta^{-} \quad . \quad . \quad . \quad . \quad . \quad . \quad (1)$$

with an energy release of 16·75 MeV. (Hornyak and Lauritsen 1950). The spectrum of alpha particles emitted in this process has been studied be several workers and an analysis of their results up to 1941 is given by Wheeler (1941 a). The main conclusion drawn by Wheeler is that the distribution of alpha particles at low energies can be accounted for by supposing the existence of a broad level in the $^{8}$Be nucleus at an excitation energy of about 3 MeV.; reasons are given for believing this level to be distinct from another level in $^{8}$Be at about the same excitation which is observed in the $^{11}\mathrm{B}(p\alpha)$ reaction (Dee and Gilbert 1936) and in the scattering of alpha particles by helium (Devons 1939, Wheeler 1941 b). Recently new observations have been made on the energy distribution of both the alpha particles and beta particles emitted in reaction (1); Christy, Cohen, Fowler, Lauritsen and Lauritsen (1947) studied the momentum relations in the process and Bonner, Evans, Malich and Risser (1948) extended observations of the alpha particle spectrum to very low energies by projecting $^{8}$Li nuclei into a cloud chamber. Cassels has obtained similar results, with better statistical accuracy, by projecting $^{8}$Li nuclei into a photographic plate§. Hornyak and Lauritsen (1950) showed that existing data on the low energy alpha particle spectrum fitted

† Now at Chalk River Laboratories, Ontario, Canada.
‡ Communicated by the Authors.
§ We are grateful to Dr. Cassels for informing us of his results before publication.

with their measurements of the beta particle energy distribution, and that less than 2 per cent of all the $\beta$ transitions from $^{8}$Li proceed to the ground state of $^{8}$Be.

The present work was commenced early in 1948 with the object of improving the statistical accuracy of the existing observations of the low energy part of the alpha particle spectrum. The method of magnetic analysis used, in which the energy of only one member of the alpha particle pair from reaction (1) is observed, is inferior to methods which display the total energy release in each disintegration, and leads, as pointed out in § 3, to a broadening of the spectrum. It is felt, however, that the present results are of some interest in showing the application of a magnetic analyser to a study of the $^{8}$Li reaction.

## §2. Experimental.

The alpha particle spectrum was investigated by means of the magnetic analyser described in other papers (Burcham and Freeman 1949, 1950 a, 1950 b). In the first experiments a lithium hydroxide target deposited on a thick copper backing was bombarded with deuterons of 900 keV. energy. The energy release in the reaction $^{7}$Li($dp$)$^{8}$Li is $-0{\cdot}193\pm0{\cdot}008$ MeV. (Strait and Buechner 1949, Paul 1950) and the $^{8}$Li nuclei are all projected forwards, the maximum angle of recoil being 34° with the deuteron beam. The $^{8}$Li nuclei, therefore, recoil into the target and target backing and a correction, amounting to about 100 keV. had to be made in consequence to the observed energy of the alpha particles emitted (*cf.* Bonner, Evans, Malich and Risser 1948). This correction is entirely eliminated in the cloud chamber and photographic plate experiments ; in later work with the magnetic analyser it was reduced by using thin foils of collodion as target backing.

The collodion foil on which the lithium hydroxide was deposited was set at 34° with the deuteron beam and the radioactive alpha particles were observed in a direction at right angles to the foil. The thickness of both the foil and the target were measured by observing the 339 keV. $^{19}$F($p\gamma$) resonance with and without the foil in position, and were found to be $20\pm5$ keV. and $10\pm5$ keV. respectively for protons. The observations were made using a suitable irradiation and counting cycle ; during the 2 second irradiation period the yield of the reaction was monitored by observation of the alpha particles from the $^{6}$Li($d\alpha$) reaction through a side window, and the radioactive alpha particles were counted, for different analyser settings, in a 2 second period following the interruption of the deuteron beam. It was found possible to bombard the collodion foils with currents of about 5 $\mu$A. without damage for a period of about an hour, and as the yield was large (about 400 radioactive alpha particles per second at the peak of the spectrum) good statistical accuracy was possible. The targets became blackened by deposition of carbon during the experiment, but repeat observations showed only a small shift of the spectrum over a period of an hour. The analyser resolution was 4 per cent in energy.

## §3. Results.

The alpha particle spectrum obtained is shown in fig. 1, in which the number of alpha particles for a given number of irradiation cycles, corrected by using the monitor counts to the same intensity of irradiation, is plotted against energy. The lower energy portion of the spectrum is shown on a larger scale. The total thickness of the backing foil and target was $30\pm10$ keV. for protons of 340 keV. energy, or approximately $120\pm40$ keV. for alpha particles of about 1500 keV., and in order to correct

Fig. 1.

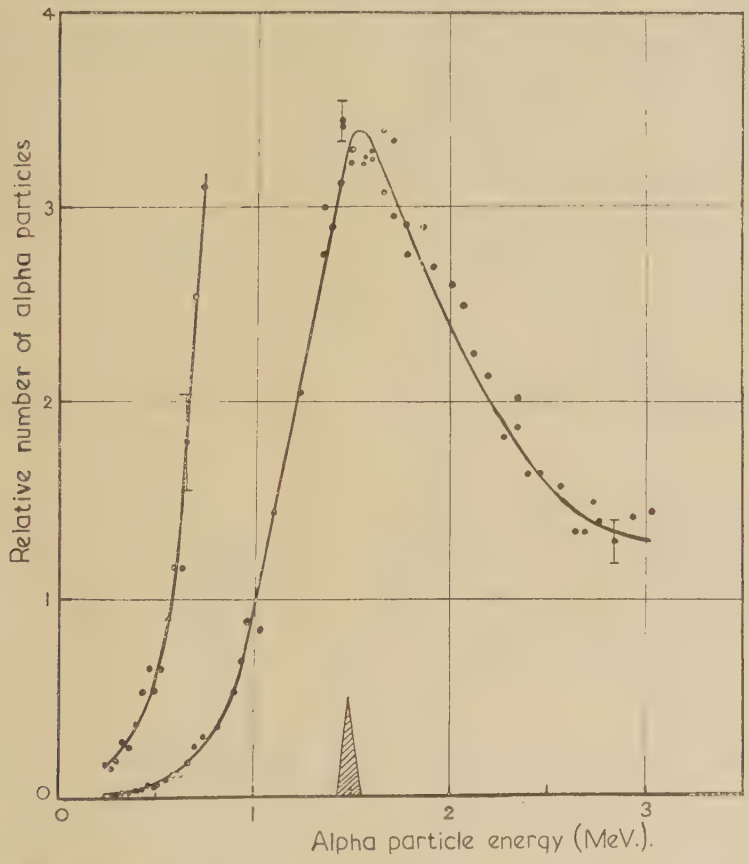


Alpha particles from the $^{8}$Li–$^{8}$Be* break-up; experimental points. The shaded triangle represents the analyser resolution.

for this it was assumed that the average retardation of the alpha particles would be $60\pm20$ keV. Correction was also made for the varying transmission factor of the analyser over the spectrum by applying an experimentally determined normalizing factor (*cf.* Burcham and Freeman 1950 b). The effect of charge exchange on the low energy particles was also allowed for by using the figures given by Briggs (1927); the ordinates at the very

low energies have been increased by the necessary factor and the corresponding high energy points reduced to allow for detection of singly charged particles. With these corrections and normalization the spectrum of fig. 2 (*a*) is obtained from the smoothed curve of fig. 1 ; this figure shows that the maximum yield occurs for an energy of $1575 \pm 25$ keV. If the alpha particles are assumed to be emitted from $^{8}$Be nuclei at rest the energy of the most probable alpha particle pair is $3150 \pm 50$ keV. which is to be compared with the value of 3300 keV. found by Bonner, Evans, Malich and Risser (1948). The points obtained by these authors are plotted for comparison in fig. 2, with the assumption that the energy of the alpha particle pair divides equally between the two alpha particles, and it is clear that the width (about 1000 keV.) of the present distribution is considerably greater. This may be due to the corrections applied to the

Fig. 2.

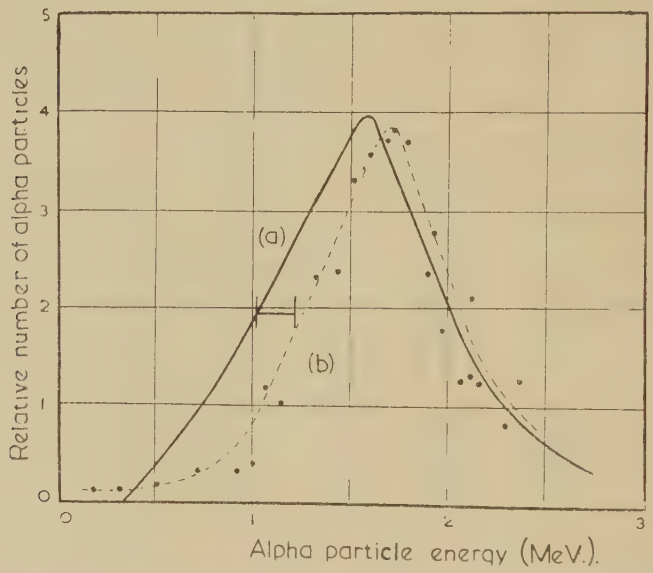


Alpha particles from the break-up of $^{8}$Li ; corrected distribution in energy. (*a*) present observations, (*b*) experimental points found by Bonner, Evans, Malich and Risser (1948). The horizontal line shows the broadening expected in curve (*a*) as a result of target thickness and recoil.

experimental points, although the increased width must in part be due to the use of a target of thickness 120 keV. as a source of activity, and to the fact that the $^{8}$Be* nucleus disintegrates into alpha paticles before it has lost its energy of recoil from the emission of the electron from $^{8}$Li, so that the two alpha particles in general have different energy. The recoil effect depends on the distribution of recoil momentum between the $^{8}$Be* nucleus and neutrino, and has been studied by Christy, Cohen, Fowler, Lauritsen and Lauritsen (1947). With the assumption of the maximum

recoil energy of about 10 keV. and an isotropic distribution of recoiling $^8$Be* nuclei in a target of 120 keV. thickness, it was found by construction that a spectrum of the form given by Bonner, Evans, Malich and Risser (1948) (theoretical curve) would be broadened by about 200 keV. in $E_\alpha$ without appreciable shift of the peak. The recoil effect is responsible for about 125 keV. of this broadening and the target thickness for about 75 keV. The broadening is indicated in fig. 2, and correction for it brings the width of the present distribution into agreement with the cloud chamber work, although it makes it unsuitable for detailed comparison with a theoretical level formula.

In deducing the position of the excited state of $^8$Be* effective in the break-up of $^8$Li, allowance must be made for the energy dependent factor $(Q-2E_\alpha)^5$ ($Q=16{\cdot}75$ MeV.) which appears in the theoretical formula for the yield of alpha particles pairs of energy $2E_\alpha$ to take account of the varying probability of the $\beta$-transition (Wheeler 1941). If the ordinates of the distribution given in fig. 2 are divided by this factor the peak is found to shift to $1610\pm25$ keV., which corresponds to an energy for the excited state of $3130\pm50$ keV., using the figure of $89\pm5$ keV. for the energy of the ground state of $^8$Be given by Tollestrup, Fowler and Lauritsen (1949).

Acknowledgments.

We wish to thank Messrs. W. Birtwhistle and D. D. Stewart for much technical assistance.

References.

Bonner, T. W., Evans, J. E., Malich, C. W. and Risser, J. R., 1948, *Phys. Rev.*, **73**, 885.

Briggs, G. H., 1927, *Proc. Roy. Soc.* A, **114**, 341.

Burcham, W. E. and Freeman, J. M., 1949, *Phil. Mag.*, **40**, 807.

Burcham, W. E. and Freeman, J. M., 1949, *Phil. Mag.*, **40**, 807 ; 1950a, *Ibid.*, **41**, 337 ; 1950b, *Ibid.*, **41**, 921.

Christy, R. F., Cohen, E. R., Fowler W. A., Lauritsen, C. C. and Lauritsen, T., 1947, *Phys. Rev.*, **72**, 698.

Dee, P. I. and Gilbert, C. W., 1936, *Proc. Roy. Soc.* A, **154**, 279.

Devons, S., 1939, *Proc. Roy. Soc.* A, **172**, 564.

Hornyak, W. F. and Lauritsen, T., 1950, *Phys. Rev.*, **77**, 160.

Paul, E. B., 1950, *Phil. Mag.*, **41**, 942.

Strait, E. N. and Buechner, W. W., 1949, *Phys. Rev.*, **76**, 1766.

Tollestrup, A. V., Fowler, W. A. and Lauritsen, C. C., 1949, *Phys. Rev.*, **76**, 428.

Wheeler, J. A., 1941a, *Phys. Rev.*, **59**, 27; 1941b, *Ibid.*, **59**, 16.

# LXXXVI. *The Energy Release in the Reaction* $^{7}$Li$(dp)^{8}$Li.

By E. B. Paul*,
Cavendish Laboratory, Cambridge†.

[Received June 27, 1950.]

Summary.

In the reaction $^{7}$Li$(dp)^{8}$Li the velocity of the centre of mass exceeds the velocity of the recoil nucleus in the centre of mass system and recoils will be observed only at angles less than a certain angle with the deuteron beam. This maximum angle has been observed for several deuteron energies and the Q-value for the reaction determined to be $-0{\cdot}187\pm0{\cdot}010$ MeV.

## §1. Introduction.

The energy release in the reaction $^{7}$Li$(dp)^{8}$Li has been determined by several methods. Rumbaugh, Roberts and Hafstad (1938) using a target enriched in the $^{7}$Li isotope observed no protons of range greater than 1·76 cm. with 0·86 MeV. deuterons. This sets an upper limit to the Q-value of 0·28 MeV. They also found no appreciable yield of $^{8}$Li at deuteron energies less than 0·36 MeV. which sets a lower limit to the Q-value of $-0{\cdot}20$ MeV. Strait and Buechner (1949) observed a proton group from bombardment of lithium with 1·36 MeV. deuterons. The protons were analysed magnetically and detected in photographic plates; the Q-value reported for the $^{7}$Li$(dp)^{8}$Li reaction is $-0{\cdot}193\pm0{\cdot}008$ MeV.

The present paper describes work done at the Cavendish Laboratory in 1948 employing a different method of finding the Q-value for this reaction, based on the observation of the maximum angle of recoil of the $^{8}$Li nuclei. This method, which can be used to study a reaction for which the velocity of the centre of mass exceeds that of the recoil nucleus in the centre of mass system, was suggested by Newson (1935) and has been discussed by Bethe (1937) who shows that the maximum angle of recoil $\phi_0$ in the laboratory system is given by

$$\sin\phi_0=\left\{\frac{M_2}{M_1M_3}\left[(M_0+M_1)\frac{Q}{E_1}+M_0\right]\right\}^{1/2}, \quad . \quad . \quad . \quad . \quad (1)$$

where $M_0$, $M_1$, $M_2$, $M_3$ are the masses of the initial nucleus and particle, and of the final particle and nucleus respectively and $E_1$ is the energy of the incident particle. For the $^{7}$Li$(dp)^{8}$Li reaction the condition that $\phi_0$

* Now at Chalk River Laboratories, Chalk River, Ontario.
† Communicated by Dr. W. E. Burcham.

shall be real is that $E_1 \geq |Q|$ approximately, so that a maximum angle of recoil should be observable for deuteron energies exceeding 0·2 MeV. An examination of relation (1) shows that the sensitivity of the method is greatest when $E_1$ is as small as possible and it may be shown that the accuracy of the Q-value so determined is least dependent on $E_1$ when Q is near zero. The number of recoils per unit solid angle reaches a maximum at the angle $\phi_0$ for an isotropic distribution of recoils in the centre of mass system and this facilitates observation of $\phi_0$.

## §2. Experimental.

The experimental arrangement is shown in fig. 1. The deuteron beam passed through a grid which supported an aluminium foil approximately 0·61 mgm./cm.$^2$ in thickness. A thin film of lithium oxide was deposited on the foil. $^8$Li recoil nuclei produced in the target by deuteron bombard-

Fig. 1.

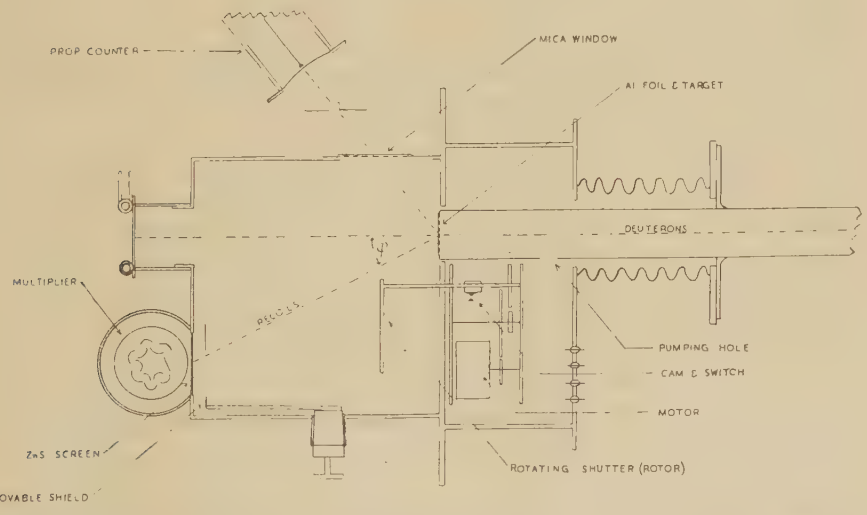


Apparatus used for detection of $^8$Li recoils produced in the $^7$Li$(dp)^8$Li reaction.

ment were received on a zinc sulphide screen set at an angle near the maximum expected. A movable shield in front of the fluorescent screen varied the angular range over which recoils could reach the screen from the target. The alpha particles from the break-up of the $^8$Li nuclei received by the fluorescent screen produced scintillations which were detected by an RCA 931A electron multiplier placed close behind the screen.

Periodic irradiations of 2·3 sec. were made and the alpha-particle activity on the screen was observed in periods of 3·2 sec. following each irradiation. During these counting periods the deuteron beam was

interrupted and a rotating shutter automatically moved between the target and the screen in order to prevent detection of any alpha particles directly from the target.

The angle fixed by the edge of the shield was measured by replacing the target by a sheet of tracing paper illuminated from behind. The distance from the point at which the beam intersected the plane of the fluorescent screen to the edge of the shadow on the screen was measured with dividers.

The movable shield allowed $^{8}$Li recoils to be recorded at angles greater than that fixed by the edge of the shield but the exposed screen area was different for each setting of the shield. This correction was found by placing a polonium source in the target position and counting for different settings of the shield. The correction curve so obtained was used to allow for the change in total solid angle with angle of recoil.

The air equivalent of the target material and supporting foil was measured before and after bombardment using a polonium source and an ionization chamber. The difference between the residual extrapolated range of the polonium alpha particles when the target foil was in place and removed was $0{\cdot}81 \pm 0{\cdot}04$ cm. air.

A proportional counter viewed the target continuously through a mica window in the side of the vacuum box. The counter was arranged to detect the alpha particles from the reaction $^{6}\mathrm{Li}(d\alpha)^{4}\mathrm{He}$ and served to monitor the conditions of irradiation.

About 40 irradiations were performed for each setting of the movable shield. The background due to dark current in the multiplier and gamma radiation from the target was measured when the shield completely covered the screen. Runs were made with primary deuteron energies of 950, 900 and 850 keV. The energies of these deuteron beams after having passed through the aluminium foil and lithium oxide target were taken to be $550 \pm 20$ keV., $460 \pm 30$ keV., and $400 \pm 30$ keV. respectively. $^{8}$Li nuclei could escape from the target from a depth of about 0·4 mm. air equivalent, that is, about 10 per cent of the thickness of the lithium target. Thus, for example, deuterons of initial energy 950 keV. produced $^{8}$Li nuclei which emerged from the target only for a deuteron energy of between 570 and 530 keV. This was assumed to give the uncertainty in $E_1$ since other sources of error were estimated to be less important. Scattering of the $^{8}$Li nuclei before emerging from the target was neglected, although such scattering probably contributed to the uncertainty in the measurement of the maximum angle of recoil.

The background count per irradiation was subtracted from the total count per irradiation and correction was also made for variations in the count from the monitor counter. Finally the count of delayed alpha particles for each angle setting was multiplied by the corresponding geometrical factor as determined with a polonium source in place of the target. This gave the mean count per unit solid angle per irradiation for each setting of the shield. A check made of the period of the activity being observed gave a half-life of $1{\cdot}3 \pm 0{\cdot}5$ sec.

## §3. Results.

The corrected results of the various runs are presented in figs. 2 and 3. The ordinates correspond to counts per irradiation for 100 counts per irradiation in the monitor counter for a solid angle equal to that subtended by the screen in the fully exposed position. The values of the maximum

Fig. 2.

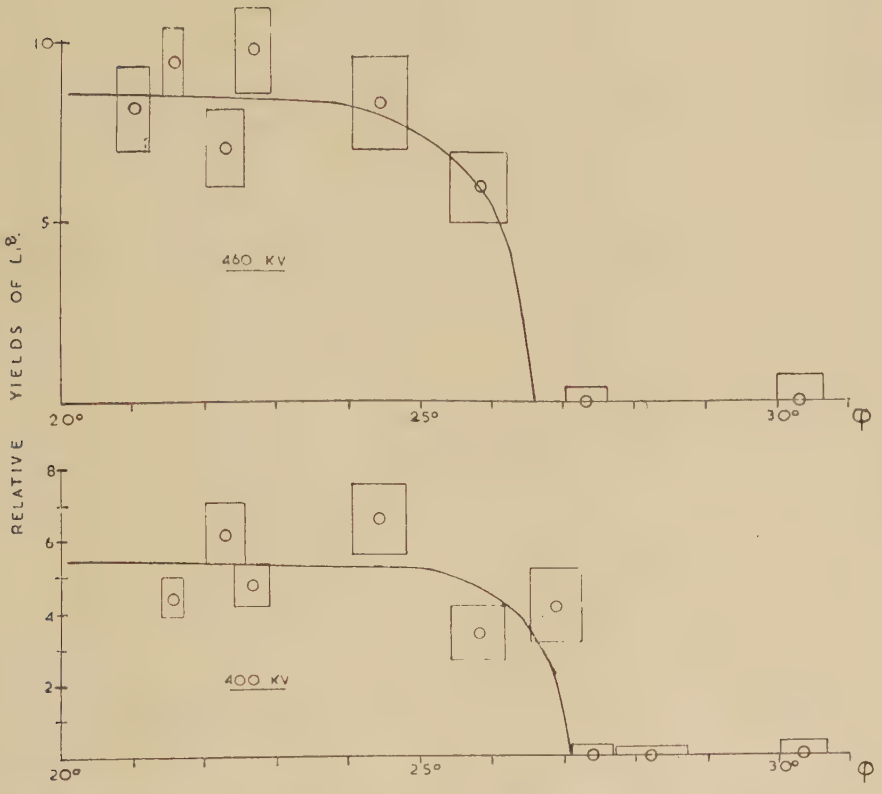


Angular distribution of recoils from the $^7$Li$(dp)^8$Li reaction. Runs 1 and 2.

Table.

| Run | $E_1$ (keV.) | $\phi_0$ (degrees) | Q (MeV.) |
|---|---|---|---|
| 1 | 460±30 | 26·6±1·5 | −0·193±0·024 |
| 2 | 400±30 | 27·2±0·5 | −0·162±0·013 |
| 3 | 550±20 | 27·8±0·8 | −0·215±0·014 |
| 4 | 460±30 | 27·7±0·8 | −0·182±0·015 |
| 5 | 400±30 | 25·2±1·4 | −0·182±0·021 |

angle are listed in the Table together with the Q-value calculated for the reaction.

Fig. 3.

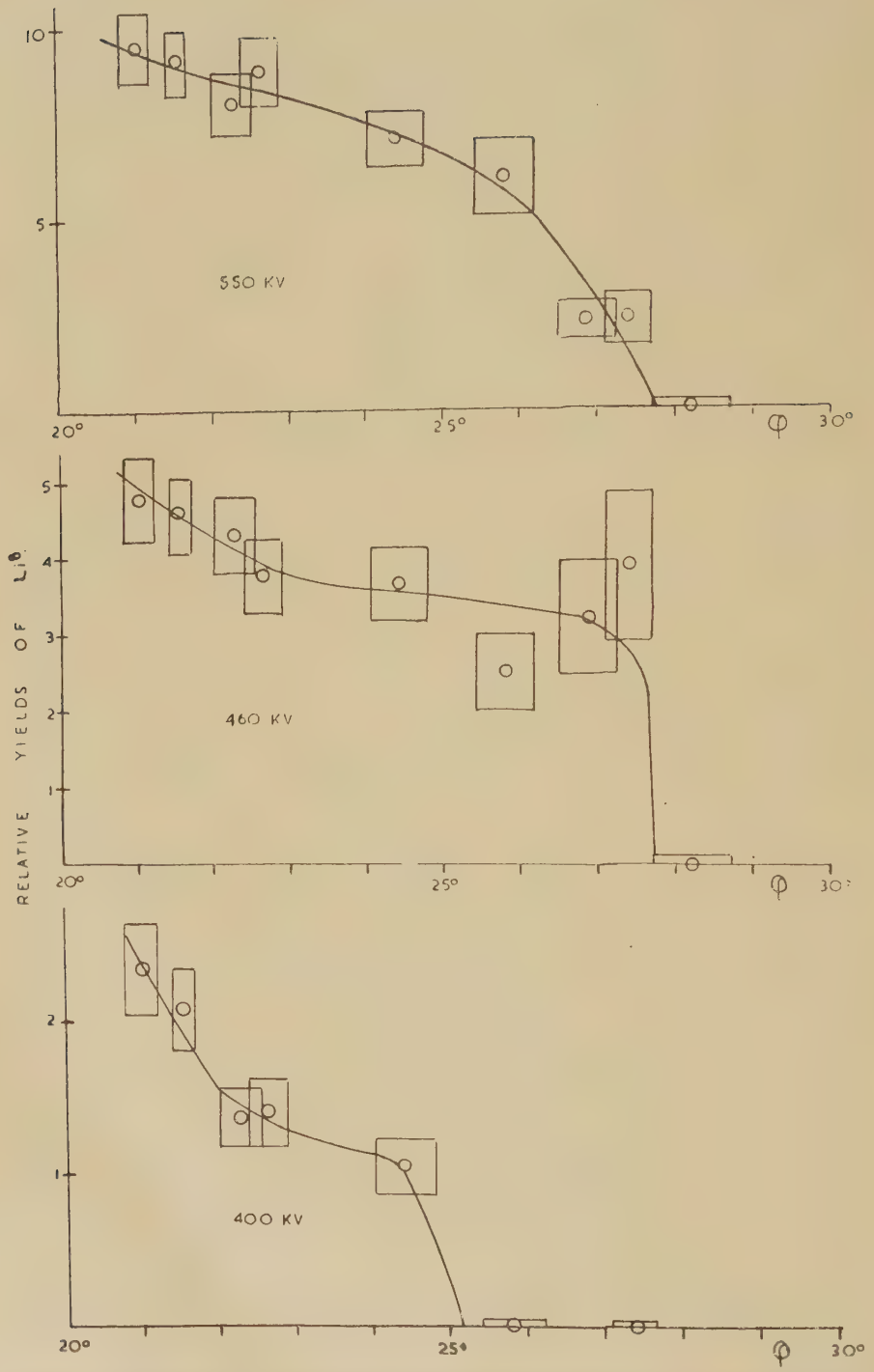


Angular distribution of recoils from the $^{7}$Li$(dp)^{8}$Li reaction. Runs 3, 4 and 5

These results have been combined and the weighted average for the energy release in the reaction $^{7}$Li$(dp)^{8}$Li is found to be

$$Q = -0{\cdot}187 \pm 0{\cdot}010 \text{ MeV}.$$

This value is in satisfactory agreement with the values of $-0{\cdot}20 \pm 0{\cdot}03$ MeV. found by Rumbaugh, Roberts and Hafstad (1938) and of $-0{\cdot}193 \pm 0{\cdot}008$ found by Strait and Buechner (1949).

Acknowledgments.

The writer is grateful to Dr. W. E. Burcham for advice in the course of this experiment and to Mr. W. Birtwhistle for technical assistance.

References.

Bethe, H. A., 1937, *Rev. Mod. Phys.*, **9**, 281.
Newson, H. W., 1935, *Phys. Rev.*, **48**, 790.
Rumbaugh, L., Roberts, R. and Hafstad, L. R., 1938, *Phys. Rev.*, **54**, 657.
Strait, E. N. and Buechner, W. W., 1949, *Phys. Rev.*, **76**, 1766.

# LXXXVII. *On the Quantum Mechanics of Fluids.*

By P. J. Price,

Royal Society Mond Laboratory, Cambridge*.

[Received July 10, 1950.]

Abstract.

The position of this paper, in the quantum theory of liquids, is principally that of a critique of the contribution by Green. The relation of his formalism to wave-mechanics is discussed, and hydrodynamical equations are derived, in wavemechanical form, which are shown to be equivalent to Green's results. A formula for the boundary stress is arrived at, and it is shown that the difference between the kinetic and thermodynamic pressures—on which Green's explanation of the thermomechanical effects in liquid helium II is based—is identically zero, confirming the conclusions of Yvon and de Boer.

## §1. Introduction.

The system discussed here is that of N identical atoms (bosons or fermions), without effective internal degrees of freedom or spin, enclosed in a volume V and interacting by a potential U. H. S. Green (Born and Green 1947, Green 1948 : referred to below as I and II respectively) has given the most complete account to date of the quantum mechanics of this model, and derived the hydrodynamical equations of motion in a suggestive form which demonstrates their correspondence to the classical equations. In this paper a treatment by conventional wavemechanical methods is given, and the results shown to be equivalent to Green's. The virial theorem is derived, and the stress on the boundary identified in the surface term. A discussion of the thermodynamic pressure follows, in which de Boer's (1949) conclusion is confirmed : that Green's expression for the difference between the kinetic and thermodynamic pressures vanishes identically.

## §2. Green's Formalism and Wave-Mechanics.

We need a means of comparing results in Green's formalism (I, §2) with those derived below. For simplicity, consider a single particle only, with wave-function $\psi(\mathbf{r})$ defined in a domain $\mathfrak{R}$ and satisfying a boundary condition B on its boundary, S. If $\{\phi_\nu\}$, $(\nu=1, 2, \ldots)$ is a complete orthonormal set of such functions, then

$$\delta(\mathbf{r}_1, \mathbf{r}_2) \equiv \sum_{\nu=1}^{\infty} \phi_\nu(\mathbf{r}_1)\phi_\nu^*(\mathbf{r}_2) \quad . \quad . \quad . \quad . \quad . \quad . \quad (1)$$

* Communicated by the Author.

has the property

$$\int^{\mathfrak{R}} \delta(\mathbf{r}_1, \mathbf{r}_2)\psi(\mathbf{r}_2)d^3\mathbf{r}_2=\psi(\mathbf{r}_1) \text{ in } \mathfrak{R},$$

and obeys B on S.

In Dirac's notation, if $\psi_k$ is the wave-function corresponding to a ket $|k\rangle$,

$$\psi_k(\mathbf{r}')\equiv\langle\mathbf{r}'|k\rangle.$$

Hence by (1)
$$\langle\mathbf{r}'|\mathbf{r}''\rangle=\delta(\mathbf{r}', \mathbf{r}''). \quad . \quad . \quad . \quad . \quad . \quad . \quad . \quad . \quad (2)$$

If
$$\Delta_1\equiv\Delta(\mathbf{r}_1)\equiv|\mathbf{r}_1\rangle\langle\mathbf{r}_1|, \quad . \quad . \quad . \quad . \quad . \quad . \quad . \quad . \quad (3)$$

then by (2),
$$\Delta_1=\delta(\mathbf{r}_1, \mathbf{r}), \quad . \quad . \quad . \quad . \quad . \quad . \quad . \quad . \quad (4)$$

where $\mathbf{r}$ is a $q$-number. An operator A is expressed in the Schrödinger notation by

$$\langle\mathbf{r}'|\mathrm{A}|k\rangle\equiv\mathrm{A}\psi_k(\mathbf{r}'), \quad . \quad . \quad . \quad . \quad . \quad . \quad . \quad . \quad (5)$$

and in Green's formalism by

$$\langle\mathbf{r}'|\mathrm{A}|\mathbf{r}''\rangle\equiv\mathrm{A}(\mathbf{r}', \mathbf{r}''). \quad . \quad . \quad . \quad . \quad . \quad . \quad . \quad . \quad (6)$$

Now if $|k\rangle\langle k|\equiv\rho_k$ is the projection operator of a pure state $k$,

$$\rho=\sum_k a_k\rho_k$$

(where the $a_k$ are real and $\geqslant 0$) is von Neumann's statistical operator (von Neumann 1943, Dirac 1947). By (5) and (6), if A and B are hermitian,

$$\begin{aligned}[\mathrm{A}\rho_k\mathrm{B}](\mathbf{r}', \mathbf{r}')&=\langle\mathbf{r}'|\mathrm{A}\rho_k\mathrm{B}|\mathbf{r}'\rangle\\ &=\langle k|\mathrm{A}\Delta(\mathbf{r}')\mathrm{B}|k\rangle\\ &=[\mathrm{A}\psi_k(\mathbf{r}')]^*\mathrm{B}\psi_k(\mathbf{r}'). \quad . \quad . \quad . \quad . \quad . \quad . \quad . \quad . \quad (7\end{aligned}$$

Hence
$$\left[\sum_\lambda \mathrm{A}_\lambda\rho\mathrm{B}_\lambda\right](\mathbf{r}', \mathbf{r}')=0 \qquad (a)$$

implies
$$\sum_\lambda[\mathrm{A}_\lambda\psi(\mathbf{r}')]^*\mathrm{B}_\lambda\psi(\mathbf{r}')=0 \qquad (b) \quad . \quad . \quad . \quad . \quad (8)$$

and conversely.

All Green's final $c$-number equations are in the form (8 $a$) (or an N-particle generalization, involving summations and integrations over the 3N coordinates), and hence have equivalent wave-mechanical forms (8 $b$). For example, Green's

$$\{\rho, \mathbf{p}\}\equiv\tfrac{1}{2}(\rho\mathbf{p}+\mathbf{p}\rho)$$

corresponds to Landau's (1941) current operator

$$\mathbf{J}(\mathbf{r}')\equiv\tfrac{1}{2}(\Delta(\mathbf{r}')\mathbf{p}+\mathbf{p}\Delta(\mathbf{r}')),$$

whose expectation

$$\langle k|\mathbf{J}(\mathbf{r}')|k\rangle=\tfrac{1}{2}i\hbar[\psi_k\nabla\psi_k^*-\psi_k^*\nabla\psi_k](\mathbf{r}'),$$

is the conventional current at the point $\mathbf{r}'$. Similarly

$$\left(\frac{1}{m}\right)\{\{\rho, \mathbf{p}\}, \mathbf{p}\} \quad \frac{\hbar^2}{4m}[(\psi^*\nabla\Gamma\psi+\psi\Gamma\nabla\psi^*)-(\Gamma\psi^*\Gamma\psi+\Gamma\psi\Gamma\psi^*)]. \quad (9)$$

(The arrow denotes the correspondence (8), and the equality—for a pure state—(7)). Each of (8) is equivalent to

$$\mathrm{Tr}\left[\rho \sum_{\lambda} \mathrm{A}_\lambda \Delta(\mathbf{r}')\mathrm{B}_\lambda\right]=0,$$

and hence to the *classical* equation

$$\iint \rho(\mathbf{p},\mathbf{r}) \sum_{\lambda} \mathrm{A}_\lambda(\mathbf{p},\mathbf{r})\mathrm{B}_\lambda(\mathbf{p},\mathbf{r})\delta(\mathbf{r}-\mathbf{r}')\,d^3\mathbf{p}\,d^3\mathbf{r}$$

$$=\int \rho(\mathbf{p},\mathbf{r}') \sum_{\lambda} \mathrm{A}_\lambda(\mathbf{p},\mathbf{r}')\mathrm{B}_\lambda(\mathbf{p},\mathbf{r}')\,d^3\mathbf{p}=0. \quad . \quad . \quad . \quad (10)$$

In generalizing these results for N particles, $\mathbf{r}$ is replaced by the set $\mathbf{r}_1, \mathbf{r}_2, \ldots, \mathbf{r}_N$. The effect of the symmetry restriction (Bose or Fermi) is that the $\rho$ of (8) is in practice confined to the appropriate subspace of the space of $\{\phi_r\}$. The restriction is formally included by replacing all observables A by AQ, where Q $=Q^+$ or $Q^-$ is the corresponding projection operator—which commutes with all A of physical interest. The correspondence (10) is not affected by the restriction.

## §3. The Equations of Motion.

Write Schrödinger's equation in the form

$$\mathrm{H}\psi(x_1, x_2, \ldots, x_{3N}) \equiv [-\omega\Delta+\mathrm{U}(x_1, x_2, \ldots, x_{3N})]\psi=i\hbar\frac{\partial}{\partial t}\psi,$$

$$. \quad . \quad . \quad (11)$$

where $\omega=\hbar^2/2m$, $m$ is the mass of a particle, and

$$\Delta \equiv \sum_{i=1}^{3N} \partial_i\partial_i, \qquad \partial_i \equiv \partial/\partial x_i.$$

Let
$$\mathbf{k}(x_1 \ldots x_{3N}) \equiv \tfrac{1}{2}i\hbar[\psi\nabla\psi^*-\psi^*\nabla\psi]. \quad . \quad . \quad . \quad . \quad (12)$$
Then

$$\nabla \,.\, \mathbf{k} \equiv \sum_i \partial_i k_i=(\tfrac{1}{2}i\hbar/\omega)[\psi^*\mathrm{H}\psi-\psi\mathrm{H}\psi^*]=-m[\psi^*\dot{\psi}+\psi\dot{\psi}^*].$$

*I. e.*
$$\nabla \,.\, \mathbf{k}=-m\frac{\partial}{\partial t}(\psi^*\psi). \quad . \quad . \quad . \quad . \quad . \quad . \quad . \quad (13)$$

Also,

$$2\frac{\partial}{\partial t}\mathbf{k}=[(\mathrm{H}\psi)\nabla\psi^*-\psi\nabla(\mathrm{H}\psi^*)]-[(-\mathrm{H}\psi^*)\nabla\psi+\psi^*\nabla(\mathrm{H}\psi)]$$

$$=-2\psi^*\psi\nabla\mathrm{U}-\omega[(\Delta\psi\nabla\psi^*+\Delta\psi^*\nabla\psi)-(\psi\nabla(\Delta\psi^*)+\psi^*\nabla(\Delta\psi))].$$

Hence, by the identity

$$\Delta\psi^*\nabla\psi+\Delta\psi\nabla\psi^* \equiv \nabla \,.\, [\nabla\psi^*\nabla\psi+\nabla\psi\nabla\psi^*]-\nabla(\nabla\psi^* \,.\, \nabla\psi),$$

$$\frac{\partial}{\partial t}\mathbf{k}+\psi^*\psi\nabla\mathrm{U}=-\omega\{\nabla \,.\, [\nabla\psi^*\nabla\psi+\nabla\psi\nabla\psi^*]$$

$$-\tfrac{1}{2}\nabla[\psi^*\Delta\psi+\psi\Delta\psi^*+2\nabla\psi^* \,.\, \nabla\psi]\}$$

$$=-\omega\{\nabla \,.\, [\nabla\psi^*\nabla\psi+\nabla\psi\nabla\psi^*]-\tfrac{1}{2}\nabla[\Delta(\psi^*\psi)]\}.$$

*I. e.*

$$\frac{\partial}{\partial t}\mathbf{k}+\psi^*\psi\nabla\mathrm{U}+\omega\nabla \,.\, [(\nabla\psi^*\nabla\psi+\nabla\psi\nabla\psi^*)-\tfrac{1}{2}\nabla\nabla(\psi^*\psi)]=0. \quad . \quad (14)$$

## § 4. The Macroscopic Equations.

Rewrite the wave-function in terms of the coordinates of the particles :

$$\psi=\psi(\mathbf{r}_1, \mathbf{r}_2, \ldots, \mathbf{r}_N),$$

where the $\mathbf{r}_i$ are vectors in subspaces of the cartesian space of § 3. If the surface S enclosing the particles is given by $\sigma(\mathbf{r})=0$, then this 3N-dimensional space is bounded by the hypersurfaces $S_i : \sigma(\mathbf{r}_i)=0$. The boundary condition is taken as

$$\psi=0 \text{ on the } S_i. \quad \ldots\ldots\ldots \quad (15)$$

We may also define a " vector " element of $S_i$: $d\mathbf{S}_i$

$$\left(\text{so that, for example, } \int^{S_i} \mathbf{r}_i \,.\, d\mathbf{S}_i = 3V \prod_{j\neq i} d^3\mathbf{r}_j\right),$$

and vector operators $\nabla_i$. ($\nabla_i \,.\, \mathbf{r}_j=3\delta_{ij}$). The hamiltonian of (11) is then

$$\mathrm{H}=-\omega \sum_i \Delta_i+\mathrm{U}(\mathbf{r}_1, \mathbf{r}_2, \ldots, \mathbf{r}_N). \quad \ldots\ldots \quad (16)$$

Let $\mathrm{I}_i'$ denote the operation

$$\int^{\mathfrak{R}_1} \ldots \int^{\mathfrak{R}_N} \prod_{j\neq i} d^3\mathbf{r}_j \ldots,$$

and $\mathrm{I}_i$ mean applying $\mathrm{I}_i'$ and dropping the suffix $i$, so that

$$\mathrm{I}_i f(\mathbf{r}_i)=\mathrm{V}^{(N-1)} f(\mathbf{r}).$$

$\mathrm{I}_{ij}''$, etc., are defined similarly. Then

$$\begin{aligned}\mathrm{I}_i'(\nabla \,.\, \mathbf{k}) &= \sum_j \mathrm{I}_i'(\nabla_j \,.\, \mathbf{k}_j)\\ &= \mathrm{I}_i'(\nabla_i \,.\, \mathbf{k}_i)+\sum_{j\neq i} \mathrm{I}_{ij}'' \int^{S_j} \mathbf{k}_j \,.\, d\mathbf{S}_j\\ &= \mathrm{I}_i'(\nabla_i \,.\, \mathbf{k}_i)=\nabla_i \,.\, (\mathrm{I}_i'\mathbf{k}_i), \text{ by (15).}\end{aligned}$$

Hence $$\mathrm{I}_i(\nabla \,.\, \mathbf{k})=\nabla \,.\, (\mathrm{I}_i \mathbf{k}_i).$$

Defining $$\mathbf{J}\equiv \sum_i \mathrm{I}_i \mathbf{k}_i, \qquad n\equiv \sum_i \mathrm{I}_i(\psi^*\psi), \quad \ldots\ldots \quad (17)$$

(13) becomes $$\nabla \,.\, \mathbf{J}=-m\frac{\partial}{\partial t} n. \quad \ldots\ldots\ldots \quad (18)$$

Since, apart from normalizing constants, $\mathbf{J}\to mn_1\mathbf{u}_1^{(1)}$ (*cf.* Green's I, 5.1) and $n\to n_1$ (I, 2.7), (18) is equivalent to (I, 5.6) with $q=1$. Green's more general cluster equations correspond to integration of (13) over fewer than (N−1) of the coordinates.

Since (14) is a vector equation, we may write it

$$-\mathrm{I}_i'\left[\frac{\partial}{\partial t}\mathbf{k}_i+\psi^*\psi\nabla_i \mathrm{U}\right]=\sum_j \mathrm{I}_i'(\nabla_j \,.\, \mathbf{T}_{ji}), \quad \ldots\ldots \quad (19)$$

where $$\mathbf{T}_{ji}=\nabla_j\psi^*\nabla_i\psi+\nabla_j\psi\nabla_i\psi^*-\tfrac{1}{2}\nabla_j\nabla_i(\psi^*\psi).$$

Now, for $j\neq i$,

$$\begin{aligned}\mathrm{I}_i'(\nabla_j \,.\, \mathbf{T}_{ji})-\mathrm{I}_{ij}''\int^{S_j} d\mathbf{S}_j \,.\, [&(\nabla_j\psi^*\nabla_i\psi+\nabla_j\psi\nabla_i\psi^*)\\ &-\tfrac{1}{2}\nabla_j(\psi^*\nabla_i\psi+\psi\nabla_i\psi^*)]=0, \text{ by (15),}\end{aligned}$$

since $\psi=0$, $\nabla_i\psi=0$, on $S_j$.

Defining

$$\left.\begin{aligned}
&\mathbf{R} \equiv \omega \sum_i \mathrm{I}_i[\nabla_i\psi^*\nabla_i\psi+\nabla_i\psi\nabla_i\psi^*],\\
&\mathbf{S} \equiv \tfrac{1}{2}\omega \sum_i \mathrm{I}_i\nabla_i\nabla_i(\psi^*\psi)=\tfrac{1}{2}\omega\nabla\nabla n,\\
&\mathbf{P} \equiv \mathbf{R}-\mathbf{S},\\
&\mathbf{F} \equiv -\sum_i \mathrm{I}_i(\psi^*\psi\nabla_i \mathrm{U}),
\end{aligned}\right\} \quad . \quad . \quad . \quad . \quad . \quad (20)$$

(19) becomes

$$\frac{\partial}{\partial t}\mathbf{J}=\mathbf{F}-\nabla\,.\,\mathbf{P}. \quad . \quad . \quad . \quad . \quad . \quad . \quad . \quad . \quad (21)$$

This result is equivalent to (I, 5.8) for $q=1$, since

$$\mathbf{J} \to mn_1\mathbf{u}_1^{(1)}, \qquad \mathbf{F} \to mn_1\boldsymbol{\eta}_1^{(1)},$$

while for the remaining term of (I, 5.8) (there is a factor $(1/m^2)$ missing):

$$(1/m)\{\{\rho_1, \mathbf{p}^{(1)}\}\mathbf{p}^{(1)}\} \to -\tfrac{1}{2}\omega \sum_i \mathrm{I}_i[(\psi^*\nabla_i\nabla_i\psi+\psi\nabla_i\nabla_i\psi^*)-(\nabla_i\psi^*\nabla_i\psi+\nabla_i\psi\nabla_i\psi^*)]$$

$$=\omega \sum_i \mathrm{I}_i[(\nabla_i\psi^*\nabla_i\psi+\nabla_i\psi\nabla_i\psi^*)-\tfrac{1}{2}\nabla_i\nabla_i(\psi^*\psi)]=\mathbf{P}.$$

The equation corresponding to (I, 5.10) follows from (21) in the same way, given the definitions of $\mathbf{v}$ and $d/dt$, and the equation of continuity (18). The quantity $\mathbf{P}$ defined in (20) is the expectation, in Landau's formalism, of

$$\left(\frac{1}{m}\right)\sum_i \{\{\mathbf{p}_i, \delta(\mathbf{r}', \mathbf{r}_i)\}, \mathbf{p}_i\},$$

which (by the considerations leading to (10)) reduces, in the classical limit, to the classical tensor of the momentum flux. Also $\mathbf{S}$ is proportional to the expectation of

$$\sum_i [[\mathbf{p}_i, \delta(\mathbf{r}', \mathbf{r}_i)], \mathbf{p}_i] \qquad (\text{where } [\mathrm{A}, \mathrm{B}]=(i\hbar)^{-1}(\mathrm{AB}-\mathrm{BA}))$$

and hence vanishes "as $h^2$", in the classical limit.

## § 5. The Virial Theorem.

From the definitions (20), the scalar of $\mathbf{S}$ is

$$\mathbf{S}_s=\tfrac{1}{2}\omega \sum_i \mathrm{I}_i\Delta_i(\psi^*\psi)=\tfrac{1}{2}\omega\Delta n, \quad . \quad . \quad . \quad . \quad . \quad . \quad (22)$$

and similarly

$$\mathbf{R}_s=\omega \sum_i \mathrm{I}_i[\Delta_i(\psi^*\psi)-(\psi^*\Delta_i\psi+\psi\Delta_i\psi^*)]=\omega\Delta n+2\mathrm{K},$$

where

$$\mathrm{K} \equiv -\omega \sum_i \mathrm{I}_i(\psi^*\Delta_i\psi+\psi\Delta_i\psi^*), \quad . \quad . \quad . \quad . \quad . \quad (23)$$

is the kinetic energy expectation. Then from (21),

$$\nabla\,.\,(\mathbf{P}\,.\,\mathbf{r})=(\nabla\,.\,\mathbf{P})\,.\,\mathbf{r}+\mathbf{P}_s=\mathbf{F}\,.\,\mathbf{r}-\frac{\partial}{\partial t}\mathbf{J}\,.\,\mathbf{r}+2\mathrm{K}+\tfrac{1}{2}\omega\Delta n. \quad . \quad (24)$$

For a stationary state, $(\partial/\partial t)\mathbf{J}=0$. Then, on integrating (24) over the whole volume,

$$\int^{s} d\mathbf{S}\,.\,\mathbf{P}\,.\,\mathbf{r}=\int^{\mathrm{V}}(2\mathrm{K}-\Gamma)\,d^3\mathbf{r}, \qquad . \quad . \quad . \quad . \quad . \quad (25)$$

where $\Gamma\equiv -\mathbf{F}\,.\,\mathbf{r}$ is the virial of the potential U, and $\int^{\mathrm{V}}(\Delta n)\,d^3\mathbf{r}$ vanishes by (15). (25) is the quantum virial theorem for an energy eigenstate, or a statistical ensemble of stationary states. Putting

$$\mathrm{U}=\mathrm{U}_1+\mathrm{U}_2\equiv \sum_i \mathrm{V}_1(\mathbf{r}_i)+\sum_{i<j}\sum \mathrm{V}_2(r_{ij}), \qquad \mathbf{r}_{ij}\equiv \mathbf{r}_i-\mathbf{r}_j, \qquad . \quad (26)$$

the virial becomes

$$\Gamma=\sum_i \mathrm{I}_i[\mathbf{r}_i\,.\,(\nabla_i \mathrm{V}_1(\mathbf{r}_i))\psi^*\psi]+\sum_{i<j}\sum \mathrm{I}_i[r_{ij}(\mathrm{V}_2'(r_{ij}))\psi^*\psi]. \quad . \quad . \quad (27)$$

Or

$$\Gamma=\mathbf{r}\,.\,(\nabla \mathrm{V}_1(\mathbf{r}))n(\mathbf{r})+\tfrac{1}{2}\int s\mathrm{V}_2'(s)n_2(\mathbf{r},\,\mathbf{r}+\mathbf{s})\,d^3\mathbf{s}, \quad . \quad . \quad . \quad (28)$$

where

$$n_2(\mathbf{r}_1,\,\mathbf{r}_2)=2\sum_{i<j}\sum \mathrm{I}_{ij}(\psi^*\psi).$$

By (15), on the boundary

$$\nabla_i\psi=\mathbf{n}_i\partial_{ni}\psi,$$

where $\mathbf{n}_i$ is the unit (outward) normal to $\mathrm{S}_i$; and hence

$$\text{on S,} \quad \mathbf{P}=\mathbf{nn}\omega\sum_i \mathrm{I}_i(\partial_{ni}\psi^*\partial_{ni}\psi). \quad . \quad . \quad . \quad . \quad . \quad . \quad . \quad (29)$$

The interpretation of (29) as the tensor of the stress on the boundary S, suggested by the form of (25), is supported by the following considerations for one dimension.

The Schrödinger equation in one dimension is

$$\left[-\omega\frac{d^2}{dx^2}+\mathrm{U}(x)-\mathrm{E}\right]\psi(x)=0, \qquad . \quad . \quad . \quad . \quad . \quad (30)$$

where

$$\lim_{x\to\pm\infty}\mathrm{U}>\mathrm{E}.$$

Suppose that, for $x>0$, the potential has the form

$$\left.\begin{aligned} &x\leqslant a, \qquad \mathrm{U}=0,\\ &x>a, \qquad \mathrm{U}=\mathrm{E}_0=\text{constant,}\end{aligned}\right\} \quad . \quad . \quad . \quad . \quad . \quad (31)$$

where $\mathrm{E}_0>\mathrm{E}$. Then the solution of (30) for $x>0$ is

$$\left.\begin{aligned} &x\leqslant a, \qquad \psi=\mathrm{A}\sin[k_1(x-a)+\phi],\\ &x>a, \qquad \psi=\mathrm{A}\sin(\phi)\exp[-k_2(x-a)],\\ &\omega k_1^2=\mathrm{E}, \qquad \omega k_2^2=\mathrm{E}_0-\mathrm{E}.\end{aligned}\right\} \quad . \quad . \quad (32)$$

Since $(d/dx)\psi$ is continuous,

$$\tan(\phi)=-k_1/k_2=-\sqrt{\left(\frac{\mathrm{E}}{\mathrm{E}_0-\mathrm{E}}\right)}. \quad . \quad . \quad . \quad . \quad . \quad (33)$$

The contribution of the "potential step" (31) to the reaction of the system is

$$\mathrm{F}=\lim_{\varepsilon\to 0}\int_{x=a-\varepsilon}^{a+\varepsilon}\psi^*\psi\,d\mathrm{U}=\mathrm{E}_0(\psi^*\psi)_{x=a}$$

$$=|\mathrm{A}|^2\mathrm{E}_0\sin^2(\phi)=\omega\left(\frac{d}{dx}\psi^*\right)_a\left(\frac{d}{dx}\psi\right)_a(\mathrm{E}_0\tan^2(\phi)/\mathrm{E}).$$

If E is fixed while $\mathrm{E}_0\to\infty$,

$$\left.\begin{aligned}&(a)\ \psi\to 0, \qquad x\geqslant a,\\ &(b)\ \mathrm{E}_0\tan^2(\phi)\,\mathrm{E}\to 1,\end{aligned}\right\} \quad . \ . \ . \quad (34)$$

and hence

$$\mathrm{F}\to\omega\left(\frac{d}{dx}\psi^*\right)_a\left(\frac{d}{dx}\psi\right)_a, \quad . \ . \ . \ . \ . \quad (35)$$

which is the one-dimensional analogue of (29).

## § 6. Application of Fröhlich's Perturbation Theory.

The interpretation of (29) suggested above, is confirmed by the theory of boundary perturbations proposed by Fröhlich (1938). In the notation of (11), let $\psi$ satisfy $\mathrm{H}\psi=\mathrm{E}\psi$ in $\mathfrak{R}$ and vanish on its boundary S, and let $\psi'$ satisfy $\mathrm{H}\psi'=\mathrm{E}'\psi'$ in $\mathfrak{R}'\subset\mathfrak{R}$ and vanish on S′. Then by Green's theorem

$$(\mathrm{E}'-\mathrm{E})\int^{\mathfrak{R}'}\psi^*\psi\Pi_i dx_i=-\omega\int^{S'}\psi^*\partial_n\psi'\,d\mathrm{S}. \quad . \ . \ . \quad (36)$$

Choose $\psi'$ so that, as $\mathrm{S}'\to\mathrm{S}$, $\psi'\to\psi$ and $\mathrm{E}'\to\mathrm{E}$. Suppose that, if $\mathbf{x}$ is on S, $\mathbf{x}'=\mathbf{x}+\lambda\mathbf{z}(\mathbf{x})$ is on S′. Then it is assumed (Fröhlich 1938) that

$$\partial_n\psi'(\mathbf{x}+\lambda\mathbf{z})=\partial_n\psi(\mathbf{x})+\mathrm{O}(\lambda) \quad . \ . \ . \ . \ . \ . \quad (37)$$

(*i. e.* $\psi$ "moves with the boundary", to the first order in $\lambda$). Then (36) gives

$$\mathrm{E}'=\mathrm{E}-\lambda\omega\int^{S}(\partial_n\psi^*)(\partial_n\psi)\mathbf{z}\,.\,d\mathbf{S}+\mathrm{O}(\lambda^2). \quad . \ . \ . \ . \quad (38)$$

In the notation of § 4, if the surface S enclosing the particles is perturbed to S′ by $\mathbf{r}'=\mathbf{r}+\lambda\mathbf{s}(\mathbf{r})$, then (38) integrates to

$$\left(\frac{d\mathrm{E}}{d\lambda}\right)_{\lambda=0}=-\omega\int^{S}\left[\sum_i \mathrm{I}_i(\partial_{n\,i}\psi^*)(\partial_{n\,i}\psi)\right]\mathbf{s}\,.\,d\mathbf{S}=-\int^{S}d\mathbf{S}\,.\,\mathbf{P}\,.\,\mathbf{s}. \quad . \ . \quad (39)$$

Conservation of energy then requires $\mathbf{P}$ to be the tensor of the stress on the boundary in a *slow* perturbation, provided Ehrenfest's theorem applies. For a Gibbs ensemble, the free energy F is given by

$$e^{-\beta\mathrm{F}}=\mathrm{Z}\equiv\sum_{\nu=1}^{\infty}e^{-\beta\mathrm{E}_\nu}, \quad . \ . \ . \ . \ . \ . \ . \quad (40)$$

where $E_\nu$ are the energy levels of the eigen-functions of H, of Bose and Fermi symmetry, and $\beta^{-1}=k\mathrm{T}$. Then

$$\left(\frac{\partial \mathrm{F}}{\partial \lambda}\right)_\beta = \mathrm{Z}^{-1}\sum_\nu e^{-\beta \mathrm{E}_\nu}\frac{d\mathrm{E}_\nu}{d\lambda} = -\int^{\mathrm{S}} d\mathbf{S}.\left[\mathrm{Z}^{-1}\sum_\nu e^{-\beta \mathrm{E}_\nu}\mathbf{P}_\nu\right].\mathbf{s}, \quad . \quad (41)$$

and therefore $$\overline{\mathbf{P}} \equiv \mathbf{Z}^{-1}\sum_\nu e^{-\beta \mathrm{E}_\nu}\mathbf{P}_\nu,$$

the average of $\mathbf{P}$ over the canonical distribution, is the boundary stress for isothermal displacements. For a simple dilation

$$\mathbf{s}=\mathbf{r}, \quad \mathrm{V}\frac{d}{d\mathrm{V}} = \left(\frac{1}{3}\right)\frac{d}{d\lambda}. \quad . \quad . \quad . \quad . \quad . \quad . \quad (42)$$

Substituting (42) in (25), (39) and (41), the thermodynamic pressure is

$$p = -\frac{d\mathrm{F}}{d\mathrm{V}} = \left(\frac{1}{3\mathrm{V}}\right)\int^{\mathrm{V}}\left[\mathrm{Z}^{-1}\sum_\nu e^{-\beta \mathrm{E}_\nu}(2\mathrm{K}_\nu - \Gamma_\nu)\right]d^3\mathbf{r}.$$

*I. e.*

$$3p\mathrm{V} = \int^{\mathrm{V}}(2\overline{\mathrm{K}}-\overline{\Gamma})d^3\mathbf{r}. \quad . \quad . \quad . \quad . \quad . \quad . \quad . \quad (43)$$

There is an arbitrariness in (39), which can be written

$$-\frac{d\mathrm{E}}{d\lambda} = \int_{\mathrm{S}} d\mathbf{S}\,.\,(\alpha\mathbf{R}-\beta\mathbf{S})\,.\,\mathbf{s}$$

where $2\alpha-\beta=1$. For the case (42), (43), $\mathbf{s}=\mathbf{r}$ we then find

$$-\frac{d\mathrm{E}}{d\lambda} = \int^{\mathrm{V}}(2\mathrm{K}-\Gamma)d^3\mathbf{r} + 3\left(\frac{\alpha-1}{\alpha}\right)\int^{\mathrm{V}}\mathbf{S}_s d^3\mathbf{r}, \quad \alpha\neq 0.$$

Since $\int^{\mathrm{V}}\mathbf{S}_s d^3\mathbf{r}=0$ by (15), we then retrieve (43).

Comparison of (23), (28) and (43) with (I, 3.21) and (I, 3.22) shows that $p$ is numerically equal to Green's $p_1$, the first term in his series for $p$. Thus the quantity $\pi = p_1 - p$, which Green identifies (II) with the energy associated with the thermomechanical effect in liquid helium II, appears to be zero. However, this conclusion has been the subject of a recent controversy (Yvon 1948), (Massignon 1949), (de Boer 1949), (Green 1949), (Horowitz 1950). A further discussion of the question is therefore attempted in the following paragraphs.

## § 7. Application of Brillouin's Theory.

The result (39) may also be obtained by the independent perturbation method originated by Brillouin (1937). For simplicity, the work is given in terms of the case $\mathrm{N}=1$. The particle is enclosed in the surface S, on which the wave-function $\psi(\mathbf{r})$ vanishes. Let S be continuously deformed to S′ by $\mathbf{r}'=\mathbf{r}+\lambda\mathbf{s}(\mathbf{r})$, and choose $\mathbf{s}$ to be normal to S. Then $\mathbf{s}(\mathbf{r})$ may be chosen *inside* S so as to agree with the boundary value, be continuous, and satisfy

$$\nabla\,.\,\mathbf{s}=\text{constant}, \quad \mathbf{s}=\nabla\phi. \quad . \quad . \quad . \quad . \quad . \quad . \quad (44)$$

The choice is unique, and has the property

$$\Delta \mathbf{s} = 0. \quad . \quad . \quad . \quad . \quad . \quad . \quad . \quad . \quad . \quad (45)$$

If $$H'\psi(\mathbf{r}) = H\psi(\mathbf{r}') = H\psi(\mathbf{r}+\lambda\mathbf{s}),$$

then $$H' = H + \lambda\{\omega[2(\nabla\mathbf{s}):\nabla\nabla + (\Delta\mathbf{s}).\nabla] + \mathbf{s}.\nabla U\} + 0(\lambda^2).$$

Or, by (45),

$$G \equiv \left(\frac{dH}{d\lambda}\right)_{\lambda=0} = 2\omega(\nabla\mathbf{s}):\nabla\nabla + [\mathbf{s}.\nabla U(\mathbf{r})]. \quad . \quad . \quad . \quad (46)$$

Since, by (44), the eigenfunctions, $\psi_\nu$, of H remain orthogonal under the deformation, the change in the eigenvalues is given by

$$\frac{dE_\nu}{d\lambda} = (\psi_\nu \,|\, G \,|\, \psi_\nu). \quad . \quad . \quad . \quad . \quad . \quad . \quad . \quad (47)$$

Now

$$\nabla.(\mathbf{P}.\mathbf{s}) = (\nabla.\mathbf{P}).\mathbf{s} + \mathbf{P}:\nabla\mathbf{s}$$
$$= -\psi^*\psi(\nabla U).\mathbf{s} + \omega\nabla\mathbf{s}:[\nabla\psi^*\nabla\psi + \nabla\psi\nabla\psi^* - \tfrac{1}{2}\nabla\nabla(\psi^*\psi)]$$

for a stationary state. Then, integrating by parts and using (45) and the boundary condition, we find

$$-\int^S d\mathbf{S}.\mathbf{P}.\mathbf{s} = \int^V [\psi^*\psi(\nabla U).\mathbf{s}]d^3\mathbf{r} + 2\omega\int^V [\nabla\mathbf{s}:\psi^*\nabla\nabla\psi]d^3\mathbf{r}$$

$$= (\psi \,|\, G \,|\, \psi) = (\psi \left|\frac{dH}{d\lambda}\right| \psi). \quad . \quad . \quad . \quad . \quad . \quad . \quad . \quad . \quad (48)$$

The generalization for N particles is quite straightforward. Thus (39) is confirmed, in a form which covers degenerate unperturbed eigenstates. If the boundary wall exerts a short-range force on the molecules, with potential $U_3$ which "moves with the wall" in the perturbation, then the derivation of (46) shows that the boundary stress is still given by (46) and (47) if $\mathbf{s}.\nabla U$ is replaced by

$$\mathbf{s}.\nabla(U_1+U_2) + z\left(\frac{dU_3(z)}{dz}\right)\partial_n s_n, \quad . \quad . \quad . \quad . \quad . \quad (49)$$

where $\mathbf{n}$ is the unit normal to S, and $-z\mathbf{n}$ is the vector from $\mathbf{r}$ to S. For the dilation case, $\mathbf{s}=\mathbf{r}$, (49) reduces to $\mathbf{r}.\nabla U$, and (43) is still valid.

## § 8. The Thermodynamic-Pressure Series.

Derivations of (43) have been given (de Boer 1949), (Green 1949) which make use of the transformation of the partition sum Z of (40) to

$$Z = \mathrm{Lim}(p, n) \sum_{k=1}^{p} \langle k \,|\, \sigma_n \,|\, k\rangle \quad . \quad . \quad . \quad . \quad . \quad . \quad (50)$$

where $$\sigma_n = \sum_{r=0}^{n} \frac{(-\beta)^r}{r!} H^r, \quad . \quad . \quad . \quad . \quad . \quad . \quad . \quad (51)$$

$\{|\, k\rangle\}$ is any complete (in the Bose or Fermi subspace) normalized orthogonal basis, and $\mathrm{Lim}(p, n)$ means

$$\lim_{p\to\infty} \quad \lim_{n\to\infty}$$

taken in the order from right to left (it is, of course, not permissible to interchange the limits in (50)). By (46),

$$\frac{d}{d\lambda}(\mathrm{H}^{r+1}) = \mathrm{H}^r\mathrm{G}+\mathrm{H}^{r-1}\mathrm{G}\mathrm{H}+\ldots+\mathrm{G}\mathrm{H}^r = \sum_{t=0}^{r}\binom{r+1}{t+1}\mathrm{G}_t\mathrm{H}^{(r-t)}. \quad (52)$$

where $\mathrm{G}_t = \mathrm{H}\mathrm{G}_{t-1}-\mathrm{G}_{t-1}\mathrm{H}, \quad \mathrm{G}_0=\mathrm{G}.$

Hence, by (50),

$$\frac{d\Xi}{d\lambda} = \mathrm{Lim}(p,n)\sum_{k=1}^{p}\sum_{r=1}^{n}\sum_{t=1}^{r}\left[\frac{(-\beta)^r}{t!\,(r-t)!}\langle k\,|\,\mathrm{G}_{t-1}\mathrm{H}^{(r-t)}\,|\,k\rangle\right]. \quad (53)$$

If we choose, for the $|\,k\rangle$, the eigenkets of the *unperturbed* hamiltonian, then

$$\langle k\,|\,\mathrm{G}_t\mathrm{H}^r\,|\,k\rangle = \langle k\,|\,\mathrm{H}\mathrm{G}_{t-1}\,|\,k\rangle\mathrm{E}_k{}^r - \langle k\,|\,\mathrm{G}_{t-1}\,|\,k\rangle\mathrm{E}_k{}^{(r+1)}.$$

If, H being hermitian, we put

$$\langle k\,|\,\mathrm{H}\mathrm{G}_{t-1}\,|\,k\rangle = \mathrm{E}_k\langle k\,|\,\mathrm{G}_{t-1}\,|\,k\rangle$$

(it is pointed out below that this step requires a special justification), then

$$\langle k\,|\,\mathrm{G}_t\mathrm{H}^r\,|\,k\rangle = 0, \quad t\geqslant 1. \quad (54)$$

Substituting (54) in (53), by (48) we retrieve (41) and (43).

Since (for $\mathbf{s}=\mathbf{r}$)

$$\mathrm{G} = 3\mathrm{V}\frac{d\mathrm{H}}{d\mathrm{V}} = (i\hbar)^{-1}(\mathrm{H}\mathbf{p}\,.\,\mathbf{r}-\mathbf{p}\,.\,\mathbf{r}\mathrm{H}), \quad (55)$$

the argument leading to (54) also requires $\langle k\,|\,\mathrm{G}\mathrm{H}^r\,|\,k\rangle$ to vanish. It has been pointed out, in this connection, by Green (1949) that expressions of the form

$$\mathrm{T}r(\mathrm{AB}-\mathrm{BA}) = \mathrm{Lim}(n,\nu)\sum_{r=1}^{n}\sum_{\varrho=1}^{\nu}[\mathrm{A}_{r\varrho}\mathrm{B}_{\varrho r}-\mathrm{B}_{r\varrho}\mathrm{A}_{\varrho r}]$$

need not vanish, with a dense or continuous basis $\{|\,r\rangle\}$, if $\langle r\,|\,\mathrm{AB}\,|\,r\rangle$ is not uniformly convergent with respect to $r$. There is, however, another approach to such questions, which was pointed out by Fuchs (1940). H is specified not simply by a differential operator, such as (11), but with respect to the linear space of a basis $\{|\,k\rangle\}$—*i. e.* to the domain symmetry and boundary condition of the corresponding wave-functions. H is then only hermitian in virtue of this boundary condition, and if $\mathrm{A}\,|\,k\rangle$ does not satisfy the latter (A is then called by Fuchs "inadmissible") we cannot assume that

$$\langle j\,|\,(\mathrm{HA}\,|\,k\rangle) = [\langle k\,|\,(\mathrm{AH}\,|\,j\rangle)]^*.$$

*Differential* relations such as (46) and (55) are still correct, but deductions by matrix algebra may be invalid. For example, a virial theorem may be deduced as follows:

$$m\frac{d^2}{dt^2}(r_i^2) = m\frac{d}{dt}[r_i^2,\,\mathrm{H}] = \frac{d}{dt}(\mathbf{r}_i\,.\,\mathbf{p}_i+\mathbf{p}_i\,.\,\mathbf{r}_i)$$

$$= \ldots = 2[p_i^2/m-\mathbf{r}_i\,.\,\nabla_i\mathrm{U}],$$

and hence for a stationary state

$$\langle\,|\,\Sigma i(p_i^2/m-\mathbf{r}_i\,.\,\nabla_i\mathrm{U})\,|\,\rangle=0.$$

The surface-integral term is missing because, although the commutator relation $[\mathbf{r}_i, \mathbf{p}_j]=\mathbf{l}_i\delta_{ij}$ is applicable to $\mathbf{r}_i$ and $\mathbf{p}_j$ *as differential operators*, the Heisenberg equation

$$\frac{d}{dt}\langle\,|\,\mathrm{A}\,|\,\rangle=\langle\,|\,[\mathrm{A},\,\mathrm{H}]\,|\,\rangle$$

is then invalid where A is not admissible. Now, with the boundary condition $\psi=0$ which we are considering, G and the $\mathrm{G}_t$ are admissible, since G−2H reduces on the boundary to a function of $\mathbf{x}$, but $\mathbf{p}\,.\,\mathbf{x}+\mathbf{x}\,.\,\mathbf{p}$ is not. It follows that the diagonal elements, in the energy representation, of $\mathrm{G}_1$, $\mathrm{G}_2$, . . . necessarily vanish, but not those of G.

## § 9. The Coordinate Representation.

Green's (1949) treatment is based on the Schrödinger representation of (50) (Slater 1931, 1933):

$$Z=\int e^{-\beta\mathrm{H}}(\mathbf{x}',\,\mathbf{x}')d^{3\mathrm{N}}\mathbf{x}'.\quad .\quad .\quad .\quad .\quad .\quad .\quad .\quad .\quad (56)$$

A typical term in the resulting series for $d\mathrm{F}\,d\lambda$ (simplified by not employing the relation (55), and not symmetrizing the operators in each term) is proportional to

$$\int d^{3\mathrm{N}}\mathbf{x}'[\mathrm{G}_t e^{-\beta\mathrm{H}}](\mathbf{x}',\,\mathbf{x}')=\int d^{3\mathrm{N}}\mathbf{x}'\sum_{\nu=1}^{\infty}\{\psi_\nu^*(\mathbf{x}')[\mathrm{G}_t\psi_\nu(\mathbf{x}')]e^{-\beta\mathrm{E}_\nu}\},\quad .\quad (57)$$

where the $\psi_\nu$ are the eigenfunctions of H. For $t\geqslant 1$, since $|\,\psi_\nu\,|$ is bounded and (at least in the dilation case (42)) $\mathrm{G}_t$ reduces to a finite function of position, (57) is

$$\sum_{\nu=1}^{\infty}e^{-\beta\mathrm{E}_\nu}\left[\int d^{3\mathrm{N}}\mathbf{x}'\psi_\nu^*(\mathbf{x}')[\mathrm{G}_t\psi_\nu(\mathbf{x}')]\right]=\sum_{\nu=1}^{\infty}e^{-\beta\mathrm{E}_\nu}\langle\nu\,|\,\mathrm{G}_t\,|\,\nu\rangle=0.$$

Thus de Boer's (1949) statement, that Green's series reduces to its first term, is confirmed. A recent paper by Horowitz (1950) appears to suggest:

(*a*) that G is inadmissible, in Fuchs' sense,

(*b*) that the reasoning, corresponding to (53), which leads to Green's series is therefore invalid.

We have seen that G (though not Green's operator) *is* admissible for the boundary condition $\psi\ \ 0$, which Horowitz also adopts in the context of his criticism (G is not admissible for a periodic boundary condition, which leads to difficulties if applied in this problem). But in any case, from the present point of view, the admissibility of G affects, not the validity of the derivation of Green's series, but the vanishing or non-vanishing of the terms of this series. However, the validity of the use of (50), in the form (56), needs examination—since the transformation matrix

$$\mathrm{T}_{\mathbf{x}'\nu}=\langle\mathbf{x}'\,|\,\nu\rangle=\psi_\nu(\mathbf{x}')\quad .\quad .\quad .\quad .\quad .\quad .\quad .\quad (58)$$

is singular ($T^{\dagger}T(\mathbf{x}', \mathbf{x}'')=\delta(\mathbf{x}', \mathbf{x}'')$).

$$\text{If} \quad I(\Xi, n, \lambda)=\int^{\Xi} d^{3N}\mathbf{x}' \sum_{r=0}^{n} \sum_{\nu=1}^{\lambda} \frac{(-\beta)^r}{r!} \psi_\nu^*(\mathbf{x}')[H^r\psi_\nu(\mathbf{x}')]$$

$$=\int^{\Xi} d^{3N}\mathbf{x}' \sum_{r=0}^{\infty} \sum_{\nu=1}^{\lambda} \frac{(-\beta)^r}{r!} E_\nu^r \psi_\nu^*(\mathbf{x}')\psi_\nu(\mathbf{x}'), \quad . \quad . \quad . \quad (59)$$

and Lim ($\mathfrak{S}$) means the limit $\mathfrak{S}\to\mathfrak{R}$, then of the six expressions

$$\left.\begin{aligned} Z_1&=\text{Lim}\,(n, \mathfrak{S}, \lambda)I,\\ Z_2&=\text{Lim}\,(n, \lambda, \mathfrak{S})I,\\ Z_3&=\text{Lim}\,(\lambda, n, \mathfrak{S})I,\\ Z_4&=\text{Lim}\,(\lambda, \Xi, n)I,\\ Z_5&=\text{Lim}\,(\mathfrak{S}, \lambda, n)I,\\ Z_6&=\text{Lim}\,(\Xi, n, \lambda)I, \end{aligned}\right\} \quad . \quad . \quad . \quad . \quad . \quad . \quad (60)$$

$Z_1$, $Z_2$ and $Z_6$ are divergent. Using the fact that the $|\psi_\nu|$ are bounded, $Z_3=Z_4=Z_5$. But

$$Z_3=\sum_{\nu=1}^{\infty} e^{-\beta E_\nu}=Z, \quad . \quad . \quad . \quad . \quad . \quad . \quad . \quad . \quad (61)$$

while $Z_5$ is evidently the Slater (1933) sum, (56). Then, by (52) and (59),

$$\frac{dZ}{d\lambda}=\frac{dZ_5}{d\lambda}$$

$$=\text{Lim}\,(\mathfrak{S}, \lambda, n)\int^{\mathfrak{S}} d^{3N}\mathbf{x}' \sum_{r=1}^{n} \sum_{\nu=1}^{\lambda} \sum_{t=1}^{r} \frac{(-\beta)^r}{t!\,(r-t)!} \psi_\nu^*(\mathbf{x}')[G_{t-1}H^{(r-t)}\psi_\nu(\mathbf{x}')]$$

$$=\text{Lim}\,(\Xi, \lambda, n)\int^{\Xi} d^{3N}\mathbf{x}' \sum_{\nu=1}^{\lambda}\left\{\sum_{r=1}^{\infty} \sum_{t=1}^{r} \frac{(-\beta)^r E_\nu^r}{t!\,(r-t)!} \psi_\nu^*(\mathbf{x}')[G_{t-1}\psi_\nu(\mathbf{x}')]\right\}. \quad . \quad . \quad . \quad (62)$$

Since

$$\sum_{s=0}^{r} \frac{(-\beta)^s}{s!} E_\nu^s \psi_\nu^*(\mathbf{x}')[G_{t-1}\psi_\nu(\mathbf{x}')]$$

converges uniformly with respect to $t$, $\mathbf{x}'$ and $\nu$,

$$\text{Lim}\,(n)\{\ \}=\sum_{t=1}^{\infty} \frac{(-\beta)^t}{(t+1)!} e^{-\beta E_\nu}\psi_\nu^*(\mathbf{x}')[G_{t-1}\psi_\nu(\mathbf{x}')] \quad . \quad . \quad . \quad (63)$$

which also converges uniformly with respect to $\mathbf{x}'$ and $r$, and hence

$$\frac{dZ}{d\lambda}=\text{Lim}(\Xi, r)\int^{\Xi} d^{3N}\mathbf{x}'\left[\sum_{t=1}^{r} \frac{(-\beta)^t}{t!}(G_{t-1}e^{-\beta H})\,(\mathbf{x}', \mathbf{x}')\right]. \quad . \quad (64)$$

Interchange of the remaining two limits results in

$$\frac{dZ}{d\lambda}=(-\beta)\sum_{t=0}^{\infty} \frac{(-\beta)^t}{t+1}\int^{\mathfrak{R}} d^{3N}\mathbf{x}'(G_t e^{-\beta H})(\mathbf{x}', \mathbf{x}'), \quad . \quad . \quad (65)$$

which is essentially Green's series, and which we have shown to reduce to its first term.

## Conclusion.

Of the mathematical results in (I), the work in this paper confirms the dynamical equations (5.6), (5.11), and thus vindicates the formalism which led to them, but is at variance with the more controversial conclusion of §3 : that the thermodynamic stress on the boundary (or on a " probe " inserted in the liquid) differs from the kinetic stress. However, it is not clear how far the theory in (II) really depends on (I). The formulæ for the thermodynamic stress necessarily refer to the whole volume of the system, the integrals over which involve a boundary contribution associated with **S**, (20). The theory given in (II) of the thermo-mechanical effects (*cf.* II, 3.20) must be regarded as an empirical one ($\pi$ was in fact computed from Kapitza's experimental results), while the discussion of the normal viscosity (I, 6.1) (II, §2) seems to depend on a conception, of the local order in the liquid, whose foundation is not clear. Further progress will probably depend on the development of a theory of the structure of the quantum liquid when almost in equilibrium. It may be, for example, that there is a long-range order which makes it meaningless to speak of local quasi-isothermal processes, to which results similar to (41) would apply.

I wish to express my thanks to Mr. H. N. V. Temperley, of the Royal Society Mond Laboratory, for his advice and encouragement, and I am indebted to the D.S.I.R. for a maintenance award.

## References.

Born, M., and Green, H. S., 1947, *Proc. Roy. Soc.* A, **191**, 168.
Brillouin, L., 1937, *Comptes Rendus*, **204**, 1863.
de Boer, J., 1949, *Physica*, **15**, 843.
Dirac, P. A. M., 1947, *Principles of Quantum Mechanics*, 3rd ed., p. 130 (Oxford : University Press).
Fröhlich, H., 1938, *Phys. Rev.*, **54**, 945.
Fuchs, K. E., 1940, *Proc. Roy. Soc.* A, **176**, 214.
Green, H. S., 1948, *Proc. Roy. Soc.* A, **194**, 244 ; 1949, *Physica*, **15**, 882.
Horowitz, J., 1950, *J. de Phys.*, **11**, 241.
Landau, L., 1941, *J. Phys. U.S.S.R.*, **5**, 71:
Massignon, D., 1949, *Comptes Rendus*, **228**, 62.
Slater, J., 1931, *Phys. Rev.*, **38**, 237 ; 1933, *J. Chem. Phys.*, **1**, 687.
von Neumann, J., 1943, *Mathematische Grundlagen der Quanten Mechanik*, ch. 4. New York : Dover.
Yvon, J., 1948, *Comptes Rendus*, **227**, 763.

# LXXXVIII. CORRESPONDENCE.

## *Latitude Effect of Cosmic Ray Stars.*

By S. Lattimore,
Imperial College of Science and Technology, London*.

[Received July 25, 1950.]

Ilford 200 $\mu$ G.5 emulsions were exposed vertically for 27 days at altitudes of 11,550 ft. and 41,400 ft. at a latitude of approximately 12° S., in the Bolivian Andes. The plates were exposed under a corrugated iron roof. Since the time required for transporting the plates to and from Bolivia was considerable, control plates of a similar type to those actually exposed were used to find the number of stars collected before and after the exposures.

The results are given in Table I., together with figures for the Jungfraujoch. The latter were calculated from results at 11,500 ft., obtained using 200 $\mu$ G.5 plates, assuming a range of $145 \pm 10$ gm./cm.$^2$ of air for the star producing radiation.

Table I.

| Height (feet) | No. of stars (< 3 prong)/c.c./day. Andes | Jungfrau | Ratio Jungfrau/Andes |
|---|---|---|---|
| 11,550 | $7{\cdot}7 \pm 1{\cdot}5$ | $16{\cdot}4 \pm 0{\cdot}5$ | $2{\cdot}1 \pm 0{\cdot}4$ |
| 14,400 | $13{\cdot}4 \pm 1{\cdot}7$ | $27{\cdot}5 \pm 1{\cdot}3$ | $2{\cdot}05 \pm 0{\cdot}27$ |

The value of $2{\cdot}1 \pm 0{\cdot}4$ for the ratio of the number of stars with three or more prongs at the Jungfraujoch to the number at 12° S. is in fair agreement with results of Beets, Morand and Winard (1949) who found a value of 2·4 for the ratio between 44° N. and 1° S. at a height of 14,700 ft.

In Table II. are shown the size distributions for all stars at the Andes, and those at the Jungfraujoch, normalized so that the ratio of all stars with three or more prongs at the Jungfraujoch to all stars with three or more prongs at the Andes is equal to 2·1. As can be seen, the latitude effect decreases as the star size increases.

Table II.

| Star size | No. of Stars. Andes | Jungfraujoch | Ratio Jungfrau=R Andes |
|---|---|---|---|
| 3, 4 | $193 \pm 25$ | $498 \pm 22$ | $2{\cdot}6 \pm 0{\cdot}35$ |
| 5, 6 | $83{\cdot}5 \pm 14$ | $161 \pm 13$ | $1{\cdot}93 \pm 0{\cdot}35$ |
| 7, 8 | $42 \pm 9$ | $52 \pm 7$ | $1{\cdot}24 \pm 0{\cdot}32$ |
| >8 | $41{\cdot}5 \pm 8{\cdot}5$ | $46 \pm 7$ | $1{\cdot}10 \pm 0{\cdot}27$ |
| Total | 360 | 755 | 2·10 |

* Communicated by Professor Sir George Thomson, F.R.S.

The figures in Table II. are plotted graphically in fig. 1 and are shown to lie on a smooth curve.

Now the magnetic cut-off energy at the Andes is 15,000 MeV. and at the Jungfraujoch is 2000 MeV., and it is possible to estimate from the ratio of the number of stars at the Jungfraujoch to the number at the Andes the proportion of the stars at the Jungfraujoch that are produced by primaries with energies between 2000 and 15,000 MeV.

Fig. 1.

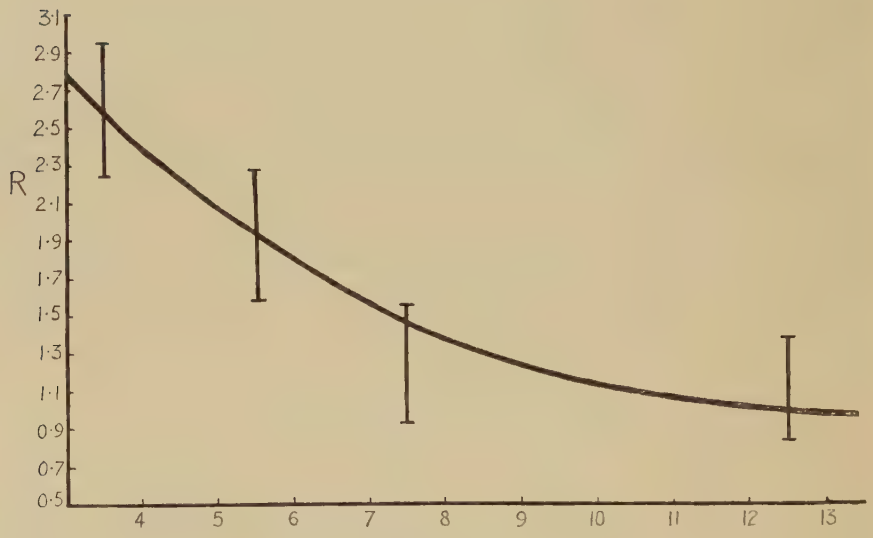


Let $x$ be this fraction. Then

$$2{\cdot}1 = 1/(1-x) \qquad \therefore \quad x \sim \tfrac{1}{2};$$

*i. e.* only one-half of the stars at the Jungfraujoch are produced by primaries with energies between 2000 and 15,000 MeV., although, assuming an $E^{-3}$ energy spectrum for the primaries, there are approximately 50 times as many primaries in this range as there are with energy greater than 15,000 MeV. This result is, at first sight, rather surprising, since most of the stars have energies below 300 MeV. However, the majority of the stars are produced by neutral particles, probably neutrons, which must have been produced by the primaries high in the atmosphere, and further, the work of Harding (1949) shows that a star producing particle can probably produce more than one star. It would, therefore, seem probable that a primary produces several particles high in the atmosphere each of which can produce several stars, in which case the lower energy primaries would become less important.

Acknowledgments.

We have pleasure in expressing our gratitude to Mr. Clifford Waite of Consolidated Tin Smelters Ltd., and to Mr. D. C. Deringer, Jr. of Platino Mines and Enterprises Cons. Inc. for exposing the Andes plates used in this experiment. Our thanks are also due to Sir Roger Makins, K.C.B., of the Foreign Office, who arranged for the transport of the plates to and from Bolivia. We are grateful to Professor Sir George Thomson for interesting discussions on this work.

Imperial College London. S. Lattimore.

References.

Beets, C., Morand, M., and Winard, L., 1949, *C.R. Acad. Sci.*, Paris, **229**, 1227–8.

Harding, J. B., 1949, *Phil. Mag.* (7) **40**, 530.

---

## *Note on the Heavy Nuclei of the Cosmic Radiation.*

By A. D. Dainton and D. W. Kent,
H. H. Wills Physical Laboratory, University of Bristol *.

[Received July 30, 1950.]

[Plates XXX. and XXXI.]

It is now well known that the atomic nuclei among the primary cosmic radiation are rapidly absorbed in the atmosphere as a result of nuclear interactions and loss of energy through ionization (Bradt and Peters 1948, 1950, Freier *et al.* 1948). Further, in the nuclear collisions which they make, these primary particles are often not absorbed catastrophically. They frequently suffer fragmentation so that fast heavy particles of smaller mass emerge from the encounter—see Pls. XXX. and XXXI. It follows that the distribution in mass and energy of the heavy particles, as well as their intensity, changes rapidly as they penetrate towards the earth.

Recent experiments in this laboratory with plates exposed at 68,000 feet, showed the presence of substantial numbers of heavy particles at this altitude. The observations have allowed us to determine the characteristics of the flux of heavy particles at this altitude. The deduced values of the intensity of the heavy nuclei at the top of the atmosphere, and their mean free path, are in good agreement with the results of other workers.

The exposure was made with 400 $\mu$ Ilford G5 emulsions by means of free balloons at a geomagnetic latitude of 54° N. Level flight was maintained at 68,000 feet ($52 \pm 1$ gm./cm.$^2$) for 100 minutes. Since very few heavy nuclei are observed at altitudes lower than 55,000 feet, and since

---

* Communicated by Professor C. F. Powell, F.R.S.

the time of ascent and descent above this altitude was small compared with the time of level flight, it was a sufficient approximation to assume that the observed nuclei entered the plates at 68,000 feet.

Our observations were made on 118 nuclei with charge $Z \geqslant 5$. The charge of each nucleus was determined by the delta-ray method described by Bradt and Peters (1948). The number, $\nu$, of delta-rays having an energy greater than $W_1$, produced per unit length of its trajectory by a particle of charge Z, is given by :

$$\nu = \frac{CZ^2}{\beta^2}\left\{\frac{1}{W_1} - \frac{1}{\beta^2}\right\}, \quad . \quad . \quad . \quad . \quad . \quad . \quad . \quad . \quad . \quad (1)$$

where $\beta c$ is the velocity of the incident particle. Using the range-energy relation, the charge can thus be determined within an error of plus or

Fig. 1.

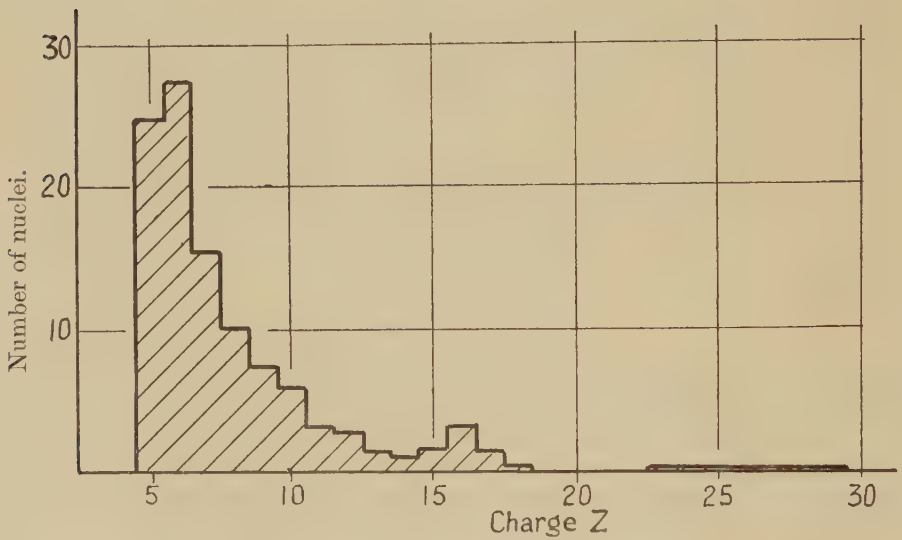


Distribution in charge of 118 nuclei.

minus one unit in the majority of cases, if the length of the track is sufficiently great. In cases where particles of low charge cannot be observed over a long range, the uncertainty in the charge determination is greater. The spectrum determined in this investigation is shown in fig. 1.

In order to obtain a value of the flux at the top of the atmosphere it was convenient to consider only those tracks which passed through the emulsion of the outside plates of the stack. The angle of each track with respect to the zenith was determined from the dip and the angle between the projection of the track on the plane of the emulsion and the vertical side of the plate. The observed distribution was then corrected for absorption in the stack and for geometrical orientation of the plates. The number of tracks observed having a zenith angle between $\theta$ and $\theta+d\theta$ is given by

$$dn = I(\theta) \, . \, t \, . \, \mathrm{A} \, . \, 4 \sin^2\theta \, . f(\theta) \, . \, d\theta, \quad . \quad . \quad . \quad . \quad . \quad . \quad (2)$$

where $t$ is the time of exposure, A is the area surveyed, and $4\sin^2\theta\,.f(\theta)$ is the correction factor due to plate orientation and to the choice of minimum track length (500 $\mu$ in this investigation). The function

$$f(\theta)=1-\left[1-\left(\frac{d}{l\sin\theta}\right)^2\right]^{1/2},$$

where $d$ is the depth of the emulsion and $l$ is the minimum track length considered, is operative only when the zenith angle exceeds $\sin^{-1}d/l=53°$. Assuming the absorption in the atmosphere to be exponential, $I(\theta)$, the intensity of the radiation at an angle $\theta$, is related to the flux at the top of the atmosphere by the equation

$$I(\theta)=\mathrm{I}_0\exp\left[(\mathrm{L}/\lambda)\sec\theta\right],$$

Fig. 2.

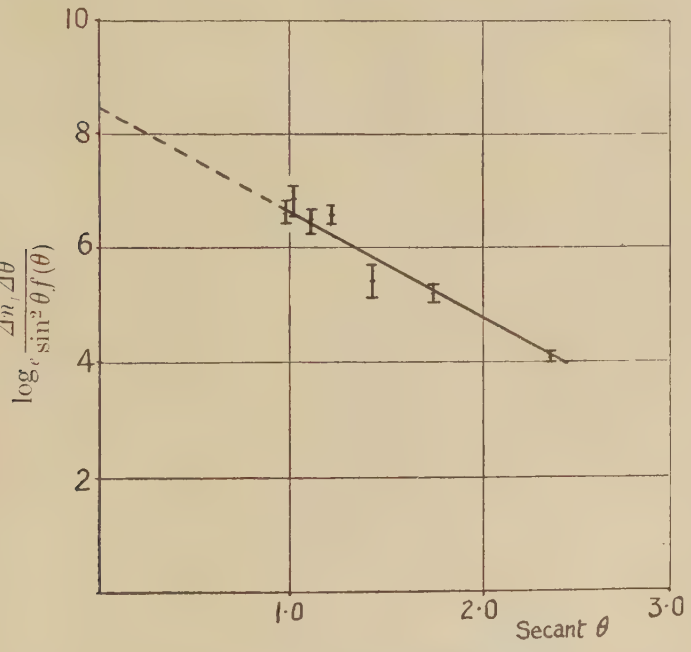


Angular distribution function.

L being the distance in gm. cm.$^{-2}$ from the level of the exposure to the top of the atmosphere, and $\lambda$ the mean free path for disappearance in air. We can express equation (2) in the form (Hoang Tchang-Fong 1950)

$$\log_e\left[\frac{\Delta n}{\Delta\theta}\Big/\sin^2\theta f(\theta)\right]=\log_e(4\,.\,\mathrm{I}_0\,.\,\mathrm{A}\,.\,t)-\frac{\mathrm{L}}{\lambda}\sec\theta.$$

A plot of this function, shown in fig. 2, gives a value $-\mathrm{L}\,\lambda$ for the slope and for the intercept at $\sec\theta=0$, $\log_e(4\,.\,\mathrm{I}_0\,.\,\mathrm{A}\,.\,t)$. From these two values we obtain for the mean free path

$$\lambda\sim 28\ \mathrm{gm./cm.^2},$$

and for the flux $\mathrm{I}_0\sim 1{\cdot}3\times10^{-3}$ particles cm.$^{-2}$ sec.$^{-1}$ steradian$^{-1}$.

It is probable that an appreciable fraction of the nuclei observed at this altitude are not of primary origin. Of eight observed collisions caused by nuclei of charge $Z > 6$, four cases resulted in a reduction in the charge of the primary, but little change in its velocity and direction.

In 34 cases in which an increase in the delta-ray density with range was observed, it was possible to determine the kinetic energy of the nucleus. The values thus obtained were corrected for ionization losses in the air to determine the corresponding values of the kinetic energy at the top of the atmosphere. Since collisions involving degradation of the charge occur, it is reasonable to assume that some of the particles are splinters of larger, more heavily ionizing nuclei. The values obtained, which lie between 0·45 BeV. and 2·0 BeV. per nucleon, therefore represent lower limits for the energies of the particles at the top of the atmosphere.

The present experiments are being continued with the application of new techniques.

The authors wish to express their gratitude to Professor C. F. Powell, F.R.S., for making this investigation possible, and to Dr. C. Franzinetti for helpful guidance and discussion.

## References.

Bradt, H. L., and Peters, B., 1948, *Phys. Rev.*, **74,** 1828; 1950, *Ibid.*, **77,** 54.
Freier, P., Lofgren, E. J., Ney, E. P., and Oppenheimer, F., 1948, *Phys. Rev.*, **74,** 1818.
Hoang Tchang-Fong, 1950, *Thesis*, Paris.

---

## *Loss of Energy of Fast Protons in Matter with Particular Reference to their Range in Carbon.*

By A. E. Taylor,
Atomic Energy Research Establishment, Harwell, Berks.*

[Received August 3, 1950.]

In using the 110-inch cyclotron at Harwell for measurements of total scattering cross sections and neutron energy spectra (Taylor, Pickavance, Cassels and Randle 1950) carbon absorbers of varying thickness have been used in a triple coincidence telescope detecting protons scattered from a polythene radiator. The range in carbon was used to deduce the energy of the protons, since carbon was a convenient material having a low atomic number. This choice was made in order to minimize multiple coulomb scattering and nuclear absorption for efficient operation of the detecting telescope. It was therefore required to compute the range energy relation in carbon for protons up to 200 MeV.

---

* Communicated by the Author.

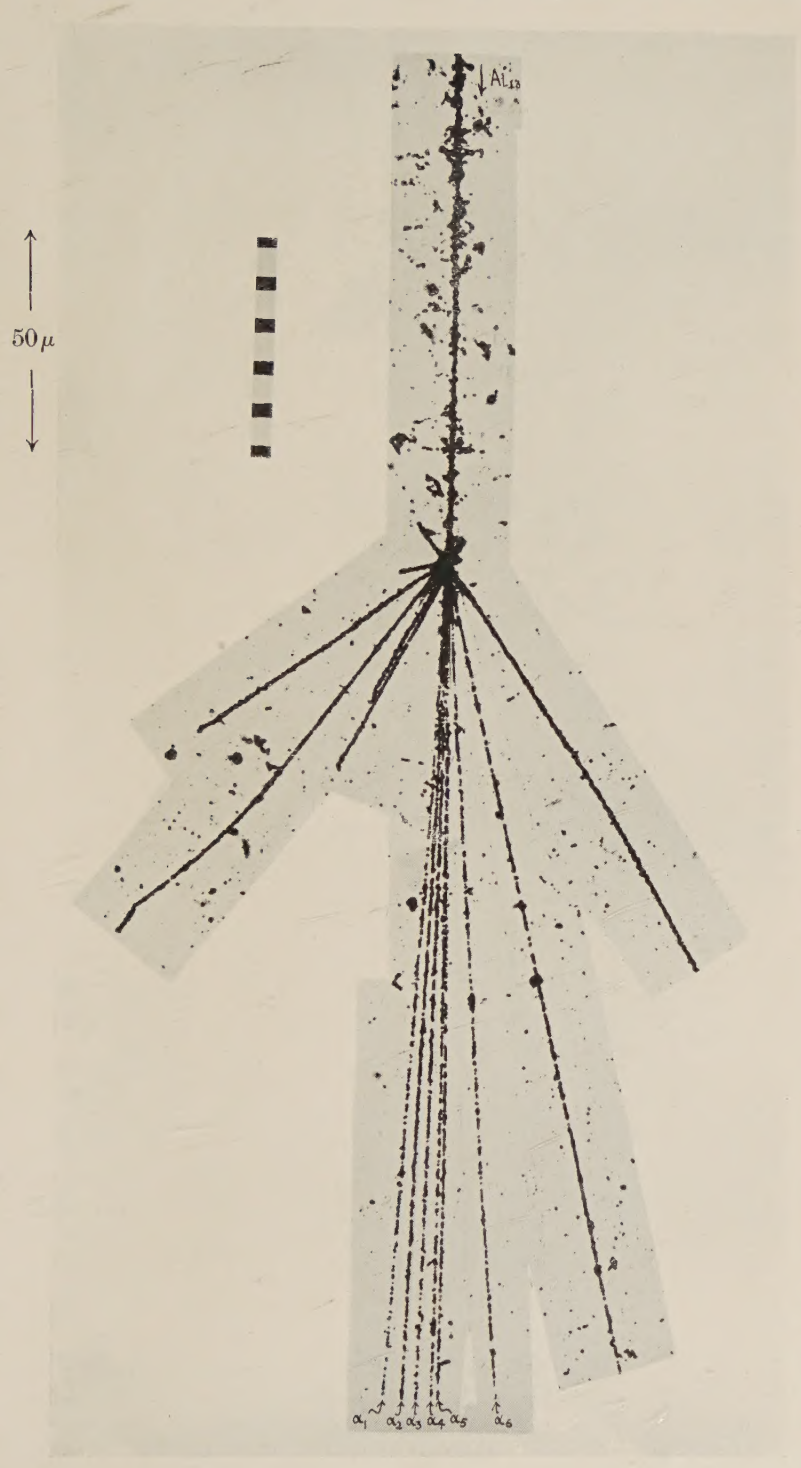


PLATE I.

A nucleus of charge Z=13±1 with a velocity $\beta=0{\cdot}55$ suffers a collision in the emulsion and gives rise to a "jet" of six $\alpha$-particles (considered to be components of the primary particle) and low energy disintegration fragments of the target nucleus. Observer: Miss J. HERAPER.

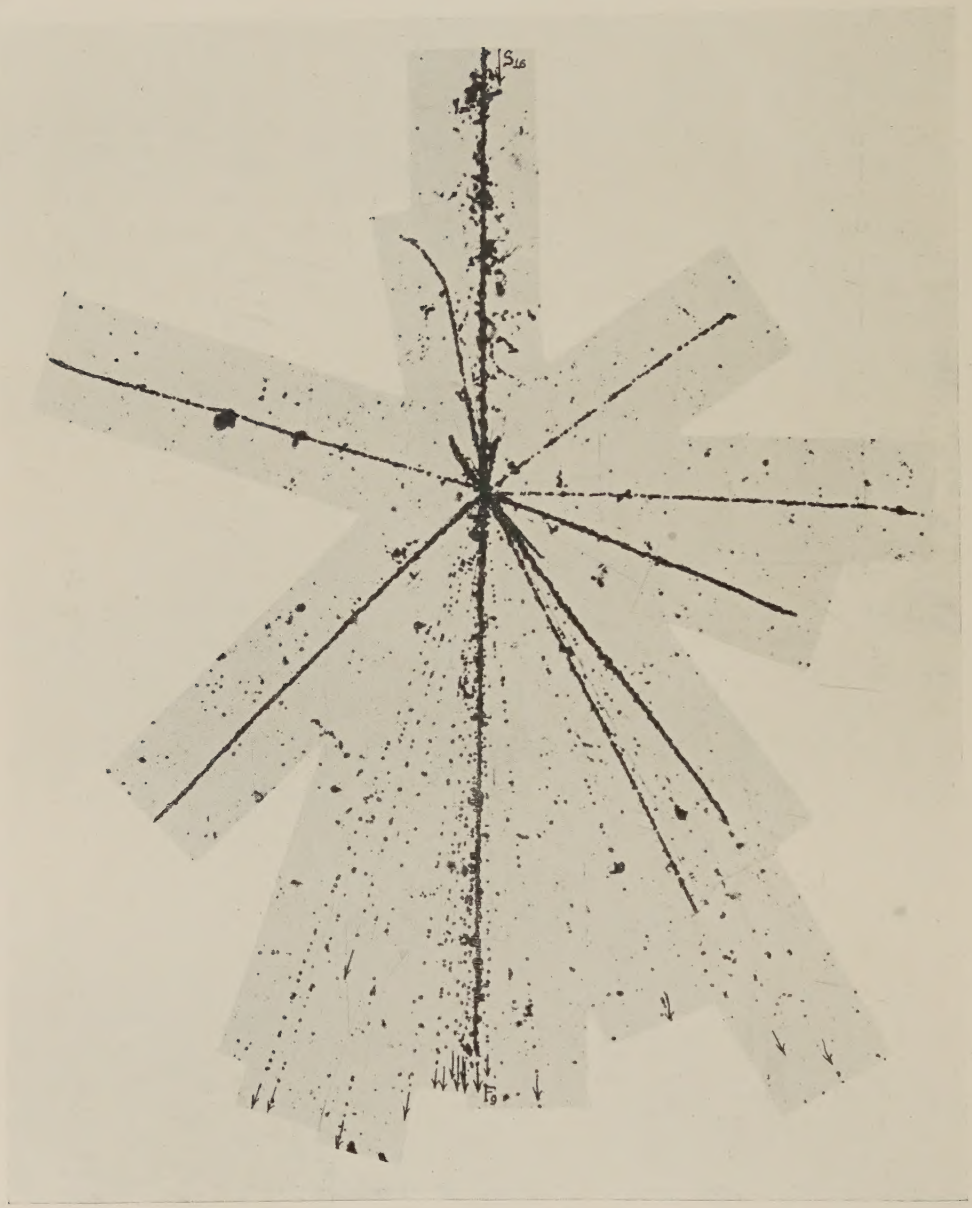


PLATE II.

A fast nucleus of charge $Z=16\pm1$ interacts with one of silver or bromine in the emulsion. The nucleus emerging from the encounter has a charge $Z=9\pm1$ and is accompanied by twenty-five singly charged particles moving at relativistic velocities, and in directions contained by a cone of semi-vertical angle 30°. The tracks of fifteen of these particles have been reproduced in this photomicrograph. Observer : Miss E. JAMES.

The calculations have been made using the theoretical equation for protons given by Livingston and Bethe (1937)

$$-\frac{dE}{dx}=\frac{4\pi Ne^4}{mv^2}\left[Z'\left(\ln\frac{2mv^2}{I(1-\beta^2)}-\beta^2\right)-C_K\right],$$

where $-dE/dx$ is the rate of loss of energy, $Z'$ the effective number of electrons per atom, I the mean excitation energy of the atom of the absorber and $C_K$ a correction term.

For elements of low atomic number, $Z'$ is taken as the total number of electrons, Z, and the non-excitation of the inner shell electrons for low proton energies is corrected by the term $C_K$. Values of $C_K$ are given by Livingston and Bethe (1937) in terms of the energy of the proton and a critical energy depending on the ionization potential of the electrons. For elements of high atomic number $Z'$ is taken as the effective number of electrons (Hönl 1933).

The value of I is usually chosen to give agreement with experimental values for the energy loss at low energies. On the basis of the Fermi Thomas model of the atom, Bloch (1933) showed that approximately a linear relationship should hold between I and Z for elements of high atomic number. The constant of proportionality, $\alpha$, given by Wheller (1941), is 11·5 eV. while Mano (1934 a, b) has given the value of 10·5 eV. for elements with Z greater than 20 but shows that $\alpha$ fluctuates for Z less than 20. The values adopted by Livingston and Bethe (1937) for hydrogen, helium, aluminium, air and gold differ slightly from those of Mano, but the variation of $\alpha$ with Z follows the same pattern.

Before the computation of the range energy relation in carbon can be carried out, an appropriate value of I must be found. In view of the variation of $\alpha$ for elements of low atomic weight, it was decided to find a value which gave an atomic stopping power relative to aluminium in agreement with experimental values, rather than take the theoretical value of 11·5 eV. Using for $Z'$ the total number of electrons both for aluminium and carbon and a value of I for aluminium as 150 eV., the value of I for carbon was found to be 50·3 eV., and hence $\alpha$ is 8·4 eV. This value seems to fit in with the pattern of variation of $\alpha$ with Z. Similarly for silver and copper the calculated values of I were 365 eV. for silver and 293 eV. for copper, using values of $Z'$ 39·6 and 27·4 respectively.

Using the value of I as 50·3 eV. for carbon and the appropriate values of $C_K$, $dE/dx$ was calculated at 20 MeV. intervals up to 200 MeV. Below 20 MeV. the known experimental values were taken. The range was then computed by numerical integration and is given in Table I.

These values for the range have been used as a measure of the energy of protons scattered into a triple coincidence telescope from a polythene radiator bombarded by neutrons ejected from beryllium and carbon targets. The end point of the spectrum of the scattered protons was compared with that using aluminium for the absorber. The energy in this case was deduced from the range energy curves of Smith (1947).

TABLE I.

| Energy MeV. | $\frac{1}{\rho}\frac{dE}{dx}$ MeV./gm. cm.$^{-2}$ | Range gm. cm.$^{-2}$ |
|---|---|---|
| 2·5 | 132·5 | 0·0113 |
| 5 | 77·3 | 0·0374 |
| 10 | 44·15 | 0·127 |
| 15 | 31·58 | 0·264 |
| 20 | 24·96 | 0·442 |
| 40 | 14·16 | 1·55 |
| 60 | 10·23 | 3·24 |
| 80 | 8·16 | 5·45 |
| 100 | 6·89 | 8·13 |
| 120 | 6·03 | 11·24 |
| 140 | 5·39 | 14·76 |
| 160 | 4·91 | 18·65 |
| 180 | 4·54 | 22·89 |
| 200 | 4·23 | 27·45 |

The energies so determined agree with each other to 2 MeV. and to within 2 MeV. of the value expected from the theoretical energy of the neutrons, the experimental error being also about 2 MeV.

August 2nd, 1950. A. E. TAYLOR.

REFERENCES.

BLOCH, F., 1933, *Zeits f. Phys.*, **81,** 363.
HÖNL, H., 1933, *Zeits. f. Phys.*, **84,** 1.
LIVINGSTON, M. S., and BETHE, H. A., 1937, *Rev. Mod. Phys.*, **9,** 261.
MANO, G., 1934 a, *Ann. Phys., Lpz.*, **1,** 407.; 1934 b, *J. Phys. Radium*, **5,** 628.
SMITH, J. H., 1947, *Phys. Rev.*, **71,** 32.
TAYLOR, A. E., PICKAVANCE, T. G., CASSELS, J. M., and RANDLE, T. C., 1950, *Nature, Lond.*, **165,** 4207, 967–968.
WHELLER, J. A., 1941, *Phys. Rev.*, **60,** 754.